Feedforward activation in metabolic systems

by

Marnette Coetzee

Thesis presented in partial fulfilment of the requirements for the degree of Master of Science (Biochemistry) in the Faculty of Science at Stellenbosch University

Supervisors: Prof. J.-H.S. Hofmeyr (supervisor)
Prof. J.M. Rohwer (co-supervisor)

March 2016

Declaration

By submitting this thesis electronically, I declare that the entirety of the work contained therein is my own, original work, that I am the sole author thereof (save to the extent explicitly otherwise stated), that reproduction and publication thereof by Stellenbosch University will not infringe any third party rights and that I have not previously in its entirety or in part submitted it for obtaining any qualification.

Date: March 2016 .....

Acknowledgements

I would like to thank:

- Prof Jannie Hofmeyr for being my supervisor. This study would not have been possible without your encouragement, guidance and patience.
- Prof Johann Rohwer for co-supervision of this study.
- Dr Danie Palm for always taking the time to explain.

Contents

List of Figures

List of Tables

Summary

This thesis describes an analytical and quantitative analysis of the regulatory phenomenon of feedforward activation in metabolic pathways. The necessary background in kinetic modelling of metabolic pathways, enzyme kinetics of allosteric enzymes, metabolic control analysis and supply-demand analysis are provided. A few selected examples of feedforward activated enzymes are discussed, focussing on their classification into the two major mechanistic classes, namely K-enzymes, for which the allosteric activator acts by increasing the affinity for the enzyme substrate (specific activation), and V-enzymes, for which the allosteric activator acts by increasing the limiting rate (V_f) of the enzyme (catalytic activation).

Feedforward activation is then studied by means of metabolic control analysis and supply-demand analysis of a minimal system subject to feedforward activation. An initial control analysis of the full system suggests that saturation of the allosteric enzyme with its substrate would allow it to control the flux through the demand pathway for the allosteric activator. The enzyme kinetics of K-enzymes however show that under these conditions the allosteric effect is abolished, and other conditions should be sought under which the allosteric enzyme controls its demand flux. This was done using supply-demand analysis, which showed that the allosteric enzyme would have the necessary control of the activator demand flux if the nested supply flux for its substrate was near equilibrium. V-enzymes do not exhibit this problem, and the catalytic allosteric effect operates under conditions of substrate saturation of the allosteric enzyme. A kinetic model of feedforward-regulated system was constructed and used to provide data for a graphical

analysis of the theoretical results.

The last part of the study is concerned with a particular allosteric enzyme, lactate dehydrogenase (LDH) in glucose fermentation metabolism in *Lactococcus lactis*, which is activated through feedforward action by fructose-1,6-bisphosphate (FBP), with the interesting twist that it also has an absolute requirement for FBP. An existing kinetic model of this metabolic pathway contained a rate equation for LDH that only incorporated a non-cooperative V-effect of FBP, but omitted other potentially important effects that have been described in the literature, such as the competitive inhibition of FBP binding by inorganic phosphate (Pi), cooperative binding of both FBP and Pi, and the alteration of the K_M-values of both the substrates pyruvate and NADH (K-effects). A new rate equation for LDH that incorporated these effects was developed and parameterised with data from the literature. The kinetic model with the original and one with the new rate equation were compared in terms of their steady-state behaviour as the external glucose concentration was increased from 0 to 2mM. The only observable differences occurred at glucose concentrations below 50μM and are probably of physiological significance only in the very last stage of glucose depletion. With our new LDH rate equation there was a decrease in the mixed acid fermentation fluxes as compared to the original model. We were able to relate the observed differences to the different types of allosteric effects through a series of 'what-if' experiments in which we compared the effects of four forms of our rate equation: the full equation, one which was completely desensitised to FBP, one with V-effects only and one with K-effects only. We also studied the effects of binding cooperativity of FBP and Pi-binding, and of Pi-inhibition of FBP-binding. We found that the activating V-effect of FBP on LDH operated mostly at very low glucose concentrations, while the K-effect of FBP onLDH operated only at higher glucose concentrations. The K-effect still dominated in the region between exclusively V-effect and exclusively K-effect, and it is only in this region that the cooperative binding of FBP and Pi and the Pi-inhibition of FBP-binding had any visible effect.

Opsomming

Hierdie tesis beskryf 'n analitiese and kwantitatiewe analise van die regulatoriese verskynsel van allosteriese vooruitvoeraktivering in metaboliese paaie. Die nodige agtergrond in kinetiese modellering van metaboliese paaie, ensiemkinetica van allosteriese ensieme, metaboliese kontrole analise en aanbod-aanvraag analise word verskaf. 'n Paar uitgesoekte voorbeelde van allosteriese ensieme word bespreek, met spesifieke fokus op hul klassifikasie in twee hoof meganistiese klasse, naamlik K-ensieme, waar die allosteriese aktiveerder die affiniteit van die ensiemsubstraat verhoog (spesifieke aktivering), en V-ensieme, waar die allosteriese aktiveerder die limiterende snelheid (V_f) van die ensiem verhoog (katalitiese aktivering).

Vooruitvoeraktivering word dan bestudeer met behulp van metaboliese kontrole analise and aanbod-aanvraag analise van 'n kernmodel wat aan vooruitvoeraktivering onderwerp is. 'n Aanvanklike kontrole analise van die model suggereer dat versadiging van die allosteriese ensiem met sy substraat die ensiem in staat stel om die fluksie deur die aanvraagpad vir die allosteriese aktiveerder te beheer. Die ensiemkinetika van K-ensieme toon egter dat die allosteriese effek onder hierdie kondisies opgehef word, sodat ander kondisies gevind moet word wat ook die allosteriese ensiem in staat stel om sy aanvraag fluksie te beheer. Dit is gedoen met aanbod-aanvraag analise, wat getoon het dat die allosteriese ensiem die nodige beheer oor sy aanvraagfluksie sou hê wanneer die aanbodfluksie vir sy subtraat naby ewewig is. V-ensieme het nie hierdie probleem nie, en die katalitiese allosteriese effek funksioneer wanneer die allosteriese ensiem met substraat versadig is. 'n Kinetiese model van die vooruitvoergereguleerde sisteem is gebou en

gebruik om data te verskaf vir 'n grafiese analise van die teoretiese resultate.

Die laaste gedeelte van die studie het gekonsentreer op 'n bepaalde allosteriese ensiem, naamlik laktaatdehidrogenase (LDH) in glukose metabolisme van *Lactococcus lactis*, wat deur vooruitvoer deur glukose-1,6-bisfosfaat (FBP) geaktiveer word, en interessant genoeg 'n absolute vereiste vir FBP het. 'n Bestaande kinetiese model van hierdie metaboliese pad het 'n snelheidsvergelyking vir hierdie ensiem bevat wat slegs 'n nie-koöperatiewe V-effek van FBP geïnkorporeer het, en ander potensieel belangrike effekte wat in die literatuur beskryf word uitgelaat het, soos kompeterende inhibisie van FBP-binding deur anorganiese fosfaat (Pi), koöperatiewe binding van beide FBP en Pi, en die wysiging van die K_M-waardes van beide die substrate pirovaat en NADH (K-effekte). 'n Nuwe snelheidsvergelyking vir LDH wat hier die effekte inkorporeer is ontwikkel en geparameteriseer met data uit die literatuur. Die kinetiese model met die oorspronklike en 'n model met die nuwe snelheidsvergelyking is in terme van hulle bestendige toestandsgedrag vergelyk soos wat die eksterne glukose konsentrasie toeneem van nul tot 2mM. Die enigste waarneembare verskille het by glukose konsentrasies laer as 50μM voorgekom en is waarskynlik net fisiologies belangrik in die heel laaste stadium van glukose uitputting. Met ons nuwe LDH snelheidsvergelyking was daar in vergelyking met die oorspronklike model 'n afname in die gemengde suurfermentasie fluksies. Ons kon hierdie waargenome verskille toewys aan die verskillende tipes allosteriese effekte deur 'n reeks van 'wat-as' eksperimente waarin ons die effekte van vier vorms van ons snelheidsvergelyking vergelyk het: die volle vergelyking, een wat volledig vir FBP gedesensiteer is, een met alleenlik V-effekte, en een met alleenlik K-effekte. Ons het ook die effekte van koöperatiewe binding van FBP en Pi, en van kompeterende inhibisie van FBP-binding deur Pi ondersoek. Ons het gevind dat die aktiverende V-effek van FBP op LDH slegs by baie lae glukose konsentrasies gefunksioneer het, terwyl die K-effek slegs by hoër glukose konsentrasies gefunksioneer het. In die gebied tussenin het die K-effek steeds gedomineer, en dit was slegs in hierdie gebied wat die koöperatiewe binding van FBP en Pi, en die kompeterende inhibisie van FBP-binding deur Pi waarneembare effekte gehad het.

Chapter 1

Introduction

A major aim of the field of systems biology is to understand the systemic properties of cellular reaction networks in terms of the local properties of the enzyme-catalysed reactions. The theoretical framework of choice for such studies is metabolic control analysis (MCA) [16, 30], which allows the expression of systemic control and response coefficients in terms of elasticity coefficients of individual enzymes. MCA often goes hand-in-hand with computational studies using one of the many software packages for kinetics modelling, such as PySCeS, the Python Simulator for Cellular Systems [44]. Many of the models developed by various systems biology groups worldwide are now available in curated online databases, such as JWS Online [45].

One outcome of studies using these approaches is a deeper understanding of the regulation of metabolism. The analytical procedure called supply-demand analysis [22–24] is tailor-made for this purpose, focussing on the pathways leading into and out of a regulatory metabolite, the so-called supply of and demand for that metabolite. In particular, it enables one to study the degree of functional differentiation of the supply and demand blocks around the metabolite, the functions in question being the locus of steady-state flux control and the homeostatic maintenance of the concentration of the regulatory metabolite. One of the general results of supply-demand analysis is that one block cannot fully fulfil both functions at the same time. The more, for example, the demand controls the flux, the more the properties of the sup-

ply block determines the degree to which the metabolite is homeostatically maintained, and *vice versa*. Whereas supply-demand analysis originally considered systems in which the supply and demand could communicate only through the metabolite that links them, it has now been generalised to systems where there can be multiple regulatory linkages between the blocks [55]. A recent example of the application of generalised supply-demand analysis to the study of the regulation of complex metabolic pathways is that of Christensen *et al.* [8].

The phenomenon of inhibitory feedback regulation of allosteric enzymes has been well studied using the above mentioned analytical tools [22, 23]. In such systems, for the feedback loop to be functional, the demand for regulatory metabolite that inhibits the upstream allosteric enzyme should control the flux through the full supply-demand system. Under such conditions the allosteric enzyme can maintain homeostasis in the concentration of the regulatory metabolite through the feedback loop, but only if the allosteric enzyme controls the flux local to the supply block; this is ensured if the allosteric enzyme is insensitive to its immediate product.

Regulation through feedforward activation, on the other hand, has not yet been subjected to such an analysis, and the aim of the study described in this thesis was to rectify this situation. Although in many respects the properties of a system regulated by feedforward activation are just the opposite of one regulated by feedback inhibition (flux-control by supply and homeostatic concentration maintenance by demand), feedforward regulation faces a particular problem that needs to be overcome, and which does not arise in feedback systems. Similar to feedback, a feedforward loop can only work if the allosteric enzyme controls the flux local to the demand block for the regulatory metabolite. This is automatically satisfied if the allosteric enzyme is saturated with its substrate(s). However, under these conditions the so-called K-effect (the increase in substrate binding affinity by the allosteric activator) is abolished and the feedforward loop does nothing. Only so-called V-effects (the increase in the limiting rate V_f by the allosteric activator) can function under such conditions. A major part of our analysis of feedforward systems was to find conditions where the allosterically regulated enzyme can

still control its local flux without being saturated with its substrate(s).

Chapter 2 provides the necessary background in kinetic modelling of metabolic pathways, enzyme kinetics of allosteric enzymes, metabolic control analysis and supply-demand analysis. A supply-demand analysis of a typical feedback-regulated system is also provided.

In Chapter 3 a few selected examples of feedforward activated enzymes are discussed, focussing on their classification into the two major mechanistic classes, namely K-enzymes, for which the allosteric activator acts by increasing the affinity for the enzyme substrate (specific activation), and V-enzymes, for which the allosteric activator acts by increasing the limiting rate of the enzyme (catalytic activation).

In Chapter 4 feedforward activation is then studied by means of metabolic control analysis and supply-demand analysis, supplemented with a kinetic model of feedforward regulation system that was used to provide computational data for a graphical analysis of the theoretical concepts.

Chapter 5 considers a particular allosteric enzyme, lactate dehydrogenase (LDH) in glucose fermentation metabolism in *Lactococcus lactis*, which is activated through feedforward action by fructose-1,6-bisphosphate (FBP). The rate equation for LDH of an existing kinetic model of this metabolic system [17, 18] is modified to account for potentially important allosteric effects described in the literature but not incorporated into the original LDH rate equation. Models with the original and the new LDH rate equations are compared and the observed differences analysed by a series of 'what-if' experiments with different forms of the new LDH equation.

Chapter 6 is a general discussion of the results generated in the study described in this thesis.

Chapter 2

Background

This chapter summarises the concepts of metabolic systems, kinetic modelling, enzyme kinetics, metabolic control analysis and supply-demand analysis necessary for the study of feedforward regulation of metabolic pathways developed in this thesis.

2.1 Metabolic systems

Cells are complex systems that sustain life through encoding and executing the many functions necessary to grow, reproduce, maintain their structures and respond to their environments. Metabolism is the entire network of chemical reactions occurring in cells. These chemical reactions are organised into metabolic pathways of which the intrinsic properties have been moulded by evolution to fulfil specific functions essential to life.

A metabolic system is defined as an open network of enzyme-catalysed reactions linked by common intermediates, the product of one reaction being the substrate for the next reaction. Metabolic systems include membrane transport steps because the network spreads across membrane-bounded compartments [19]. Metabolic maps describe the topological structure of a metabolic network in terms of the stoichiometry of the individual reactions. Communication between reactions is through mass action by reactants and products, and through regulatory feedforward and feedback loops where a me-

tabolite affects the rate of a reaction for which it is neither a substrate nor a product.

Reaction networks can exist in one of three possible states. The first state is **equilibrium**. Here the chemical species do not vary over time and the individual reaction rates are zero. Since this state can only be reached in closed systems, it holds little interest for open metabolic systems.

The second possible state is **steady state**. Metabolic systems are open systems through which a flow of mass occurs. Source reactions 'push' and sink reactions 'pull' the system from the outside, ensuring that the metabolic state approaches steady state. The net rate of change of the metabolic pools are zero, but the individual reaction rates are not zero ensuring a constant flux of matter through the system. In a non-growing system the net import of mass into the system equals the net export per unit time. In a steady-state growing system mass will accumulate in the system, but the metabolite concentrations and the flux per unit volume will remain constant.

Steady states are stable in various ways and to various degrees. An asymptotically stable steady-states is a unique state for a particular set of parameters and is reached irrespective of the initial concentrations of the variable metabolites. Such a state can be a point attractor or an oscillating limit cycle. A dynamically stable steady-state relaxed back into the same steady-state after perturbation in the concentration of any one of the variable metabolites. A structurally stable state relaxed to a closely-neighbouring steady state after a perturbation in one of the parameters of the system.

Finally, a **transient state** is where a metabolic system is moving from one steady state to another or back to the original steady state after a perturbation in a parameter or fluctuation in internal metabolites.

2.2 The kinetic model in steady state

One of the aims of computational systems biology is to build kinetic models of cellular pathways. The components of the pathway (enzymes) are quantitatively described by mathematical rate laws, each of which describes the rate, v, of an enzyme-catalysed reaction. Well-known examples of such

rate laws include the Michaelis-Menten [36], Hill [20] and Monod-Wyman-Changeux [37] equations. Though there is a linear relationship between enzyme rate, v, and enzyme concentration, the rate laws are non-linear functions of substrate, product and allosteric modifier concentrations and include phenomenological constants such as k_{cat}, K_{eq} and K_{M}.

To describe the rates at which the metabolite concentrations in the system change we consider a system consisting of n steps converting m metabolites. S_i represents any enzymatic intermediates, metabolite pools or groups of metabolite pools with concentration s_i, where i is a counter for 1 to m metabolites. The rate of any functional step, which can be elementary, translocator, non-catalysed or group of reactions is denoted by v_j. The stoichiometric coefficient c_{ij} describes the stoichiometry by which metabolite S_i participates in step j, where j is a counter for the 1 to n steps. The rate at which S_j changes is

$$\frac{ds_i}{dt} = c_{i1}v_1 + c_{i2}v_2 + c_{i3}v_3 + ... + c_{i(n-1)}v_{n-1} + c_{in}v_n \tag{2.1}$$

or, using summation notation,

$$\frac{ds_i}{dt} = \sum_{j=1}^{n} c_{ij}v_j \qquad \text{for } i = 1, \ldots, m \tag{2.2}$$

For the construction of the model all external metabolites that are only produced or consumed and all external effectors are fixed at a specific concentration. The internal metabolites are the variables of the system. For a kinetic model in *steady state* the total rate of production for each variable is equal to the rate of consumption of that variable, so that $ds_i/dt = 0$. For the whole system

$$\sum_{j=1}^{n} c_{ij}J_j = 0 \qquad \text{for } i = 1, \ldots, m \tag{2.3}$$

The symbol J represents a steady state reaction rate and is called a *flux*. Note that although the balance equations are linear functions of reaction rates the individual reaction rates are non linear functions of metabolite concentrations and system parameters.

2.3 Metabolic regulation

Metabolism is highly regulated. Mass action is considered the basic driving force for self-organization [19]. Thus, one way of defining metabolic regulation is the alteration of reaction properties to counteract or augment the mass-action trend in metabolic systems [19]. This can be achieved through a multitude of regulatory mechanisms such as allosteric feedforward activation or end-product inhibition, covalent modification cycles, induction and repression of enzyme synthesis, etc. The focus of this study is allosteric feedforward activation of enzymes.

To begin to understand metabolic regulation it is essential to know the function of a metabolic pathway. Enzymes are essential to metabolism and function on different levels. First and foremost enzymes catalyse reactions, i.e., increase their reaction rate. On a systemic level enzymes perform higher level functions, namely determining (i) the steady state, (ii) the control of steady-state fluxes and concentrations, (iii) structural and dynamic stability, i.e., the response to perturbations in system parameters and system variables respectively, (iv) the transition time from one steady state to another and (v) the dynamic form of the transient or steady state (point, monotonic, oscillatory, trigger or chaotic) [23].

Enzymes regulate metabolic pathways by responding to signals that originate from inside or outside the cell. These responses range from fine-tuning to drastic reorganisation of metabolic processes that control the synthesis and degradation of biomolecules and the generation or consumption of energy. The response time can vary from milliseconds to hours or longer and the control processes can affect more than one pathway.

Regulation is achieved on two levels. The first level involves the evolution of enzymes with high catalytic and binding specificity, the ability of enzymes to alter activity, concentration and binding properties and the evolution of allosteric and other signals. The second level involves the evolution of network structures such as moiety-conserved cycles and auto-catalytic cycles [19].

The regulation of metabolic enzymes play a crucial role in the mainte-

nance of metabolic homeostasis. For a metabolic system to be effectively regulated the concentrations of major metabolites need to be maintained within a small concentration range while reaction rates must be able to change sensitively in response to small changes in metabolite concentration. One of the ways of achieving this sensitivity is through cooperative binding of substrates, products and modifiers to the regulated enzyme [11].

Enzymes that exhibit cooperative kinetics have multiple binding sites for substrates and the binding of one substrate molecule changes the affinity of the other binding sites. With positive cooperativity the affinity for substrate is increased and with negative cooperativity binding affinity is decreased. The plot of reaction rate against substrate concentration has a sigmoidal shape which is quite different from the rectangular hyperbola obtained from the Michaelis-Menten equation. The steepest part of the curve, which represents the maximum activation for those conditions, is typically at a concentration in the physiological range of the particular metabolite. Enzymes following Michaelis-Menten kinetics require an 81-fold increase in substrate concentration to increase the nett rate from $0.1V_f$ to $0.9V_f$ ('switch on'), whereas enzymes following cooperative Hill kinetics only need a 9-fold increase in substrate concentration to achieve the same effect (for a Hill coefficient of 2). The Hill equation will be discussed in some detail in section 2.4). Thus, cooperative enzymes are sensitive to small changes in substrate concentration and a high degree of precision is essential in the regulation of these enzymes [54].

Many regulated enzymes have evolved sites for effector binding which are separate from the catalytic sites. These are allosteric enzymes. Allosteric regulation is the regulation of the activity of an enzyme through the binding of an effector molecule at the allosteric binding site. Allosteric activators enhance the activity of the enzyme, whereas allosteric inhibitors decrease the activity of the enzyme. Allosteric regulation can be homotropic, i.e., the substrate and the allosteric effector are both the same molecule (cooperative binding) or heterotropic where the substrate and the effector molecules are different.

Allosteric regulation occurs throughout metabolism. The most common

type is feedback inhibition, while feedforward activation is relatively rare. With feedback inhibition the product of a metabolic pathway (usually the final product) controls the rate at which it is synthesised by inhibiting an earlier step in the pathway, normally the first reaction that is unique to the pathway (committed step). With feedforward activation a metabolite early in a metabolic pathway activates an enzyme that catalysis a reaction further along the pathway.

2.4 Two classes of allosteric enzymes

Allosteric enzymes alter reaction properties by changing catalytic and or binding properties of enzymes [23]. We distinguish between two classes of allosteric enzymes. These enzymes are classed according to the effect the allosteric effector has on the binding properties (the half-saturating concentration, e.g., $s_{0.5}$) and/or the catalytic properties (the limiting velocity, V_f) of the enzyme. When referring to cooperative enzymes, the terminology $s_{0.5}$ is used instead of K_M; $s_{0.5}$ is the concentration of the substrate S required to saturate the enzyme by 50% in the absence of other species that can bind to the enzyme. Similarly, $p_{0.5}$ and $x_{0.5}$ refer to the half-saturating concentrations of product P and allosteric modifier X.

With a **K-enzyme** the binding of modifier changes the binding affinity of the enzyme for its substrates and products, but not its maximum velocity V_f. With a **V-enzyme** the binding of modifier changes the maximal velocity, V_f, of the reaction, but it does not affect the half-saturating concentrations of its substrates and products. For **Mixed V-K enzymes** the modifier affects both the binding of substrates and products and the V_f.

Two mechanistic models for describing the kinetic behaviour of cooperative enzymes with allosteric modifiers will be discussed, namely the reversible Hill model developed by Hofmeyr and Cornish-Bowden [20] and the concerted model of Monod, Wyman and Changeux (MWC model) [37].

The reversible Hill equation

The rate laws used in kinetic models of metabolic systems need to describe the kinetics of an enzyme within the context of the system where the enzyme functions. Hofmeyr and Cornish-Bowden [20]'s reversible Hill equation can be considered as a universal rate equation for systems biology because it describes (i) the kinetic properties of reactions catalysed by enzymes, (ii) reversible reactions in a thermodynamically consistent way, and (iii) enzyme regulation through allosteric modification by effectors, both of binding and catalysis (the latter through a modification made by Westermark *et al.* [65]), so that both K and/or V-enzymes can be modelled with the reversible Hill equation. In addition, substrate/modifier saturation, which will be discussed further on, is accounted for by the Hill equation.

We consider the case where an allosteric, cooperative enzyme E, with substrate S and product P, is modified by effector X. The reversible Hill equation describes the rate v of enzyme E as:

$$v = V_{\mathrm{f}} \cdot \frac{1 + \gamma\alpha\xi^h}{1 + \alpha\xi^h} \cdot \frac{\sigma(\sigma + \pi)^{h-1}}{(\sigma + \pi)^h + \dfrac{1 + \xi^h}{1 + \alpha\xi^h}} \left(1 - \frac{p/s}{K_{\mathrm{eq}}}\right) \tag{2.4}$$

with

- h, Hill coefficient
- α, strength of modifier effect on substrate/product binding
- γ, strength of modifier effect on catalysis, V_{f} and V_{r}
- $s_{0.5}$, $p_{0.5}$ and $x_{0.5}$, half-saturating concentrations
- $\sigma = \dfrac{s}{s_{0.5}}$, $\pi = \dfrac{p}{p_{0.5}}$ and $\xi = \dfrac{x}{x_{0.5}}$, where s, p and x denote the concentrations of the respective metabolites.

In the absence of product P the Hill-equation reduces to the irreversible form:

$$v = V_{\mathrm{f}} \cdot \frac{1 + \gamma\alpha\xi^h}{1 + \alpha\xi^h} \cdot \frac{\sigma^h}{\sigma^h + \dfrac{1 + \xi^h}{1 + \alpha\xi^h}} \tag{2.5}$$

The degree of cooperativity in the binding of S, P and X is determined by the Hill coefficient, h. In eqn. 2.4 h is the same for the substrate, product and modifier. Whereas microscopic reversibility in the reversible enzyme mechanism requires the Hill coefficient of the substrate and product to be the same, that of the modifier need not be. To model non-cooperative enzymes the Hill-coefficient is set to one.

In order to demonstrate the empirical meaning of h, $x_{0.5}$, α, γ, and s in the Hill equation, we consider their effects in both K and V-enzymes (Fig. 2.2). Because this thesis is mainly concerned with allosteric activation we portray the effects on the rate of changes of a positive modifier, which implies that $\alpha > 1$ (for K-enzymes) $\gamma > 1$ (for V-enzymes). For values of $\alpha < 1$ or $\gamma < 1$ the modifier would act as an allosteric inhibitor of K-enzymes and V-enzymes respectively. For simplicity's sake, the irreversible form of the Hill equation (eqn. 2.5) is considered by setting the product concentration p to zero.

The simplest effect is that of changes in the limiting rate V_f. Increasing V_f increases the total capacity of the enzyme, moving the entire curve up as shown on Fig. 2.1.

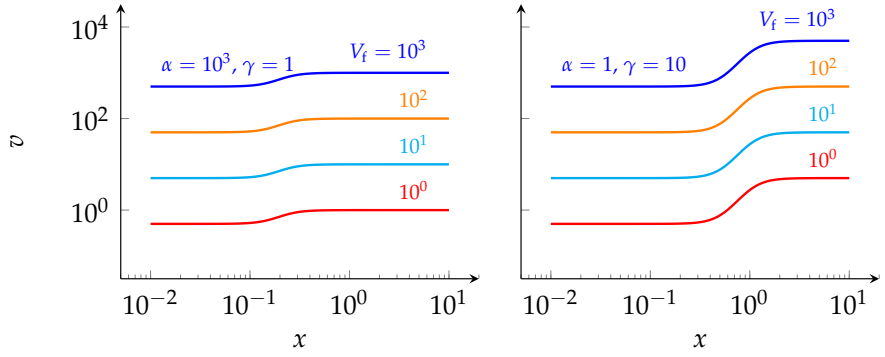

Figure 2.1: The effect of changing the value of V_f of the irreversible Hill-equation 2.5 on the rate of K-enzymes (left) and V-enzymes (right) . The parameter values are: $s = s_{0.5} = x_{0.5} = 1$, $h = 4$, $p = 0$.

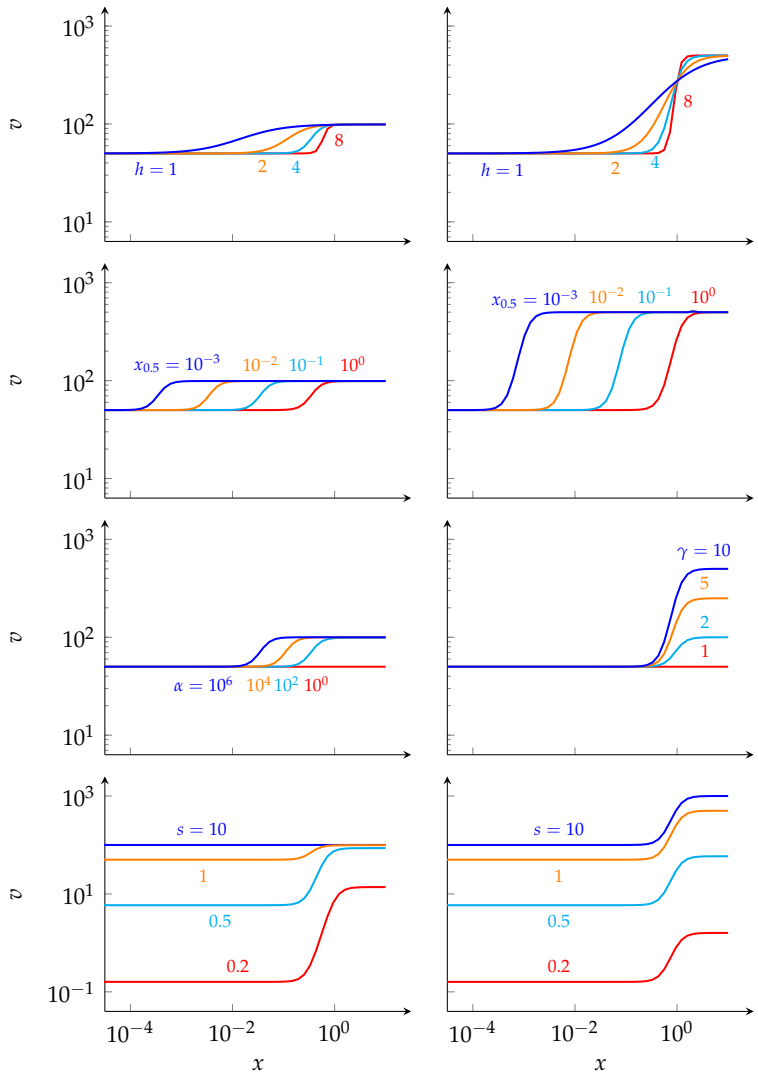

Figure 2.2: The effect of changing the values of parameters of the irreversible Hill-equation 2.5 on the rate of K-enzymes (left) and V-enzymes (right). The parameter values are: $V_f = 100$, $s = s_{0.5} = x_{0.5} = 1$, $h = 4$, $p = 0$. For the K-enzyme $\alpha = 10^3$ and $\gamma = 1$, while for the V-enzyme $\alpha = 1$ and $\gamma = 10$.

The Hill equation for K-enzymes

For a K-enzyme, where the allosteric modifier acts by affecting only the binding of substrate/product, i.e., when $\gamma = 1$, the reversible Hill-equation reduces to:

$$v = V_f \cdot \frac{\sigma(\sigma+\pi)^{h-1}}{(\sigma+\pi)^h + \frac{1+\xi^h}{1+\alpha\xi^h}} \left(1 - \frac{p/s}{K_{eq}}\right) \tag{2.6}$$

As h increases the degree of cooperativity increases and with that the steepness Sensitivity) of the response of v to the concentration of X (and, of course, S and P; not shown). A decrease in $x_{0.5}$ shifts the rate vs. x curve to the left, lowering the concentration range in which the rate responds to X. The the modifier strength α has an effect similar to that of $x_{0.5}$: the larger the value α, the lower the concentration range in which the rate responds to X.

An important feature of K-enzymes is that of abolishment of the modifier effect as the enzyme approaches saturation by substrate. This implies that allosteric modification of K-enzymes can only occur at non-saturating substrate concentrations. This property will play a crucial role in our subsequent analysis of metabolic regulation through feedforward activation.

The Hill equation for V-enzymes

For V-enzymes a distinction is made between enzymes with an absolute requirement for the activator, i.e., no enzyme activity in the absence of activator and enzymes that are active in the absence of activator. In both cases the enzyme rate is multiplied by a factor representing the V effect. For an enzyme with an absolute requirement for the activator the rate varies between zero and V_f, whereas for enzymes without the absolute requirement V_f is increased from its value in the absence of activator by the factor representing the V effect.

When the allosteric modifier acts by affecting only catalysis (V_f and V_r), i.e., when $\alpha = 1$, the reversible Hill-equation for a V-enzyme with no absolute requirement for modifier 2.4 reduces to:

$$v = V_f \cdot \frac{1+\gamma\xi^h}{1+\xi^h} \cdot \frac{(\sigma+\pi)^h}{(\sigma+\pi)^h + 1} \left(1 - \frac{p/s}{K_{eq}}\right) \tag{2.7}$$

Here γ represents the modifier strength. Increasing γ increases the maximum forward rate by increasing the plateau of maximum activation of the enzyme (see Fig. 2.2). When $\gamma = 1$ there is no activation. The other parameters act as they did for K-enzymes, except for the important difference that substrate saturation does not abolish the effect of the modifier, as it did with K-enzyme. In fact, it has not effect whatsoever, and this fact will become a crucial part of our argument in Chapter 4 that V-enzymes are more effective targets for feedforward regulation than K-enzymes.

The rate equation for a V-enzyme with an absolute requirement for activator is:

$$v = V_f \cdot \frac{\xi^h}{1+\xi^h} \cdot \frac{(\sigma+\pi)^h}{(\sigma+\pi)^h+1}\left(1-\frac{p/s}{K_{eq}}\right) \tag{2.8}$$

Here the multiplier term varies from 0 (in the absence of X) to 1 (at $\xi \gg 1$).

In the analysis of feedforward regulation in Chapter 4 we us the Hill equation 2.7 as representative of V-enzymes, while in Chapter 5 we use the Hill equation 2.8.

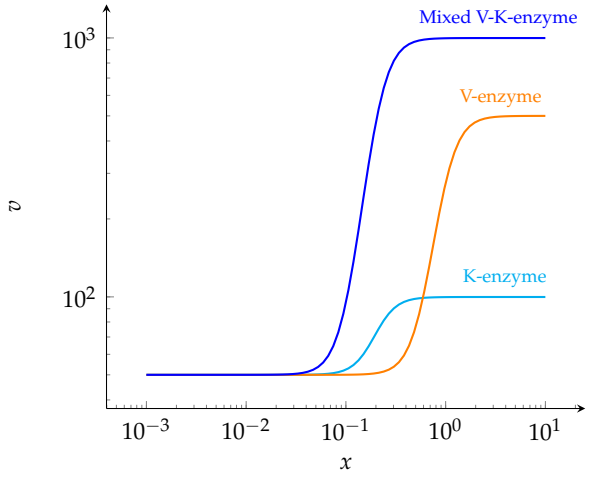

Figure 2.3: Comparing the effect of activator X on the rate of a K-enzyme (eqn. 2.6), a V-enzyme (eqn. 2.7), and a mixed V-K-enzyme (eqn. 2.4). All the parameters are kept constant except α and γ. For the K-enzyme $\alpha = 10^3$, for the V-enzyme $\gamma = 10$, and for the mixed V-K-enzyme $\alpha = 10^3$ and $\gamma = 10$. Other parameter values are: $s = s_{0.5} = x_{0.5} = 1$, $p = 0$, $h = 4$, $V_f = 10^2$.

Fig. 2.3 compares the effect of X on the rate of a K-enzyme, a V-enzyme, and a mixed V-K-enzyme. The effect of α on the K-enzyme is to increase the affinity of the enzyme to X, while the effect of γ on the V-enzyme is to increase the V_f by a factor of 10 (in this case). Note that the actual rate is $0.5V_f$ because $\sigma = 1$. In the mixed V-K-enzyme the α-term enhances the effect of γ so that the actual enhanced $V_f = 10^3$ is reached. To understand why this is so consider that at the high $\alpha = 10^3$ the α-containing denominator term in eqn. 2.5 tends to zero, and the α-containing term tends to 1.

The reversible Monod-Wyman-Changeux equation

The rate law commonly employed to model cooperative, allosteric enzymes is the Monod-Wyman-Changeux rate equation [37]. For computational systems biology the more useful form is that derived by Popova and Sel'kov [49, 50, 51, 52] for reversible multi-substrate, multi-product reactions. We consider the case where an MWC enzyme E with substrate S and product P, is modified by effector X.

The MWC model is based on the following assumptions [11]:

- A subunit of the enzyme can exist is one of two conformational states, R and T.
- All subunits of a particular enzyme molecule must be in the same conformational state, i.e., for a dimeric protein the only allowed conformational states are RR and TT; RT does not exist.
- In the absence of any binding to a ligand, i.e., for the free forms of the enzyme R_0 and T_0, the two states of the enzyme are in equilibrium with an equilibrium constant $L_0 = \dfrac{T_0}{R_0}$.
- Any ligand can bind to the R or T state, but the dissociation constant for the two states are different. For each subunit in the R conformation the dissociation constant $K_{s[R]} = \dfrac{[R][S]}{[RS]}$ similarly for each ligand binding to

the T conformation the dissociation constant $K_{s[T]} = \frac{[T][S]}{[TS]}$. The ratio of $\frac{K_{s[R]}}{K_{s[T]}}$ is often written as c.

The shape of the saturation curve is determined by the values of n, L and $K_{s[R]}/K_{s[T]}$. If $n = 1$ there is only one binding site per molecule and no cooperativity is possible. If $L = 0$ only the R-form of the enzyme exists. Simplification again yields an equation independent of n. Similarly, if $L \to \infty$ only the T-form of the enzyme exists and no cooperativity is observed. For cooperativity to be possible it thus is essential for both the R and T forms to exist. In addition the R and T also need to be functionally different, i.e., $K_R \neq K_T$ to exhibit cooperative behaviour [11].

Monod , Wyman and Changeux describe *heterotropic effects* as the interaction between different ligands such as substrates and allosteric effectors. If the allosteric effector binds preferentially to R but at a different site as the substrate, the fraction of the enzyme in the R-state will increase and the effector therefore acts as a positive allosteric effector (activator). Similarly, a ligand which binds preferentially to the T-state will decrease the binding of substrate by decreasing the fraction of the molecule in the R-state and therefore act as an negative allosteric effector (inhibitor) [11].

The rate v of the enzyme, E, modelled with the MWC-equation as generalised by Popova and Sel'kov is [25]:

$$v = V_{f[R]}\sigma \cdot \frac{(1+\sigma+\pi)^{n-1} + aL(1+c_s\sigma+c_p\pi)^{n-1}}{(1+\sigma+\pi)^n + L(1+c_s\sigma+c_p\pi)^n}\left(1 - \frac{\Gamma}{K_{\text{eq}}}\right) \tag{2.9}$$

where

- $\sigma = \frac{s}{K_{s[R]}}$ and $\pi = \frac{p}{K_{p[R]}}$, where s and p symbolise the concentrations of S and P
- L is the allosteric constant and incorporates the modifier effect (see below)
- n = number of subunits (each with one active site)

- $K_{s[R]}$, $K_{p[R]}$ and $K_{x[R]}$ are the intrinsic dissociation constants for the complexes of S, P and X for the R-form of the enzyme
- $K_{s[T]}$, $K_{p[T]}$ and $K_{x[T]}$ are the intrinsic dissociation constants for the complexes of S, P and X for the T-form of the enzyme
- $c_s = \dfrac{K_{s[R]}}{K_{s[T]}}$, and $c_p = \dfrac{K_{p[R]}}{K_{p[T]}}$ describe the relative binding to the R and T forms
- $a = \dfrac{V_{f[T]}}{K_{s[T]}} / \dfrac{V_{f[R]}}{K_{s[R]}}$, where $V_{f[T]}$ and $V_{f[R]}$ are the respective forward limiting rates for the R and T forms

If the R and T-forms have different affinities for the ligand and the R-form catalyses the reaction at a higher rate than the T-form, this rate equation describes a mixed V-K enzyme for which allosteric effectors have both catalytic and binding effects.

Allosteric modifiers affect the binding of substrates, products and other modifiers by decreasing or increasing L, as follows:

$$L = L_0 \frac{(1+\xi_T)^n}{(1+\xi_R)^n} = L_0 \frac{(1+c_x\xi_R)^n}{(1+\xi_R)^n} = L_0 \frac{(1+\xi_T)^n}{(1+c'_x\xi_T)^n} \tag{2.10}$$

where x is the allosteric modifier and $c_x = K_{x[R]}/K_{x[T]}$ and $c'_x = K_{x[T]}/K_{x[R]}$.

An allosteric activator binds with a higher affinity to the R-form than to the T-form, thereby stabilising the R-form and decreasing L. If $c_x = 0$ the effector binds exclusively to the R-form and L reduces to

$$L = \frac{L_0}{(1+\xi_R)^n} = \frac{L_0}{(1+c'_x\xi_T)^n} \tag{2.11}$$

An allosteric inhibitor binds with a higher affinity to the T-form than to the R-form, thereby stabilising the T-form and increasing L. If $c'_x = 0$ the effector binds exclusively to the R-form and L reduces to

$$L = L_0 (1+\xi_T)^n = L_0 (1+c_x\xi_R)^n \tag{2.12}$$

The MWC-equation for K-enzymes

If it is assumed that S and P bind only to the R state, i.e., that $c_s = c_p = 0$, and that $V_{f[T]} = 0$, i.e., that $a = 0$, then eqn. 2.9 reduces to

$$v = V_{f[R]}\sigma \cdot \frac{(1+\sigma+\pi)^{n-1}}{(1+\sigma+\pi)^n + L}\left(1 - \frac{\Gamma}{K_{\text{eq}}}\right) \tag{2.13}$$

which is structurally analogous to the reversible Hill eqn. 2.6 for K-enzymes.

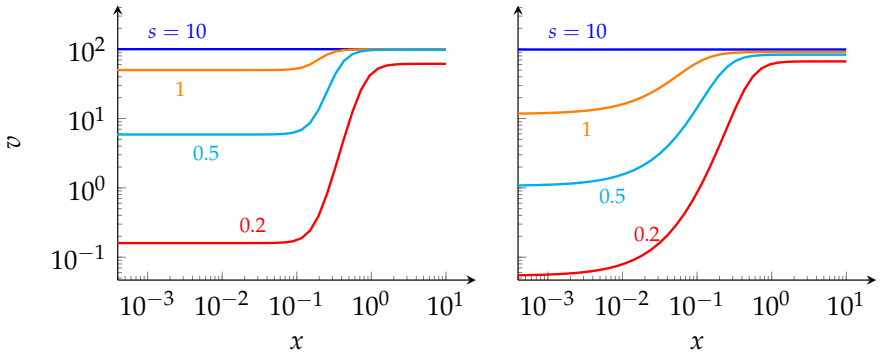

Figure 2.4: Comparison of the Hill-eqn. 2.6 and MWC-eqn. 2.13 with respect to saturation of the activator effect by increasing substrate concentration. For both enzymes $V_{\text{f}} = 100$ and $p = 0$. For the Hill equation $s = s_{0.5} = x_{0.5} = 1$, $\gamma = 1$, $\alpha = 10^3$, $h = 4$. For the MWC equation $K_{\text{s[R]}} = K_{\text{s[X]}} = 0.1$, $L_0 = 3.5 \times 10^4$, $n = 4$.

As with the Hill equation, the MWC equation shows the abolishment of the effect of the modifier as the enzyme saturates with substrate, Fig. 2.4.

The MWC-equation for V-enzymes

If it is assumed that substrates and products have equal affinities for both the R- and T-forms, but the reaction catalysed by the R-form is faster than that of the T-form, the MWC equation reduces to a form that describes a V-enzyme [25]:

$$v = V_{f[R]} \cdot \frac{1+aL}{1+L} \cdot \frac{\sigma}{1+\sigma+\pi}\left(1 - \frac{\Gamma}{K_{\text{eq}}}\right) \tag{2.14}$$

As with the V-enzyme form of the Hill-equation, the binding of substrates and products are unaffected by allosteric modifiers. Only the limiting rate V_{f}

is affected by the term $(1 + aL)(1 + L)$. In the absence of modifier and at saturating substrate concentrations the rate tends to the limiting rate V_f, so that this form of the rate equation is for a MWC V-enzyme that is active in the absence of modifier.

Although both the Hill and MWC equations described above can be used interchangeably in kinetic models, the Hill equation has the advantage that it is much less complicated and its parameters can be determined experimentally and have empirical meanings. The 13 MWC parameters all have clear mechanistic interpretations, but are difficult to relate to experimentally observable properties [20]. In the remainder of this thesis we shall only use forms of the reversible Hill equation.

2.5 Metabolic control analysis

Metabolic control analysis (MCA) originated from the work of Kacser and Burns [30] and Heinrich and Rapoport [16]. MCA can be used to understand and explain the relationship between the steady-state properties of the network as a whole and the properties of the individual reactions of that system. The steady state is determined by the parameters of the system, which describe the nature, kinetics and activities of the individual enzymes, temperature and the concentration of external effector molecules. For a given set of parameters there is usually a unique steady state. The concentrations and rates of the internal reactions (variables of the system) characterise the steady state. Metabolites directly affect enzyme rates as substrates and products and indirectly by longer range interactions such as allosteric effects which are transmitted via feedback and feedforward loops.

Metabolic interactions can be grouped according to the time-scale on which they operate. Broadly speaking, three time scales can be distinguished. Very rapid reactions usually reach equilibrium within milliseconds and are often considered as frozen. In the intermediate time scale metabolic interactions happen within seconds to minutes. This metabolic time-scale is applicable to the behaviour and control of intermediate metabolism where we observe changes in enzyme rate and metabolite concentrations. The third time scale

stretches over hours to days and involves changes in the parameters that are regarded as constant in the intermediate time-scale; the rate of synthesis and degradation of enzymes and conserved moieties typically fall in this slow time scale.

Within the metabolic time scale certain quantities can be regarded as constant parameters of the system. They include environmental factors such as temperature and, in a well buffered system, pH. Besides these, the following quantities are regarded as constant in the metabolic time scale:

- The concentrations of enzymes, translocators and moieties in cofactors. These chemical species are synthesised and degraded very slowly relative to the metabolic time scale.
- The concentration of the initial substrates, final products and external effectors such as inhibitors, activators and hormones. We consider these metabolites to be buffered by the environment, thereby creating an open system which can approach a steady state.
- Equilibrium constants, K_{eq}, and enzymatic constants such as k_{cat}, K_M and K_i.

The variables of the metabolic system are determined by the parameters of the system, the stoichiometry and the rate function of each reaction. These are:

- Fluxes
- Metabolite concentrations
- Gibbs-energy changes, chemical and membrane potentials, mole fractions and ratios of concentrations. These quantities are all functions of metabolite concentrations.

The degree of control that a single reaction or a block of reactions (reaction blocks will be discussed in section 2.6) has over a steady-state flux or metabolite concentration is quantified by a control coefficient. A control coefficient

is defined as:

$$C^{y}_{v_i} = \frac{\partial \ln y}{\partial \ln v_i} \tag{2.15}$$

where y is a steady-state flux J or metabolite concentration s_j. Operationally, a control coefficient is the percentage change in y in response to a one percent change in enzyme activity, v_{i}.

An elasticity coefficient is a local enzyme property and is defined as

$$\varepsilon^{v_i}_{s_j} = \frac{\partial \ln v_i}{\partial \ln s_j} \tag{2.16}$$

where S_j is a metabolite or parameter that has a direct effect on the enzyme (for the purposes of this study S_j would be a substrate, product or allosteric modifier of enzyme i).

The theory of MCA is built upon a set of relationships between flux-control coefficients and elasticity coefficients called partitioned response, summation and connectivity theorems. Together these theorems allow control coefficients to be expressed as functions of elasticity coefficients, thereby allowing systemic properties to be understood in terms of local enzyme properties (see, for example, section 2.6).

The effect of an system parameter p on a steady-state variable is quantified by a response coefficient, defined as:

$$R^{y}_{p} = \frac{\partial \ln y}{\partial \ln p} \tag{2.17}$$

where y is a steady-state flux J or metabolite concentration s_j.

The partitioned response property described a fundamental relationship between a response, a control and an elasticity coefficient:

$$R^{y}_{p} = C^{y}_{v_i} \varepsilon^{v_i}_{p} \tag{2.18}$$

where y is a steady-state flux J or metabolite concentration s_j and p a parameter that affects enzyme i directly. Operationally, a response coefficient can understood as a combination of the direct effect of the parameter on enzyme i

(a local change in v_i quantified by the elasticity coeffient), followed by the effect of the change in v_i on the steady-state variable y (a systemic change in y quantified by the control coefficient).

If p interacts with more than one enzyme the partitioned response property is expressed as the sum of all the terms contributing to the response:

$$R_p^y = \sum_i C_{v_i}^y \varepsilon_p^{v_i} \tag{2.19}$$

The combined response equation shows how changes in an external regulator must be mediated by the enzymes (regulatory enzymes) which are directly affected by the regulator. Thus the response of the system depends on the ability of these enzymes to transmit the changes caused by the external regulator and to what extent the enzyme can be regulated by the regulator [22].

2.6 Supply-demand analysis

Metabolic supply-demand analysis is a quantitative framework developed by Hofmeyr and Cornish-Bowden [23] to study the regulation of metabolism in terms of a cellular economy. Within the framework of supply-demand analysis metabolic regulation and function are clearly defined. The framework allows the integration of the different parts of metabolism with each other as well as the integration with other intracellular processes.

Cellular metabolism can be divided into supply and demand blocks. These blocks are linked by metabolic products and cofactor cycles. With supply-demand analysis the behaviour, control and regulation of metabolism as a whole can be determined quantitatively because control can be expressed in terms of supply and demand elasticities. The elasticity for the supply and demand blocks can be measured experimentally.

To understand the function of a metabolic network it is essential to understand the organisation of the metabolic network. Metabolism is organised into a catabolic block which provides phosphorylation and reducing power and carbon skeletons, a biosynthetic block which provide building blocks

for macromolecular synthesis and an anabolic ('growth') block which maintains the cellular structure, genes and enzymes. These blocks are coupled either by a common intermediate such as a amino acid or nucleotide or by a pair of common intermediates that form a moiety-conserved cycle such as NAD(P)H-NAD(P), ATP-ADP or ATP-ADP-AMP. The sum of concentrations of moiety-conserved members remains constant [23].

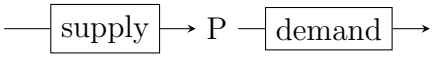

Figure 2.5: A metabolic pathway divided into a supply block that produces the product P, and a demand block that consumes P.

In a system consisting of a biosynthetic supply block that produces a product P and a demand block which consumes P, where P is the only link between the blocks, the flux control coefficients for the supply and demand block can be expressed in terms of the supply and demand elasticities using the connectivity and summation theorem of control analysis [22, 23]. The supply and demand flux-control coefficients are:

$$C^J_{\text{supply}} = \frac{\varepsilon_p^{v_{\text{demand}}}}{\varepsilon_p^{v_{\text{demand}}} - \varepsilon_p^{v_{\text{supply}}}} \quad \text{and} \quad C^J_{\text{demand}} = \frac{-\varepsilon_p^{v_{\text{supply}}}}{\varepsilon_p^{v_{\text{demand}}} - \varepsilon_p^{v_{\text{supply}}}} \tag{2.20}$$

It follows that:

$$C^J_{\text{demand}} / C^J_{\text{supply}} = -\varepsilon_p^{v_{\text{supply}}} / \varepsilon_p^{v_{\text{demand}}} \tag{2.21}$$

The higher the ratio, the more flux is controlled by the demand block, i.e. $C^J_{\text{demand}} \rightarrow 1$. It should be noted that $\varepsilon_p^{v_{\text{supply}}}$ is a negative quantity because product inhibits the supply [23].

The supply and demand concentration control coefficients can be expressed in terms of the respective block elasticities:

$$C^p_{\text{supply}} = -C^p_{\text{demand}} = \frac{1}{\varepsilon_p^{v_{\text{demand}}} - \varepsilon_p^{v_{\text{supply}}}} \tag{2.22}$$

Whereas the distribution of flux control is determined by the ratio of flux-control coefficients (eqn. 2.21), the the magnitude of the variation in the linking metabolite P is determined by the sum of the elasticities of the respective

blocks, $\varepsilon_p^{v_{\text{demand}}} - \varepsilon_p^{v_{\text{supply}}}$. The higher the sum, the smaller the absolute value of the concentration-control coefficients of the supply and demand blocks, C^p_{supply} and C^p_{demand}, and the better the homeostatic maintenance of P [23].

Supply-demand analysis of feedback inhibition

In order to understand the specific problems with which a regulatory strategy based on feedforward activation has to cope, we contrast it with a typical instance of regulation by feedback inhibition Hofmeyr and Cornish-Bowden [22].

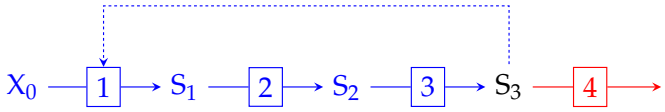

Figure 2.6: A linear metabolic pathway consisting of four sequentially coupled enzymes. The supply block comprises E_1, E_2 and E_3 and the demand block E_4. E_1 is allosterically inhibited by S_3.

To analyse the system the system partitioned into a supply-block consisting of E_1, E_2 and E_3, and a demand-block consisting of E_4. These two blocks communicate via the linking metabolite S_3. A control analysis of the resulting supply-demand system yields:

$$C^J_{v_{123}} = \frac{\varepsilon^{v_4}_{s_3}}{\varepsilon^{v_4}_{s_3} - \varepsilon^{v_{123}}_{s_3}} \quad \text{and} \quad C^J_{v_4} = \frac{-\varepsilon^{v_{123}}_{3}}{\varepsilon^{v_4}_{s_3} - \varepsilon^{v_{123}}_{s_3}} \tag{2.23}$$

$$C^{s_3}_{v_{123}} = -C^{s_3}_{v_4} = \frac{1}{\varepsilon^{v_4}_{s_3} - \varepsilon^{v_{123}}_{s_3}} \tag{2.24}$$

The respective block elasticities $\varepsilon^{v_{123}}_3$ and $\varepsilon^{v_4}_{s_3}$ represent the supply and demand block elasticities [22], which quantify the sensitivities of the conversion block fluxes J_{123} and J_4 to changes in s_3.

From eqn. 2.23 it follows that:

$$\frac{C^J_{v_4}}{C^J_{v_{123}}} = \frac{-\varepsilon^{v_{123}}_{s_3}}{\varepsilon^{v_4}_{s_3}} \tag{2.25}$$

If $-\varepsilon_{s_3}^{v_{123}} \gg \varepsilon_{s_3}^{v_4}$, then $C_{v_4}^{J} \to 1$ and the demand effectively controls the flux. This would be achieved if E_4 is saturated with substrate S_3, so that $\varepsilon_{s_3}^{v_4} \to 0$. Under such conditions eqn. 2.24 reduces to:

$$C_{v_{123}}^{s_3} = -C_{v_4}^{s_3} = \frac{1}{-\varepsilon_{s_3}^{v_{123}}} \tag{2.26}$$

from which it follows that the larger $-\varepsilon_{s_3}^{v_{123}}$ (the absolute value of the supply elasticity), the smaller the concentration-control coefficients and the better the homeostasis in the concentration of S_3.

The supply elasticity, $\varepsilon_{s_3}^{v_{123}}$ can be expressed in terms of the partitioned response equation [22]. S_3 can affect E_1 directly by acting as allosteric inhibitor, or indirectly up the reaction chain via S_2 and S_1:

$$\varepsilon_{s_3}^{v_{123}} = C_{v_1}^{J_{123}} \varepsilon_{s_3}^{v_1} + C_{v_3}^{J_{123}} \varepsilon_{s_3}^{v_3} \tag{2.27}$$

For the feedback loop to determine $\varepsilon_{s_3}^{v_{123}}$, E_1 must control the supply flux, i.e., $C_{v_1}^{J_{123}} = 1$, which implies, according to the flux-summation theorem, that $C_{v_1}^{J_{123}} = 0$ so that $\varepsilon_{s_3}^{v_{123}} = \varepsilon_{s_3}^{v_1}$. The conditions under which this is ensured can be ascertained by expressing $C_{v_1}^{J_{123}}$ and $C_{v_3}^{J_{123}}$ in terms of elasticities:

$$\varepsilon_{s_3}^{v_{123}} = \frac{\varepsilon_{s_1}^{v_2}\varepsilon_{s_2}^{v_3}}{\varepsilon_{s_1}^{v_2}\varepsilon_{s_2}^{v_3} - \varepsilon_{s_1}^{v_1}\varepsilon_{s_2}^{v_3} + \varepsilon_{s_1}^{v_1}\varepsilon_{s_2}^{v_2}} \varepsilon_{s_3}^{v_1} + \frac{\varepsilon_{s_1}^{v_1}\varepsilon_{s_2}^{v_2}}{\varepsilon_{s_1}^{v_2}\varepsilon_{s_2}^{v_3} - \varepsilon_{s_1}^{v_1}\varepsilon_{s_2}^{v_3} + \varepsilon_{s_1}^{v_1}\varepsilon_{s_2}^{v_2}} \varepsilon_{s_3}^{v_3} \tag{2.28}$$

If $\varepsilon_{s_1}^{v_1} = 0$ (a condition easily established in such systems for an enzyme-reaction that is far from equilibrium and insensitive to its product) this expression reduces to

$$\varepsilon_{s_3}^{v_{123}} = \varepsilon_{s_3}^{v_1} \tag{2.29}$$

so that the supply block-elasticity coefficient is the equivalent to the elasticity of E_1 to its allosteric inhibitor S_3. The larger $\varepsilon_{s_3}^{v_1}$ the better the homeostasis of s_3. From our description of the abolishment of modifier effects by substrate saturation it also follows that effective functioning of the feedback loop depends on the supply substrate, X_0, to be buffered at a non-saturating concentration.

The specific problem of feedback regulation alluded to in the opening paragraph of this section thus refers to the conditions necessary to ensure

that the feedback loop functions effectively, which translates to conditions ensuring that the allosteric enzyme controls the flux through the supply block. Here that condition was that $\varepsilon_{s_1}^{v_1} = 0$. In Chapter 4 we shall search for similar conditions for feedforward activation.

Chapter 3

Allosterically activated enzymes: a few examples

In this chapter five representative enzymes regulated via a feedforward mechanism are discussed: lactate dehydrogenase (LDH), pyruvate kinase (PK), acetyl coenzyme-A carboxylase (ACC), glycogen synthase (GS) and sucrose phosphate synthase (SPS). All these enzymes are sensitive to the energy status of the cell since phosphorylation/dephosphorylation or inhibition/activation by inorganic phosphate forms an integral part of their regulation. However, this review specifically focusses on the allosteric regulation of these enzymes and the distinction between K and V-enzymes. Lactate dehydrogenase is discussed in greater depth than the other examples since it is the subject of study in Chapter 5.

3.1 Lactate dehydrogenase

In a reaction common to anaerobic bacteria, yeasts and mammals, the enzyme lactate dehydrogenase (LDH) interconverts pyruvate and lactate using the NADH/NAD^+ pair as a redox cofactor.

$$\text{pyruvate} + \text{NADH} \rightleftharpoons \text{lactate} + \text{NAD}^+ \tag{3.1}$$

Lactate is an important end product of bacterial fermentation of glucose

and certain carbohydrates. Though many species of bacteria form some lactate through heterofermentation, the main genera of bacteria forming lactate through homofermentation are the lactic acid bacteria which convert at least 85% of glucose to lactate. Lactic acid bacteria include *Enterococcus*, *Lactobacillus*, *Lactococcus*, *Leuconostoc*, *Oenococcus*, *Pediococcus*, and *Streptococcus*. The species *Lactococcus lactis*, formerly known as lactic or group N Streptococcus, consists of 3 subspecies: *L. lactis* subsp. *cremoris*, *L. lactis* subsp. *lactis* and *L. lactis* subsp. *hordniae*. Lactic acid bacteria are very diverse and are used in the food industry, are present in human and animal digestive tracts, and some are serious pathogens [64]. Lactic acid bacteria are classified according to the isomer or isomers of lactate formed [14].

LDH is an important enzyme used in industrial processes such as chemical preparation of enantiometrically pure pharmaceutical intermediates and the development of lactate biosensors for monitoring serum lactate levels [2].

Different LDH isoenzymes have been isolated from different prokaryotes and eukaryotes. Lactate dehydrogenases exist in four distinct enzyme classes. Two of these are cytochrome c-dependent enzymes, acting either on D-lactate (EC 1.1.2.4) or L-lactate (EC 1.1.2.3). The other two are NAD(P)-dependent enzymes, acting either on D-lactate (EC 1.1.1.28) or L-lactate (EC 1.1.1.27). In homofermentative lactic acid bacteria pyruvate is reduced to two isomeric forms of lactate by two distinct NAD-dependent, stereospecific lactate dehydrogenases, namely L-lactate dehydrogenase (L-LDH) (EC 1.1.1.27) and D-lactate dehydrogenase (D-LDH) (EC 1.1.1.28). The evolutionary relationship between L-LDH and D-LDH is not fully known. These enzymes have been classified into the L and D-2-hydroxyacid dehydrogenase families. L-LDH enzymes are either allosteric enzymes activated by fructose-1,6-phosphate (FBP) or non allosteric enzymes. All the lactic acid bacteria have cytoplasmic NAD-linked lactate dehydrogenases (nLDH). Both L-nLDHs and D-nLDHs differ in different genera and species. nLDHs are key enzymes in energy production for lactic acid bacteria [14]. Here we focus on the allosterically activated NAD(P)-dependent enzymes. Allosteric L-LDHs have been purified, characterized, and cloned from a variety of eukaryotes and prokaryotes, and their primary and tertiary structures have been exten-

sively studied [56]. nLDHs are also found in non lactic acid bacteria and yeast such as enterobacteria *Staphylococci*, *Clostridium thermohydrosulfuricum* and *Escherichia coli* [14, 38, 62].

Catalytic and substrate binding properties of LDH

In addition to binding substrate and NADH, bacterial lactate dehydrogenases have a third ligand binding site which binds fructose-1,6-bisphosphate (FBP), which is one of the few differences between bacterial and mammalian dehydrogenases. This is a form of prokaryotic regulation which makes the cell sensitive to available levels of glucose [9]. At cellular protein concentration the enzyme is a dimer that has weak substrate affinity. Each subunit of the dimer has a positively charged pocket. Two dimers do not easily combine to form a tetramer because of the repulsion of the positive charges, but in the presence of FBP two dimers are 'stapled' together to form a tetramer. The FBP-tetramer complex has a 50-fold higher substrate affinity than the dimer [9]. The rearrangement of the active site was confirmed by an experiment where LDH was mixed with pyruvate and NADH in one syringe and FBP in another. A lag was observed before a steady state is reached. Premixing the enzyme with FBP abolishes the lag, suggesting that FBP induces a conformational change in the enzyme resulting in increased substrate sensitivity [15].

Regulation

There is great biodiversity amongst lactic acid-producing bacteria which is reflected in the considerable differences with respect to kinetic properties [31].

LDH is allosterically regulated by FBP, tagatose-1,6-bisphosphate (TBP), inorganic phosphate (Pi), ATP, GTP and several other ligands. FBP is generally believed to be the most important allosteric modifier of LDH. Several studies have reported that FBP increases substrate affinity, catalytic rate or both. In some species LDH is inhibited by Pi [12] in other species by ATP [5] and in some species by both [28].

Lactococcus lactis LDH only binds substrate tightly in the presence of FBP. For a comprehensive list of bacterial LDHs activated by FBP see Garvie [14]. Thomas [60] reported that several species of *Lactobacillus* were equally stimulated by FBP and TDP. The lactate dehydrogenases of several species of *Streptococcus* are activated by FBP or TDP and depend on pH [60]. LDHs from *Butiribacterium rettgeri, Escherichia coli* and *Lactobacillus plantarum* are inhibited by ATP, while LDHs from certain fungi are inhibited by GTP [5].

Substrate, product and effector binding

Some of the variations in earlier studies are attributed to different experimental conditions. In most cases the binding of substrate in hyperbolic. However, *Streptococcus mutans* NCTC 10449, *E. coli* and *B. rettgeri* bind pyruvate cooperatively, but not the other substrate, NADH [5]. For the non lactic acid bacterium, *Clostridium thermohydrosulfuricum*, NADH binding is cooperative at lower FBP concentrations [62].

The binding of the allosteric activator, FBP, appears cooperative in most cases. Examples include *L. lactis* where the Hill coefficient varies between 1-7 and 2.1 [12], and *L. faecalis* where the Hill coefficient varies between 1.6 and 2.1 [66]. LDH from some species have an absolute requirement for FBP, others don't.

Enzymes have also been reported where the binding of substrate alters the sensitivity of the enzyme for the activator, FBP. In *Streptococcus mutans* NCTC 10449 the binding of pyruvate alters the affinity of the enzyme for the activator FBP. The K_{FBP} decreases from 8.0 to 3.0mM as the pyruvate concentration increased from 5.0 to 20.0mM

In *Streptococcus mutans* NCTC 10449, which has an absolute requirement for FBP, LDH is activated by FBP and inhibited by ATP. The Hill coefficient for FBP binding is 1.73, which is the same as for *S. faecalis*. Binding of the allosteric effector FBP is cooperative [5]. The binding of the FBP has no effect on the K_{NADH}. ATP is a potent competitive inhibitor of FBP activation. LDH from *L. lactis* is activated by FBP and inhibited competitively by Pi. Substrate binding is not cooperative, but FBP binding appears cooperative with a Hill coefficient of 1.7-2.1 [12]. Pi does not have the same effect on lactococcal

lactate dehydrogenases. *S. faecalis* is not sensitive to phosphate inhibition, but Mn^{2+} increases the enzyme's sensitivity to FBP [12]. In *L. lactis* FBP decreases the K_M for both substrates and increases the V_f. For the non lactic acid bacterium *Clostridium thermohydrosulfuricum* NADH binding is cooperative at lower FBP concentrations [62].

Effect of activator and inhibitors

The binding of activators can increase the enzyme's sensitivity towards its substrate, increase the catalytic rate, or do both. Enzymes of which substrate affinity is increased will be referred to as K-enzymes, and those of which the limiting rate V_f is increased as V-enzymes. Enzymes activated by FBP fall into one or both of these categories, depending on species and strain. In addition to being activated by FBP, LDH is also inhibited by Pi and trinucleotides. Inhibition by both Pi and ATP is competitive as these metabolites compete with FBP and NADH-binding, respectively. A few examples follow:

In *Streptococcus mutans* NCTC 10449 the binding of the pyruvate altered the affinity of the enzyme for the activator FBP. The K_{FBP} decreases from 8.0 to 3.0mM as the pyruvate concentration increases from 5.0 to 20.0 mM. In *Streptococcus cremoris US3* FBP has an effect on both the K_M for NADH and pyruvate and the V_f-values of LDH, which thus appears to be a mixed K and V-enzyme [28]. *L. faecalis* LDH appears to be an example of a pure K-enzyme since activation by FBP decreases the K_M for both pyruvate and NADH [66]. *S. faecalis* LDH is not sensitive to phosphate inhibition and the K_{FBP} of 50μM is high compared to other *streptococcal* species [12]. For *L. lactis* LDH FBP decreases the K_M for both substrates and increases the V_f. The binding of FBP is cooperative and competitive inhibition by Pi is also cooperative [12]. LDH from *Clostridium thermocellum* shows a marked increase in activity in the presence of 1 mM FDP. V_f increased from 87 to 503μmol.min^{-1} and the K_M for pyruvate is decreased from 7.3 to 0.3mM, and thus also appears to be a mixed K and V-enzyme [2]. *Bifidobacterium longum* LDH (BLLDH) is activated by FBP and also appears to be a mixed K and V-enzyme as activation with FBP causes the K_{FBP} to decrease and the V_f to double [57]. In *Clostridium thermohydrosulfuricum* an ethanol and a lactate-producing LDH is present

(LDH_{EtOH} and LDH_{Lac}). LDH_{EtOH} has an almost absolute requirement for FBP. LDH_{Lac},however, only shows activation by FBP at temperatures above 40°C. Both enzymes show marked activation by FBP (22-fold and 5-fold respectively). The temperature optimum for both enzymes is 70°C. LDH_{Lac} is inhibited by Pi,while LDH_{EtOH} is activated by Pi[62]. Increased FBP concentration markedly decreases the K_M for pyruvate for LDH_{EtOH} but only slightly for LDH_{EtOH}. The affinity for NADH is increased for both forms.

The effect of pH and temperature

The activation of LDH by FBP in *L. faecalis* decreases V_f as the pH increases from 5.8 to7.5. Also, the affinity of the enzyme for the activator decreases as the pH increases [66]. Interestingly, the enzyme appears more sensitive to heat upon activation by FBP [66]. FBP activation in *Thermus caldophilus* stabilizes LDH towards heat treatment at 95°C [2].

Other effectors

The addition of 20 to 30 mg of Mg^{2+} increases activity of LDH from *Clostridium thermocellum* by approximately 10%. Also in *Discorea cayenesis* the addition of 1mM Mg^{2+} results in a decrease in K_M-values and an increase in V_f. ATP inhibition as a result of competition with NADH differs depending on the source of the enzyme and the concentration of ATP. At high concentrations of ATP (10mM) enzyme activity is inhibited by 23% [2]. LDHs from a number of microorganisms are subject to negative regulation by trinucleotides.

Why is LDH regulated?

The reason for LDH regulation remains unresolved with different groups giving different explanations. Also, the type of regulation playing the most important role may be strain-dependent, as was shown for the regulation of LDH enzymes of different strains of *L. lactis* [13, 48]. Types of regulation include the NADH/NAD or ATP/ADP ratio, the concentration of FBP or triose phosphate or the levels of PFL or LDH. Regulation of lactate dehydrogenase

activity *in vivo* may ensure homolactic fermentation during anaerobic growth at rapid rates. By ensuring a low intracellular pyruvate concentration other pathways of pyruvate metabolism are not expressed and fermentation is homolactic. Growth conditions resulting in heterolactic fermentation may be achieved by reducing lactate dehydrogenase activity which is accompanied by a drastic decrease in the intracellular concentration of FBP for the streptococci. Examples are the growth of *S. mutans*, *S. bovis* and *Lactobacillus casei* in continuous cultures at high dilution rates with excess glucose, where homolactic fermentation is observed, and at low dilution rates with limiting glucose where heterolactic fermentation is observed [60].

According to Teusink *et al.* [58], lactic acid bacteria are selected for rate and not yield or efficiency. They suggest that the switch between homolactic and heterolactic fermentation is the result of all the different regulatory motifs, i.e., allosteric feedback and feedforward regulation.

Melchiorsen *et al.* [35] suggests that in *L. lactis* altered levels of enzymes competing for pyruvate, i.e., LDH and PFL, seem to regulate the metabolic shift from mixed acid to homolactic fermentation, in addition to allosteric regulation. Regulation by allosteric modulation is more rapid than regulation by altering enzyme levels because the *de novo* synthesis and/or degradation of protein is involved.

The regulation of LDH in yeast is similar to the regulation in lactic acid bacteria where the lack of carbon source causes a metabolic change that leads to the production of formic and acetic acids, ethanol, and in a lower proportion, lactate [38].

Moreno-Sanchez *et al.* [38] showed that glycolysis in *L. lactis* is controlled by the ATP-demand when working below its maximum capacity, and under high-rate conditions, the glucose and lactate transporters exerted the main flux control.

3.2 Acetyl-coenzyme A carboxylase

Acetyl-coenzyme A carboxylase (E.C.6.4.1.2, ACC) catalyses the ATP and biotin-dependent (irreversible) carboxylation of acetyl-CoA to produce malo-

nyl-CoA. This reaction proceeds in two half reactions, a biotin carboxylase (BC) reaction and a carboxyltransferase (CT) reaction.

$$\text{E-Biotin} + \text{ATP} + \text{Mg}^{2+} \rightleftharpoons \text{E-Biotin-CO}_2^- + \text{ADP} + \text{Pi} \tag{3.2}$$

$$\text{E-Biotin-CO}_2^- + \text{acetyl-CoA} = \text{E-Biotin} + \text{malonyl-CoA} \tag{3.3}$$

Acetyl-coenzyme A carboxylase (ACC) plays a critical role in fatty acid metabolism [61]. Malonyl-CoA is a metabolic signal for the control of fatty acid production and utilization in response to dietary changes and altered nutritional requirements. It can therefore be considered to control the switch between carbohydrate and fatty acid utilization in liver and skeletal muscle. ACC-2 deficient mice have drastically reduced levels of malonyl-CoA in their heart and skeletal muscles, resulting in continuous fatty acid oxidation, a reduction in body fat mass and body weight, despite higher consumption of food. ACC is also found in bacteria, plants and yeast. Archae utilise ACCs for CO_2 fixation as these organisms do not use fatty acids in there lipids [61].

The regulation of ACC through short and long term mechanisms plays a key role in the control of the synthesis and oxidation of fatty acids [40]. The activity of mammalian ACC is regulated by a variety of dietary, hormonal and other physiological responses that proceed via allosteric feedforward activation by citrate, allosteric feedback inhibition by long chain fatty acids, reversible phosphorylation and inactivation and modulation of enzyme production through altered gene expression. Long-chain acyl-CoA inhibits ACC by promoting the dissociation of the polymer into protomers [61].

Activation of ACC by citrate is through a citrate-induced conformational change at the active site [59]. Acetyl CoA carboxylases from animal tissues oscillate between catalytically-inactive protomeric and catalytically-active polymeric states. The active form of animal ACC is a linear polymer consisting of 10-20 protomers made up of ACC dimers. The level of carboxylase activity is determined by the position of the protomer-polymer equilibrium. Citrate and isocitrate are capable of shifting this equilibrium in favour of the catalytically-active form. The binding of citrate to ACC1 and ACC2 precedes polymerisation. Activation may precede polymerization which could mean that citrate causes a conformational change which leads to activation. The

K_{citrate} for both ACC1 and ACC2 is about 2mM. Isocitrate, malonate, sulphate and phosphate also promote polymerization [61].

The activity of ACC does not change in parallel to the citrate concentration. This is ascribed to phosphorylation. In addition to allosteric regulation animal ACCs are also regulated by covalent modification through phosphorylation of critical serine residues. AMP-activated protein kinase (AMPK) is the critical kinase and becomes activated in response to stress signals, exercise and adipokines such as leptin and adiponectin. This enzyme regulates catalytic activity of various enzymes and cellular processes through phosphorylation by monitoring the energy status of the cell and regulating the ATP-consuming and the ATP-producing pathways accordingly [40]. Activated AMPK phosphorylates and thereby inhibits both isoforms of ACC under physiological conditions. The phosphorylated enzymes have much lower V_{f}-values and are desensitised to citrate binding [61]. Also, citrate inhibits the rate of phosphorylation of native ACC by AMPK. Thus, the polymerization of ACC in the presence of citrate protects the enzyme from being phosphorylated [40].

Phosphorylation and allosteric activation of ACC therefore appear to be interactive regulatory mechanisms.

3.3 Pyruvate kinase

Pyruvate kinase (EC 2.7.1.40; PK) catalyses the final step of glycolysis with the conversion of phosphoenolpyruvate (PEP) and ADP to pyruvate and ATP.

$$\text{PEP} + \text{ADP} \rightleftharpoons \text{pyruvate} + \text{ATP} \tag{3.4}$$

PK is found in almost all prokaryotic and eukaryotic organisms. This reaction is a committed step leading to either anaerobic fermentation or oxidative phosphorylation of pyruvate. Monovalent (K^+) and divalent (Mg^{2+} or Mn^{2+}) cations are essential for activity for all known PKs [63]. In most cells the reaction is essentially irreversible under physiological conditions ($K_{\text{eq}} = 10^3$–10^4) [29]. The reaction is a major control point in glycolysis. PK plays a critical role in the regulation of glycolytic flux which effects the

concentration of glycolytic intermediates, biosynthetic precursors and nucleotide triphosphates [3]. In certain tissues PK serves as a switch between glycolysis and gluconeogenesis [3, 29].

Four isozymes have been isolated from mammalian tissues. The kinetic properties of the isozymes differ according to the metabolic requirements of the expressing tissue. The L isozyme is found in the liver, the R isozyme in erythrocytes, the M_1 isozyme in the brain and skeletal muscles and the M_2 isozyme in the kidney and lungs [41].

PK plays a central role in cellular metabolism and therefore is a highly regulated allosteric enzyme, both homotropically and heterotropically. PK is regulated by physiological effectors such as H^+, Mn^{2+} and K^+, cooperative binding of PEP, and heterotropic effectors [29]. The nature of the effectors depends on the organism.

In mammalian tissue the M_2, L and R are considered to be allosterically regulated because of the sigmoidal kinetic responses to the binding of FBP, PEP and metal ions. These isozymes are also allosterically regulated via feedback inhibition by ATP and inhibited by phosphorylation [29]. The M_1 isozyme is regarded as unregulated because of hyperbolic binding of substrates and effectors [29, 63]. In trypanosomatid protozoans fructose 2,6-bisphosphate is the allosteric effector. Though most bacterial PKs are regulated via a feedforward mechanism by FBP, some bacterial PKs are regulated by monophosphorylated sugar such as ribose 5-phosphate [63].

Yeast PKs, which are allosterically regulated by PEP, ATP, H^+, Mn^{2+}, Mg^{2+} and FBP, have been classed as K-type enzymes where the effectors increase the affinity and reduces the cooperativity of substrate binding. The allosteric effect is dependent on bound cations in the active site and is bidirectional, i.e., the presence of substrate and metal ions in the active site also increases the affinity of the active site for FBP [3]. All known PKs have an absolute requirement for two divalent metal ions. Also, most PKs have a requirement for a monovalent metal ion per monomer. The one divalent metal ion binds the enzyme and facilitates the binding of the substrate PEP and triggers allosteric activation through a metal ion-mediated allosteric relay mechanism. The other divalent ion binds the enzyme via a complex with

the substrate ADP [29].

Also in animal and yeast PKs reversible protein kinase-mediated phosphorylation aids in coordinating the activity of the enzyme with energy and carbohydrate metabolism [41].

The binding of the substrate, PEP, appears sigmoidal in most cases, however plant cytosolic and plastid PK bind the substrate PEP hyperbolically [41]. Yeast PK is an example of a classical K-enzyme as both substrates and allosteric effectors modulate the binding affinity of each other. In was previously thought that FBP increased the affinity of the enzyme for its substrate PEP. However it now appears that regulation occurs through the enzyme-bound divalent metal ion via an allosteric relay mechanism. The binding of FBP displays negative cooperativity [29].

PK from *L. lactis* exhibits cooperative binding of both substrates PEP and ADP. This cooperativity is lost upon the addition of an excess of FBP [10].

PK is activated by a variety of heterotropic effectors. The nature of the effector depends on the organism [41]. PK isoenzymes from *E. coli* and *Salmonella typhimurium*, type I and II are the most studied allosteric enzymes. Type is activated by FBP and type II by AMP. In *E.coli* the type II enzymes is also activated by intermediates of the hexose phosphate pathway such as ribose 5-phosphate. In trypanosomatid protozoans PK is activated by fructose 2,6-bisphosphate (F2,6BP) [41].

In *L. lactis* PK is activated by FBP and inhibited by Pi. The binding of FBP decreases PEP cooperativity from h = 3.3 (in the absence of FBP) to h = 1 in the presence of FBP. ATP was similarly influenced though to a lesser degree. Saturating FBP (0.8 mM) increases the sensitivity of the enzyme for its substrates and the V_f. K_{PEP} decreased from 4 mM in the absence of FBP to 0.14 mM in the presence of saturating FBP. Similar results were found for *L. lactis* C_{10} and *S. cremoris* AM_2. Inhibition by Pi has also been reported for *B. licheniformis* PK [10].

In was previously thought that FBP increased the affinity of the enzyme for its substrate PEP directly. However it now appears that regulation occurs through the enzyme-bound divalent metal ion via an allosteric relay mechanism [29]. It was proposed that highly conserved residues in the subunit

interface relays conformational changes in the allosteric binding site to corresponding conformational changes in the active site. These changes increases the enzymes affinity for its substrate PEP. Also, the structure of rabbit PK supports the concept of domain movement playing a functional role in enzyme activity [29]. It should nevertheless be noted that this hypothesis is based on the comparison of data from prokaryotic and eukaryotic sources [29].

3.4 Glycogen synthase

Glycogen synthase (UDP-glucose-glycogen glucosyltransferase) (GS) is generally regarded as a key enzyme in the regulation of glycogen metabolism. It catalyses the reaction in which the glucose moiety of UDP-glucose (UDPG) is incorporated into glycogen. This is achieved by the formation of an $\alpha(1 \rightarrow 4)$ glycosidic bond and the release of the UDP-moiety. Therefore glycogen is both a substrate and a product of the reaction [46].

$$\mathrm{Glc}_n + \mathrm{UDPG} \rightleftharpoons \mathrm{Glc}_{n+1} + \mathrm{UDP} \tag{3.5}$$

GS is extensively regulated by allosteric and covalent modification. GS is allosterically regulated by G6P, ATP and several other ligands. G6P activates GS via a feedforward mechanism and is considered the most important allosteric modifier of GS. In the majority of kinetic studies, UDP-Glc exhibits hyperbolic saturation curves. A few studies report deviations from Michaelian kinetics, mostly in the form of negative cooperativity. The observed negative cooperativity may be the result of UDP product inhibition and disappears if appropriate measures are taken to minimize the inhibition [46].

ATP inhibits GS by decreasing the affinity of the enzyme for UDP-Glc. Kinetic studies that include both G6P and ATP indicate competitive binding. Activation and inhibition curves of G6P and ATP have been found to be either hyperbolic or sigmoidal in various studies. Cooperative G6P binding has mostly been observed for the phosphorylated enzyme, and the dephosphorylated form exhibit mild cooperativity. ATP cooperativity has been observed for the dephosphorylated enzyme. There also appears to be positive

heterotropic cooperativity in G6P and ATP binding. ATP and ADP are probably equally important GS inhibitors although detailed kinetic data for ADP is limited. AMP has also been reported as a weak inhibitor of GS at high concentrations. However it is unlikely that AMP is a significant effector of GS given the low AMP concentration in muscle in vivo [46].

G6P affects GS activity through four mechanisms: (i) as a substrate precursor, (ii) as an allosteric activator, (iii) as a GS kinase inhibitor, and (iv) as a GS phosphatase activator. Ultimately the activation of GS by G6P is due to a significant conformational change which have an affect on the kinetics of GS. Higher apparent k_{cat}-values in the presence of G6P indicates catalytic activation. The extent on catalytic activation appears to correlate with the degree of phosphorylation [46].

Even for the most phosphorylated forms, G6P decreases the apparent K_{UDPG} dramatically. G6P also activates GS by suppressing ATP-binding at the allosteric site. This is seen as an apparent increase in K_{ATP}.

In addition to allosteric regulation GS is also modulated via covalent modification. Phosphorylation occurs at at least nine serine residues, but not all phosphorylation sites affect the activity of the enzyme. Phosphorylation has a potent inhibitory effect on GS. Inhibition by phosphorylation is the result of altered affinity of GS for its reactants and modifiers, and possibly a decrease in the turnover number. G6P not only reverses the effects of phosphorylation on the kinetics of GS, but also enhances the reversal of covalent phosphorylation by inhibition of GS kinases and activation of GS phosphatases [46].

Phosphorylation by protein kinase A (PKA) inactivates GS. Insulin inhibits PKA by competitive binding with respect to cAMP, resulting in a increase in G6P concentration. G6P inhibition of phosphorylation appears specific to PKA and GS. Inhibition is brought about by a change in GS conformation upon G6P binding to the allosteric site. The ability of GS to activate PKA is hindered by the conformational change and the kinetics of the previously activated PKA is not altered. GS also inhibits one or more yeast kinases [46].

G6P also promotes dephosphorylation, and concomitant activation of GS. G6P does not directly activate the phosphatases but causes a conformational

change in GS, rendering it a better substrate. The affinity of the phosphatases for GS was not altered by G6P. Activation involves an increase in the V_f and thus the catalytic constant k_{cat} [46].

Recent studies a link between GS phosphorylation state and subcellular localization has been suggested. As G6P stimulates net dephosphorylation of GS, it is expected that it will also influence the sub-cytosolic distribution of GS by promoting the dephosphorylation of sites that are associated with targeting GS to various fractions in the cytosol. G6P-stimulated translocation of GS to the cytosol would effectively increase the total GS concentration in the cytosol [46].

3.5 Sucrose phosphate synthase

Sucrose phosphate synthase (UDP-glucose: D-fructose 6-phosphate 2-glucosyl-transferase; EC 2.4.1.14) (SPS) is a key enzyme in the sucrose synthesis pathway in plants and plays an important role in carbon partitioning [7]. Cytosolic sucrose formation starts with triose-P exported from the chloroplast, which is converted to hexose-P and ultimately to sucrose [27]. SPS is a cytoplasmic enzyme and catalyses the reversible reaction:

$$\text{UDP-glucose} + \text{fructose-6-phosphate} \rightleftharpoons \text{UDP} + \text{sucrose-6-phosphate} \quad (3.6)$$

The rate of sucrose synthesis is strongly regulated by feedforward activation, which coordinate it with the rate of photosynthesis. It is also regulated by feedback inhibition which allow the rate of sucrose synthesis to be decreased, so more photosynthate is stored in the chloroplast as starch. The control of the partitioning of the assimilated carbon is shared by SPS and fructose-2,6-bisphosphatase [27, 42].

SPS is highly regulated by a hierarchy of several interacting mechanisms that include metabolic fine control (allosteric control by G6P and Pi), coarse control via covalent modification and the amount of protein. The regulation varies among different plant species and according to different metabolic situations such as seasonal and light changes [34]. Huber and Huber [27] classed SPS into groups according to regulatory properties. Class I SPS (e.g.,

from *Zea mays*, maise and monocotyledons) is regulated allosterically and via covalent modification. A two to threefold increase in the V_f is observed as well as altered sensitivity to effectors. Class II SPS (e.g., from spinach) is allosterically activated by glucose-6-phosphate (G6P), inhibited by Pi and the sensitivity to the activator is covalently modified via phosphorylation or dephosphorylation [27]. Class III SPS (e.g. soybeans) is allosterically regulated but no covalent modification is observed. The different classes may reflect differences in carbon partitioning between sucrose and starch. Class I and II species accumulate sucrose in leaves and class III species accumulate starch [27]. Also, sucrose synthesis increases with irradiance and is referred to as feedforward control, whereas high endogenous sucrose levels reduces the absolute rate of sucrose synthesis and is referred to as feedback control [27].

During low to moderate photosynthetic rate phosphorylation/dephosphorylation is an effective mechanism to regulate fluxes and maintaining relative constant metabolite levels. However, during high photosynthetic rate with saturating CO_2 and light the synthesis of sucrose increases dramatically with increases in metabolite concentration. Specifically, an increase in G6P and a decrease in Pi act on two levels, (i) as allosteric effectors of SPS, and (ii) as effectors which regulate the phosphorylation status of the enzyme that regulates phosphorylation [27].

The binding of substrates, UDP-Glc and Fru-6-P, is hyperbolic. In spinach leaves and wheat germ SPS the saturation curve for F6P is sigmoidal and hyperbolic for UDP. Wheat germ SPS is similar with respect to saturation curves but is also stimulated by Mg^{2+} [1].

Sucrose phosphate synthase from stored potato (Solanum tuberosum L.) is activated by glucose-6-phosphate and inhibited by inorganic phosphate. Both effectors have large effects on the K_M-values for both substrates fructose-6-phosphate and UDP-glucose. Inorganic phosphate has an inhibitory effect on glucose-6-phosphate activation [53]. In spinach leaf SPS Pi is a potent inhibitor especially at low substrate concentration. Pi inhibition is competitive with respect to UDPG. Also, sucrose phosphate is a competitive inhibitor with respect to UDPG. Pi increases the K_{FBP} from 3 to 5.9mM. The results are

similar for wheat germ, barley leaf grape leaf, ladino clover leaf, sweet potato root and potato tuber. Wheat germ is insensitive to Pi inhibition [1]

Maize SPS is activated by glucose-6-phosphate. This is seen in an increase in V_f and a decrease in the K_M for the substrate UDP-glucose. The UDP-glucose saturation profile is biphasic ; thus two K_M-values for UDP-glucose were calculated. Inorganic phosphate only acted as an inhibitor in the presence of G6P.

Chapter 4

Feedforward activation

In order to gain a better understanding of the regulatory role of feedforward activation in metabolic systems, this chapter describes a metabolic control analysis and supply demand analysis of the regulation of a metabolic pathway allosterically activated via a feedforward loop. The distinction is made between specific and catalytic activation, and it is shown that for allosteric enzymes saturated with their substrate(s) specific activation is abolished, and only catalytic activators can function as feedforward regulators. We start with a theoretical analysis of feedforward activation, and supplement it with a computational study of the minimal metabolic model in Fig. 4.1, which is a four-enzyme linear pathway in which the last enzyme in the chain is activated by the upstream metabolite S_1. The kinetic model of the pathway in Fig. 4.1 was constructed using our modelling platform PySCeS (the Python Simulator for Cellular Systems) [44]. The PySCeS input file for this model is listed in Appendix B.

Similar to feedback inhibition [22, 23], the regulatory role of feedforward activation is to maintain homeostasis of the concentration of the linking metabolite/allosteric activator, S_1. Contrary to the mechanism and conditions for regulation by allosteric feedback inhibition, which is well understood and described [22, 23], allosteric feedforward activation has hitherto not been subjected to the same depth of analysis.

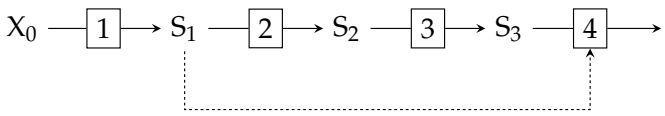

Figure 4.1: A linear metabolic pathway with four sequentially coupled enzymes E_1, E_2, E_3 and E_4. E_4 is considered to catalyse an irreversible reaction and to be insensitive to metabolites downstream from it. The external metabolite X_0 is considered to be buffered at a constant concentration. E_4 is allosterically activated by S_1 via a feedforward loop.

4.1 Control and supply-demand analysis

In order to study and describe feedforward activation we employ metabolic control analysis of the pathway in Fig. 4.1. Control analysis of the entire metabolic pathway provides insight into the relationship between local properties of the metabolic pathway, namely the sensitivities of the individual enzyme rates to changes in metabolite concentrations (elasticity coefficients), and the systemic properties which represents the contribution of each of the enzyme rates to the flux through the pathway (flux control coefficients) or the control of a metabolite concentration (concentration control coefficients) [21]. The connectivity and summation theorems of control analysis are employed to express the flux and concentration control coefficients in terms of elasticities.

Control analysis of the pathway in Fig. 4.1 yields the expressions for the flux and concentration-control coefficients in terms of elasticity coefficients:

J-control coefficients

$$C^J_{v_1} = (\varepsilon^{v_2}_{s_1}\varepsilon^{v_3}_{s_2}\varepsilon^{v_4}_{s_3} + \varepsilon^{v_4}_{s_1}\varepsilon^{v_2}_{s_2}\varepsilon^{v_3}_{s_3})/\Sigma$$
$$C^J_{v_2} = -\varepsilon^{v_1}_{s_1}\varepsilon^{v_3}_{s_2}\varepsilon^{v_4}_{s_3}/\Sigma$$
$$C^J_{v_3} = \varepsilon^{v_1}_{s_1}\varepsilon^{v_2}_{s_2}\varepsilon^{v_4}_{s_3}/\Sigma$$
$$C^J_{v_4} = -\varepsilon^{v_1}_{s_1}\varepsilon^{v_2}_{s_2}\varepsilon^{v_3}_{s_3}/\Sigma$$

s_1-control coefficients

$$C^{s_1}_{v_1} = (\varepsilon^{v_3}_{s_2}\varepsilon^{v_4}_{s_3} - \varepsilon^{v_2}_{s_2}\varepsilon^{v_4}_{s_3} + \varepsilon^{v_2}_{s_2}\varepsilon^{v_3}_{s_3})/\Sigma$$
$$C^{s_1}_{v_2} = -\varepsilon^{v_3}_{s_2}\varepsilon^{v_4}_{s_3}/\Sigma$$
$$C^{s_1}_{v_3} = \varepsilon^{v_2}_{s_2}\varepsilon^{v_4}_{s_3}/\Sigma$$
$$C^{s_1}_{v_4} = -\varepsilon^{v_2}_{s_2}\varepsilon^{v_3}_{s_3}/\Sigma$$

s_2-control coefficients

$$
\begin{aligned}
C_{v_1}^{s_2} &= (\varepsilon_{s_1}^{v_2}\varepsilon_{s_3}^{v_4} - \varepsilon_{s_1}^{v_2}\varepsilon_{s_3}^{v_3} + \varepsilon_{s_1}^{v_4}\varepsilon_{s_3}^{v_3})/\Sigma \\
C_{v_2}^{s_2} &= (-\varepsilon_{s_1}^{v_1}\varepsilon_{s_3}^{v_4} + \varepsilon_{s_1}^{v_1}\varepsilon_{s_3}^{v_3} - \varepsilon_{s_1}^{v_4}\varepsilon_{s_3}^{v_3})/\Sigma \\
C_{v_3}^{s_2} &= (-\varepsilon_{s_1}^{v_2}\varepsilon_{s_3}^{v_4} + \varepsilon_{s_1}^{v_1}\varepsilon_{s_3}^{v_4})/\Sigma \\
C_{v_4}^{s_2} &= (\varepsilon_{s_1}^{v_2}\varepsilon_{s_3}^{v_3} - \varepsilon_{s_1}^{v_1}\varepsilon_{s_3}^{v_3})/\Sigma
\end{aligned}
$$

s_3-control coefficients

$$
\begin{aligned}
C_{v_1}^{s_3} &= (\varepsilon_{s_1}^{v_2}\varepsilon_{s_2}^{v_3} + \varepsilon_{s_1}^{v_4}\varepsilon_{s_2}^{v_2} - \varepsilon_{s_1}^{v_4}\varepsilon_{s_2}^{v_3})/\Sigma \\
C_{v_2}^{s_3} &= (-\varepsilon_{s_1}^{v_1}\varepsilon_{s_2}^{v_3} + \varepsilon_{s_1}^{v_4}\varepsilon_{s_2}^{v_3})/\Sigma \\
C_{v_3}^{s_3} &= (\varepsilon_{s_1}^{v_1}\varepsilon_{s_2}^{v_2} - \varepsilon_{s_1}^{v_4}\varepsilon_{s_2}^{v_2})/\Sigma \\
C_{v_4}^{s_3} &= (-\varepsilon_{s_1}^{v_2}\varepsilon_{s_2}^{v_3} + \varepsilon_{s_1}^{v_1}\varepsilon_{s_2}^{v_3} - \varepsilon_{s_1}^{v_1}\varepsilon_{s_2}^{v_2})/\Sigma
\end{aligned}
$$

where

$$\Sigma = \varepsilon_{s_1}^{v_2}\varepsilon_{s_2}^{v_3}\varepsilon_{s_3}^{v_4} - \varepsilon_{s_1}^{v_1}\varepsilon_{s_2}^{v_3}\varepsilon_{s_3}^{v_4} + \varepsilon_{s_1}^{v_1}\varepsilon_{s_2}^{v_2}\varepsilon_{s_3}^{v_4} - \varepsilon_{s_1}^{v_1}\varepsilon_{s_2}^{v_2}\varepsilon_{s_3}^{v_3} + \varepsilon_{s_1}^{v_4}\varepsilon_{s_2}^{v_2}\varepsilon_{s_3}^{v_3}$$

At this stage we notice an important result that follows when we make two assumptions, namely that E_1 is insensitive to its immediate product S_1, i.e., $\varepsilon_{s_1}^{v_1} = 0$, and that E_4 is insensitive to its substrate S_3, i.e., $\varepsilon_{s_3}^{v_4} = 0$. The above expressions then simplify to:

J-control coefficients

$$
\begin{aligned}
C_{v_1}^{J} &= 1 \\
C_{v_2}^{J} &= 0 \\
C_{v_3}^{J} &= 0 \\
C_{v_4}^{J} &= 0
\end{aligned}
$$

s_1-control coefficients

$$
\begin{aligned}
C_{v_1}^{s_1} &= \frac{1}{\varepsilon_{s_1}^{v_4}} \\
C_{v_2}^{s_1} &= 0 \\
C_{v_3}^{s_1} &= 0 \\
C_{v_4}^{s_1} &= -\frac{1}{\varepsilon_{s_1}^{v_4}}
\end{aligned}
$$

s_2-control coefficients

$$C^{s_2}_{v_1} = \frac{-\varepsilon^{v_2}_{s_1} + \varepsilon^{v_4}_{s_1}}{\varepsilon^{v_4}_{s_1}\varepsilon^{v_2}_{s_2}}$$
$$C^{s_2}_{v_2} = \frac{-\varepsilon^{v_4}_{s_1}}{\varepsilon^{v_4}_{s_1}\varepsilon^{v_2}_{s_2}}$$
$$C^{s_2}_{v_3} = 0$$
$$C^{s_2}_{v_4} = \frac{\varepsilon^{v_2}_{s_1}}{\varepsilon^{v_4}_{s_1}\varepsilon^{v_2}_{s_2}}$$

s_3-control coefficients

$$C^{s_3}_{v_1} = \frac{\varepsilon^{v_2}_{s_1}\varepsilon^{v_3}_{s_2} + \varepsilon^{v_4}_{s_1}\varepsilon^{v_2}_{s_2} - \varepsilon^{v_4}_{s_1}\varepsilon^{v_3}_{s_2}}{\varepsilon^{v_4}_{s_1}\varepsilon^{v_2}_{s_2}\varepsilon^{v_3}_{s_3}}$$
$$C^{s_3}_{v_2} = \frac{\varepsilon^{v_3}_{s_2}}{\varepsilon^{v_2}_{s_2}\varepsilon^{v_3}_{s_3}}$$
$$C^{s_3}_{v_3} = \frac{-\varepsilon^{v_2}_{s_2}}{\varepsilon^{v_2}_{s_2}\varepsilon^{v_3}_{s_3}}$$
$$C^{s_3}_{v_4} = \frac{-\varepsilon^{v_2}_{s_1}\varepsilon^{v_3}_{s_2}}{\varepsilon^{v_4}_{s_1}\varepsilon^{v_2}_{s_2}\varepsilon^{v_3}_{s_3}}$$

Under these assumptions E_1 controls the flux J completely, i.e., is a true rate-limiting step, and the control of the concentration of S_1 is completely determined by $\varepsilon^{v_4}_{s_1}$, i.e., the sensitivity of E_4 to its allosteric activator S_1. This is clearly the ideal situation, and the analysis that follows is essentially a quest to find under which conditions the assumptions made above are tenable. There is of course no requirement for real systems to exhibit this theoretically ideal design, but our analysis in principle allows for an exploration of any set of conditions, and can show when the feedforward loop will not be functional.

Supply-demand analysis around the activator S_1

Supply demand analysis is employed to analyse the regulated responses of the metabolic pathway to varying concentrations of the allosteric activator S_1 and of S_3, the substrate of the allosteric enzyme E_4. As shown in Fig. 4.2, S_1 separates the pathway into two conversion blocks, a supply or biosynthetic block consisting of E_1 with local flux J_1, and a demand or utilisation block consisting of E_2, E_3 and E_4 with local flux J_{234}. These blocks can only communicate with each other through the activator, S_1, which is freely variable. Changes in the rate of supply is fed forward to the rate of demand via changes in S_1, both by mass-action through the linear pathway E_2, E_3 and E_4, and through feedforward activation of E_4.

The sensitivity of the local supply-block flux J_1 to S_1 is expressed by the

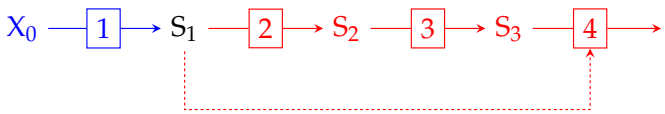

Figure 4.2: The allosteric activator S_1 separates the pathway into two conversion blocks, namely a supply block that consists of E_1 and a demand block that consists of E_2, E_3 and E_4.

elasticity coefficient $\varepsilon_{s_1}^{v_1}$. The block elasticity coefficient, $\varepsilon_{s_1}^{v_{234}}$, quantifies the sensitivity of the local demand flux, J_{234}, to changes in S_1. Both demand and supply elasticities are block elasticities, but in this specific instance the supply block is represented by only one enzyme, E_1. The fluxes J_1 and J_{234} always have the same numerical value at steady state, but to analyse block elasticities the fluxes are regarded as independent entities.

The connectivity and summation theorems provide sufficient mathematical information to express the flux and concentration control coefficients in terms of the supply and demand elasticities:

$$C_{v_1}^{J} = \frac{\varepsilon_{s_1}^{v_{234}}}{\varepsilon_{s_1}^{v_{234}} - \varepsilon_{s_1}^{v_1}} \quad \text{and} \quad C_{v_{234}}^{J} = \frac{-\varepsilon_{s_1}^{v_1}}{\varepsilon_{s_1}^{v_{234}} - \varepsilon_{s_1}^{v_1}} \tag{4.1}$$

$$C_{v_1}^{s_1} = \frac{1}{\varepsilon_{s_1}^{v_{234}} - \varepsilon_{s_1}^{v_1}} \quad \text{and} \quad C_{v_{234}}^{s_1} = \frac{-1}{\varepsilon_{s_1}^{v_{234}} - \varepsilon_{s_1}^{v_1}} \tag{4.2}$$

Inspection of eqn. 4.1 shows that the distribution of flux control is determined by the ratio of supply and demand block elasticities. For flux control by the supply, i.e., $C_{v_1}^{J} \to 1$, the demand flux J_{234} should be much more sensitive to variations in the allosteric activator, S_1, than the supply flux J_1, i.e., $\varepsilon_{s_1}^{v_{234}} \gg -\varepsilon_{s_1}^{v_1}$. Note that for flux control by the demand, i.e., $C_{v_{234}}^{J} \to 1$, $\varepsilon_{s_1}^{v_{234}} \ll -\varepsilon_{s_1}^{v_1}$, which would mean that the demand does not respond at all to the feedforward activator, thereby negating the feedforward mechanism completely. *For feedforward activation to function the supply of the activator must control the flux J through whole pathway (supply and demand) to a high degree, at best completely.* We shall now seek the conditions which make this possible. In a nutshell: we ask what makes $-\varepsilon_{s_1}^{v_1}$ small and what makes $\varepsilon_{s_1}^{v_{234}}$ large.

Conceptually the block elasticity $\varepsilon_{s_1}^{v_1}$ is the same as the J_1-response coefficient of the supply block, $R_{s_1}^{J_1}$, with respect to changes in s_1 [22]. Thus, the

sensitivity of the supply flux to changes in s_1 can be expressed in terms of the partitioned response property. S_1 interacts with only one enzyme, E_1, resulting in an expression for the response coefficient with only one term:

$$R_{s_1}^{J_1} = C_{v_1}^{J_1} \varepsilon_{s_1}^{v_1} \tag{4.3}$$

Since the supply block contains only one step, $C_{v_1}^{J_1} = 1$, so that

$$R_{s_1}^{J_1} = \varepsilon_{s_1}^{v_1} \tag{4.4}$$

Thus, the behaviour of the supply-block is determined by behaviour of the elasticity coefficient, $\varepsilon_{s_1}^{v_1}$, which in turn is determined by the kinetic and thermodynamic properties of E_1. In the kinetic model that we use to explore the concepts developed in this chapter (Appendix B) we assume E_1, E_2, and E_3 to follow reversible Michaelis-Menten kinetics, and E_4 to folow allosterically activated, reversible Hill kinetics, with the following rate equations:

$$v_1 = \frac{\frac{V_{f1}}{K_{1X0}}\left(x_0 - \frac{s_1}{K_{eq1}}\right)}{1 + \frac{x_0}{K_{1X0}} + \frac{s_1}{K_{1S1}}} \tag{4.5}$$

$$v_2 = \frac{\frac{V_{f2}}{K_{2S1}}\left(s_1 - \frac{s_2}{K_{eq2}}\right)}{1 + \frac{s_1}{K_{2S1}} + \frac{s_2}{K_{2S2}}} \tag{4.6}$$

$$v_3 = \frac{\frac{V_{f3}}{K_{3S2}}\left(s_2 - \frac{s_3}{K_{eq3}}\right)}{1 + \frac{s_2}{K_{3S2}} + \frac{s_3}{K_{3S3}}} \tag{4.7}$$

$$v_4 = V_{f4} \cdot \frac{1 + \gamma\alpha\left(\frac{s_1}{K_{4S1}}\right)^h}{1 + \alpha\left(\frac{s_1}{K_{4S1}}\right)^h} \cdot \frac{\left(\frac{s_3}{K_{4S3}}\right)^h}{\left(\frac{s_3}{K_{4S3}}\right)^h + \frac{1 + \left(\frac{s_1}{K_{4S1}}\right)^h}{1 + \alpha\left(\frac{s_1}{K_{4S1}}\right)^h}} \tag{4.8}$$

The default parameter settings used in all simulations of this set of rate equations are supplied in Table 4.1. Where relevant, changes in parameter values are given in the figure legends.

Table 4.1: Default parameter settings for the rate eqns. 4.5–4.8. For the K-form of E_4 (eqn. 4.9): $\alpha = 1000$ and $\gamma = 1$, and for the V-form of E_4 (eqn. 4.10): $\alpha = 1$ and $\gamma = 100$. The pathway substrate concentration $x_0 = 1$.

Enzyme 1	Enzyme 2	Enzyme 3	Enzyme 4
$V_{f1} = 1$	$K_{eq1} = 1$	$K_{eq1} = 1$	$V_{f4} = 1$
$K_{eq1} = 10^3$	$V_{f2} = 10^3$	$V_{f3} = 10^3$	$K_{4S3} = 1$
$K_{1X0} = 10^{-3}$	$K_{2S1} = 1$	$K_{3S2} = 1$	$K_{4S1} = 1$
$K_{1S1} = 10^8$	$K_{2S2} = 1$	$K_{3S3} = 1$	$h = 4$
			$\alpha = 1$
			$\gamma = 1$

We shall compare two forms of the rate equation for E_4, namely where S_1 only affects K_{4S3} (specific activation, the K-form of E_4) with rate equation:

$$v_{4K} = V_{f4} \cdot \frac{\left(\frac{s_3}{K_{4S3}}\right)^h}{\left(\frac{s_3}{K_{4S3}}\right)^h + \frac{1 + \left(\frac{s_1}{K_{4S1}}\right)^h}{1 + \alpha\left(\frac{s_1}{K_{4S1}}\right)^h}} \tag{4.9}$$

and where S_1 only affects V_{f4} (catalytic activation, the V-form of E_4) with rate equation:

$$v_{4V} = V_{f4} \cdot \frac{1 + \gamma\left(\frac{s_1}{K_{4S1}}\right)^h}{1 + \left(\frac{s_1}{K_{4S1}}\right)^h} \cdot \frac{\left(\frac{s_3}{K_{4S3}}\right)^h}{\left(\frac{s_3}{K_{4S3}}\right)^h + 1} \tag{4.10}$$

Partial derivation of the logarithmic form of the rate eqn. 4.5 for E_1 yields an analytical expression for the elasticity coefficient with respect to its product S_1:

$$\varepsilon_{s_1}^{v_1} = \frac{-\frac{s_1/x_0}{K_{eq1}}}{1 - \frac{s_1/x_0}{K_{eq1}}} - \frac{\frac{s_1}{K_{eq1}}}{1 + \frac{x_0}{K_{1X0}} + \frac{s_1}{K_{1S1}}} \tag{4.11}$$

where K_{eq1} is the equilibrium constant, and K_{X0} and K_{S1} are the half-saturating concentrations for substrate X_0 and product S_1. (The analytical expressions

of the elasticity coefficient $\varepsilon_{s_1}^{v_4}$ for the K and V-forms of E_4 are provided in Appendix A).

In this expression there is a clear distinction between the contribution of thermodynamics and that of kinetics. The left-hand thermodynamic term depends only on the distance from equilibrium (measured by the mass-action ratio Γ/K_{eq1}, where $\Gamma = s_1/x_0$ for E_1). Far from equilibrium $\Gamma \to 0$ and the thermodynamic term of tends to zero. Near equilibrium $\Gamma \to 1$ and the thermodynamic terms of the substrate and product elasticities tend to ∞ and $-\infty$ respectively.

The right-hand kinetic term varies between zero (when $s_1/K_{1S1} \to 0$) and one (as s_1/K_{1S1} becomes much larger than both 1 and x_0/K_{1X0}, i.e., when S_1 saturates E_1). Near equilibrium the contribution of the kinetic term is clearly negligible. Thus, for kinetic regulation of an enzyme the enzyme needs to be far from equilibrium.

We remind ourselves that for flux control by supply, $\varepsilon_{s_1}^{v_{234}} \gg -\varepsilon_{s_1}^{v_1}$. Thus, the rate of the demand block, v_{234} (more correctly, the demand flux J_{234}), should be much more sensitive to variations in the allosteric activator, S_1, than the supply block rate, v_1. For any non-zero value of $\varepsilon_{s_1}^{v_{234}}$ this is clearly achieved when $\varepsilon_{s_1}^{v_1} \to 0$. To meet these requirements E_1 must (i) be far from equilibrium so that the thermodynamic term in the elasticity expression tends to zero, and (ii) bind S_1 very weakly ($K_{1S1\gg} \to 0$) so that the kinetic term also tends to zero (this is automatically true when K_{1S1} is much larger than the physiological concentration range of s_1).

At this stage it is useful to introduce log-log rate characteristics, which show how the supply and demand fluxes respond to changes in the concentration of the metabolite that links them, here S_1. Such rate characteristics are shown in Fig. 4.3. Due to the curves being drawn in double logarithmic space the slopes of the rate characteristics are the elasticities of supply and demand with respect to s_1. Consider the blue supply rate characteristics of S_1. The slopes of the supply rate characteristics (and therefore $\varepsilon_{s_1}^{v_1}$) are zero for the entire s_1-range except where they approach $-\infty$ near equilibrium at $s_1 = 1000$ (x_0 is fixed at 1 and $K_{eq1} = 1000$ so that the equilibrium concentration of S_1 is 1000).

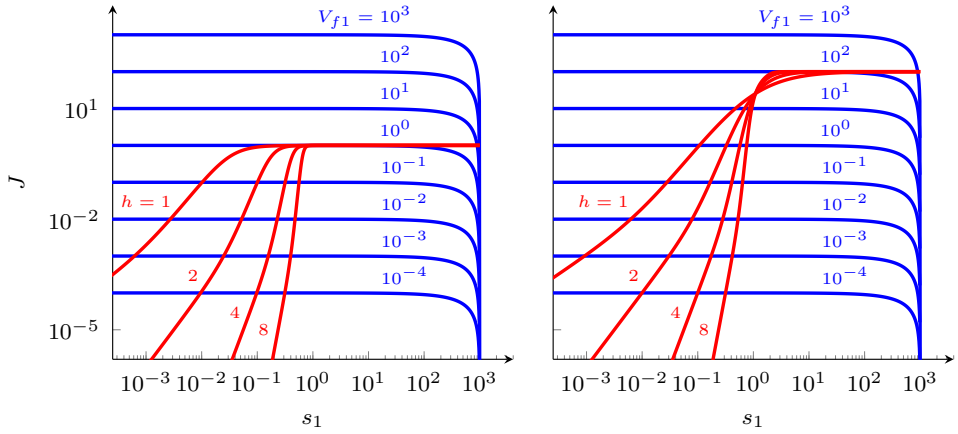

Figure 4.3: Supply and demand rate characteristics with respect to S_1 for the system in Fig. 4.2 with the K-form (left) and the V-form (right) of E_4. The S_1-supply rate characteristics vary with the limiting rate V_{f1} and the S_1-demand rate characteristics vary with the Hill coefficient in eqns. 4.10 and 4.9. Relevant parameter settings are: $K_{eq1} = 1000$, $V_{f4} = 1.0$, $K_{1S1} = 1000$; for K-E_4: $\alpha = 1000$ and $\gamma = 1$; for V-E_4: $\alpha = 1$ and $\gamma = 100$.

The slopes of the demand rate characteristis are equivalent to the demand elasticity for S_1, $\varepsilon_{s_1}^{v_{234}}$, and up to the point where S_1 no longer affects J_{234} the magnitude of the slope clearly varies with the degree of cooperativity with which S_1 binds to E_4, as determined by the Hill-coefficient.

A steady state obtains where the supply and demand rate characteristics intersect, and the ratio of the supply and demand slopes (elasticities) at steady state determines the flux-control distribution. Up to a V_{1f}-value of 1 for the K-form of E_4 the criterion of $\varepsilon_{s_1}^{v_{234}} \gg -\varepsilon_{s_1}^{v_1}$ for full flux-control by supply is met; for the V-form the criterion is met up to $V_{1f} = 100$. At higher V_{1f}-values flux-control abruptly shifts to the demand because now $\varepsilon_{s_1}^{v_{234}} \ll -\varepsilon_{s_1}^{v_1}$. Note also that during this shift the steady-state concentration of S_1 jumps by orders of magnitude to its near-equilibrium value. Here the regulation of s_1 is completely dominated by thermodynamics, while in the region where S_1-supply controls the flux, it is the kinetic properties of the demand that determine not only the steady-state concentration of S_1 but also the degree to which it varies with V_{1f}, i.e., the degree to which s_1 is homeostatically main-

tained by its demand. This is also clear from eqn. 4.2 in which we see that the degree of homeostasis in S_1 is determined by the sum of the block elasticities $(\varepsilon_{s_1}^{v_{234}} - \varepsilon_{s_1}^{v_1})$. The higher this sum, the better the homeostasis in s_1. If $\varepsilon_{s_1}^{v_1} \to 0$ homeostasis in S_1 is determined only by $\varepsilon_{s_1}^{v_{234}}$. This the opposite of what happens in a feedback-regulated system [22, 23].

The question now is what determines the magnitude of the demand elasticity of S_1.

Control analysis of the response of the S_1-demand to S_1

In terms of control analysis the effect of the activator, S_1, on the flux J_{234} is expressed by the response coefficient $R_{s_1}^{J_{234}}$, which is equivalent to the block elasticity, $\varepsilon_{s_1}^{v_{234}}$, and according to the partitioned response property is the sum of the two effects of S_1 on J_{234} via E_2 and E_4:

$$R_{s_1}^{J_{234}} = \varepsilon_{s_1}^{v_{234}} = C_{v_2}^{J_{234}} \varepsilon_{s_1}^{v_2} + C_{v_4}^{J_{234}} \varepsilon_{s_1}^{v_4} \tag{4.12}$$

If J_{234}-response to S_1 is to be via the feedforward loop then it is clear from this equation that not only should S_1 have an effect on E_4 (quantified by $\varepsilon_{s_1}^{v_4}$) but, for this effect to dominate the response, $C_{v_4}^{J_{234}}$ should also be as large as possible. In order to find conditions where this situation would obtain, we express the J_{234}-control coefficients in terms of elasticity coefficients:

$$C_{v_2}^{J_{234}} = \frac{\varepsilon_{s_3}^{v_4} \varepsilon_{s_2}^{v_3}}{\varepsilon_{s_3}^{v_4} \varepsilon_{s_2}^{v_3} - \varepsilon_{s_3}^{v_4} \varepsilon_{s_2}^{v_2} + \varepsilon_{s_3}^{v_3} \varepsilon_{s_2}^{v_2}} \tag{4.13}$$

$$C_{v_3}^{J_{234}} = \frac{-\varepsilon_{s_3}^{v_4} \varepsilon_{s_2}^{v_2}}{\varepsilon_{s_3}^{v_4} \varepsilon_{s_2}^{v_3} - \varepsilon_{s_3}^{v_4} \varepsilon_{s_2}^{v_2} + \varepsilon_{s_3}^{v_3} \varepsilon_{s_2}^{v_2}} \tag{4.14}$$

$$C_{v_4}^{J_{234}} = \frac{\varepsilon_{s_3}^{v_3} \varepsilon_{s_2}^{v_2}}{\varepsilon_{s_3}^{v_4} \varepsilon_{s_2}^{v_3} - \varepsilon_{s_3}^{v_4} \varepsilon_{s_2}^{v_2} + \varepsilon_{s_3}^{v_3} \varepsilon_{s_2}^{v_2}} \tag{4.15}$$

Substituting eqns. 4.13 and 4.15 in eqn. 4.12 yields:

$$\varepsilon_{s_1}^{v_{234}} = \frac{\varepsilon_{s_3}^{v_4} \varepsilon_{s_2}^{v_3}}{\varepsilon_{s_3}^{v_4} \varepsilon_{s_2}^{v_3} - \varepsilon_{s_3}^{v_4} \varepsilon_{s_2}^{v_2} + \varepsilon_{s_3}^{v_3} \varepsilon_{s_2}^{v_2}} \cdot \varepsilon_{s_1}^{v_2} + \frac{\varepsilon_{s_3}^{v_3} \varepsilon_{s_2}^{v_2}}{\varepsilon_{s_3}^{v_4} \varepsilon_{s_2}^{v_3} - \varepsilon_{s_3}^{v_4} \varepsilon_{s_2}^{v_2} + \varepsilon_{s_3}^{v_3} \varepsilon_{s_2}^{v_2}} \cdot \varepsilon_{s_1}^{v_4} \tag{4.16}$$

An immediate observation is that if E_4 is insensitive to (saturated with) its substrate E_3, i.e., if $\varepsilon_{s_3}^{v_4} \to 0$, then all the J_{234}-control is with E_4 and eqn. 4.12

reduces to

$$R_{s_1}^{J_{234}} = \varepsilon_{s_1}^{v_{234}} = 0 + 1 \cdot \varepsilon_{s_1}^{v_4} \tag{4.17}$$

so that the flux-response to S_1 is completely determined by $\varepsilon_{s_1}^{v_4}$. This is exactly what we already determined in section 4.1.

However, we recall from our discussion in Chapter 2 that, at least for the K-form of allosteric enzymes, there is the complication of the abolishment of the modifier effect when the substrate saturates the enzyme, i.e., when $\varepsilon_{s_3}^{v_4} = 0$ (for V-enzymes there is no such effect). For K-enzymes we therefore need to see under which conditions E_4 can still control J_{234} without being saturated with substrate.

So let us make no assumption about the value of $\varepsilon_{s_3}^{v_4}$, except to note that an allosteric enzyme it has a maximum value of the Hill coefficient, typically between 1 and 4 (see Appendix A). The other way of ensuring full J_{234}-control by E_4 is if the E_2-E_3-block is near-equilibrium, as will be explained in the following.

The ratio of substrate to product elasticity of a reaction approaches -1 near equilibrium where the thermodynamic terms of any possible elasticity expression tend to $+\infty$ and $-\infty$ for substrate and product respectively. Near equilibrium the substrate and product elasticities always are:

$$\varepsilon_s^v = \frac{1}{1 - \dfrac{\Gamma}{K_{\text{eq}}}} \quad \text{and} \quad \varepsilon_p^v = \frac{-\dfrac{\Gamma}{K_{\text{eq}}}}{1 - \dfrac{\Gamma}{K_{\text{eq}}}} \tag{4.18}$$

where Γ is the mass-action ratio p/s. The elasticity ratio therefore is

$$\frac{\varepsilon_p^v}{\varepsilon_s^v} = -\frac{\Gamma}{K_{\text{eq}}} \to -1 \tag{4.19}$$

because near equilibrium $\Gamma \to K_{\text{eq}}$. For our system this translates to $\frac{\varepsilon_{s_2}^{v_2}}{\varepsilon_{s_1}^{v_2}} \to -1$ and $\frac{\varepsilon_{s_3}^{v_3}}{\varepsilon_{s_2}^{v_3}} \to -1$.

First, divide by all numerators and denominators in eqns. 4.13–4.15 by $\varepsilon_{s_1}^{v_2}$ and substitute $\varepsilon_{s_2}^{v_2}/\varepsilon_{s_1}^{v_2}$ with -1:

$$C_{v_2}^{J_{234}} = \frac{\frac{\varepsilon_{s_3}^{v_4}\varepsilon_{s_2}^{v_3}}{\varepsilon_{s_1}^{v_2}}}{\frac{\varepsilon_{s_3}^{v_4}\varepsilon_{s_2}^{v_3}}{\varepsilon_{s_1}^{v_2}} + \varepsilon_{s_3}^{v_4} - \varepsilon_{s_3}^{v_3}} \tag{4.20}$$

$$C_{v_3}^{J_{234}} = \frac{\varepsilon_{s_3}^{v_4}}{\frac{\varepsilon_{s_3}^{v_4}\varepsilon_{s_2}^{v_3}}{\varepsilon_{s_1}^{v_2}} + \varepsilon_{s_3}^{v_4} - \varepsilon_{s_3}^{v_3}} \tag{4.21}$$

$$C_{v_4}^{J_{234}} = \frac{-\varepsilon_{s_3}^{v_3}}{\frac{\varepsilon_{s_3}^{v_4}\varepsilon_{s_2}^{v_3}}{\varepsilon_{s_1}^{v_2}} + \varepsilon_{s_3}^{v_4} - \varepsilon_{s_3}^{v_3}} \tag{4.22}$$

Because near equilibrium $\varepsilon_{s_1}^{v_2} \to \infty$, these equations reduce to:

$$C_{v_2}^{J_{234}} = 0, \quad C_{v_3}^{J_{234}} = \frac{\varepsilon_{s_3}^{v_4}}{\varepsilon_{s_3}^{v_4} - \varepsilon_{s_3}^{v_3}} \quad \text{and} \quad C_{v_4}^{J_{234}} = \frac{-\varepsilon_{s_3}^{v_3}}{\varepsilon_{s_3}^{v_4} - \varepsilon_{s_3}^{v_3}} \tag{4.23}$$

Similarly, dividing now by $\varepsilon_{s_2}^{v_3}$ and substituting $\varepsilon_{s_3}^{v_3}/\varepsilon_{s_2}^{v_3}$ with -1 yields

$$C_{v_2}^{J_{234}} = 0, \quad C_{v_3}^{J_{234}} = \frac{\frac{\varepsilon_{s_3}^{v_4}}{\varepsilon_{s_2}^{v_3}}}{\frac{\varepsilon_{s_3}^{v_4}}{\varepsilon_{s_2}^{v_3}} + 1} \quad \text{and} \quad C_{v_4}^{J_{234}} = \frac{1}{\frac{\varepsilon_{s_3}^{v_4}}{\varepsilon_{s_2}^{v_3}} + 1} \tag{4.24}$$

Because near equilibrium $\varepsilon_{s_2}^{v_3} \to \infty$ these equations reduce to:

$$C_{v_2}^{J_{234}} = 0, \quad C_{v_3}^{J_{234}} = 0 \quad \text{and} \quad C_{v_4}^{J_{234}} = 1 \tag{4.25}$$

Therefore, when both the E_2 and E_3-catalysed reactions are near equilibrium they have no control over J_{234} and all the J_{234}-control resides in E_4.

Nested supply-demand analysis around S_3 of the demand for S_1

These results can be approached from a different angle by dividing the demand for S_1 into supply and demand blocks around S_3 as shown in Fig. 4.4. This is therefore a supply-demand analysis *within* a supply-demand analyis, which we term a nested supply-demand analysis.

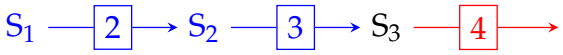

Figure 4.4: A nested supply-demand analysis of the S_1-demand block. Two conversion blocks exist around S_3, a supply block consisting of E_2 and E_3, and a demand block consisting of E_4. S_1 and X_4 are regarded as externally buffered at a constant value.

Here, E_2 and E_3 form the supply block (referred to as the S_3-supply block) and its sensitivity to changes in S_3 is represented by the nested supply elasticity coefficient $\varepsilon_{s_3}^{v_{23}}$. E_4 represents the demand block (referred to as the S_3-demand block) and its sensitivity to changes in S_3 is represented by the nested demand elasticity coefficient $\varepsilon_{s_3}^{v_4}$.

The J_{234}-control coefficients are expressed as:

$$C_{v_{23}}^{J_{234}} = \frac{\varepsilon_{s_3}^{v_4}}{\varepsilon_{s_3}^{v_4} - \varepsilon_{s_3}^{v_{23}}} \quad \text{and} \quad C_{v_4}^{J_{234}} = \frac{-\varepsilon_{s_3}^{v_{23}}}{\varepsilon_{s_3}^{v_4} - \varepsilon_{s_3}^{v_{23}}} \tag{4.26}$$

and the s_3-control coefficients as:

$$C_{v_{23}}^{s_3} = \frac{1}{\varepsilon_{s_3}^{v_4} - \varepsilon_{s_3}^{v_{23}}} \quad \text{and} \quad C_{v_4}^{s_3} = \frac{-1}{\varepsilon_{s_3}^{v_4} - \varepsilon_{s_3}^{v_{23}}} \tag{4.27}$$

From eqn. 4.26 we can deduce that the distribution of flux control depends on the ratio $-\varepsilon_{s_3}^{v_{23}}/\varepsilon_{s_3}^{v_4}$. If $-\varepsilon_{s_3}^{v_{23}} \gg \varepsilon_{s_3}^{v_4}$ then $C_{v_4}^{J_{234}} \to 1$, which is what we require for the feedforward activation loop to function. But now, instead of thinking of $\varepsilon_{s_3}^{v_4}$ being much smaller than $-\varepsilon_{s_3}^{v_{23}}$, we ask under which conditions $-\varepsilon_{s_3}^{v_{23}}$ becomes much larger than $\varepsilon_{s_3}^{v_4}$, which for an irreversible enzyme has a maximum value of the Hill coefficient, typically between 1 and 4. Following the reasoning in the previous section we see that if the E_2-E_3 supply block for S_3 is near equilibrium, $\varepsilon_{s_3}^{v_{23}} \to -\infty$ and the condition is satisfied.

To summarise the results up to now:

- In order for the feedforward activation loop to function, the supply block of the allosteric activator S_1 must control the pathway flux. This is achieved when $\varepsilon_{s_1}^{v_{234}} \gg -\varepsilon_{s_1}^{v_1}$. Under such conditions the degree of homeostatic maintenance of s_1 is determined by $\varepsilon_{s_1}^{v_{234}}$.

- The response of the demand flux J_{234} to S_1, i.e., $\varepsilon_{s_1}^{v_{234}}$, depends on the product $C_{v_4}^{J_{234}}\varepsilon_{s_1}^{v_4}$. $C_{v_4}^{J_{234}} \to 1$ when $-\varepsilon_{s_3}^{v_{23}} \gg \varepsilon_{s_3}^{v_4}$, which is satisfied when

either $\varepsilon_{s_3}^{v_4} \to 0$ or $-\varepsilon_{s_3}^{v_{23}} \to -\infty$, i.e., when the E_2-E_3 supply block for S_3 is near equilibrium. For the K-form of E_4 only the second criterion is valid, while for the V-form both criteria are valid.

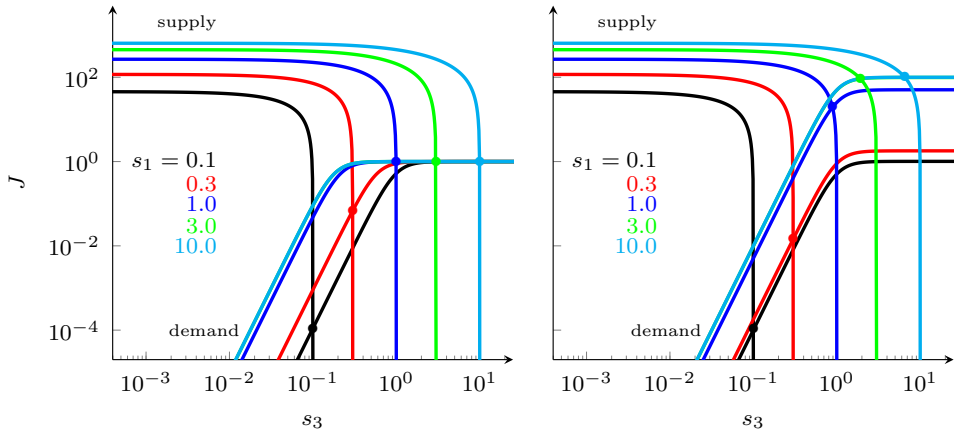

Figure 4.5: Supply and demand rate characteristics with respect to S_3 for the system in Fig. 4.4 with the K-form (left) and the V-form (right) of E_4 at different concentrations of S_1. For K-E_4 $h = 4$, $\alpha = 1000$ and $\gamma = 1$. For V-E_4 $h = 4$, $\alpha = 1$ and $\gamma = 100$. The steady states for each pair of supply-demand characteristics within the E_2-E_3-E_4 reaction block are indicated with a colored dot. In both graphs the S_3-demand rate characteristics for $s_1 = 3$ (green) and $s_1 = 10$ (cyan) are contiguous.

The above nested supply-demand analysis is visualised in Fig. 4.5, which depicts supply and demand rate characteristics with respect to S_3 for the system in Fig. 4.4 with the K and the V-forms of E_4 at different concentrations of S_1. The first important observation is that an increase in s_1 of course also increases the equilibrium concentration of S_3. K_{eq2} and K_{eq3} are both set to 1, so that the S_3-supply block also has $K_{eq23} = 1$, so that here the equilibrium concentration of S_3 increases proportionally with s_1. Now imagine that this did not happen and that, for example, only the black S_3-demand characteristic at $s_1 = 0.1$ in Fig. 4.5 existed. The steady states at the different S_1-concentrations would now all lie on this rate characteristic: the increase in J_{234} with s_1 would be due solely to the allosteric effect and there would be near-perfect homeostatic maintenance of s_3. The real effect is therefore a combination of the

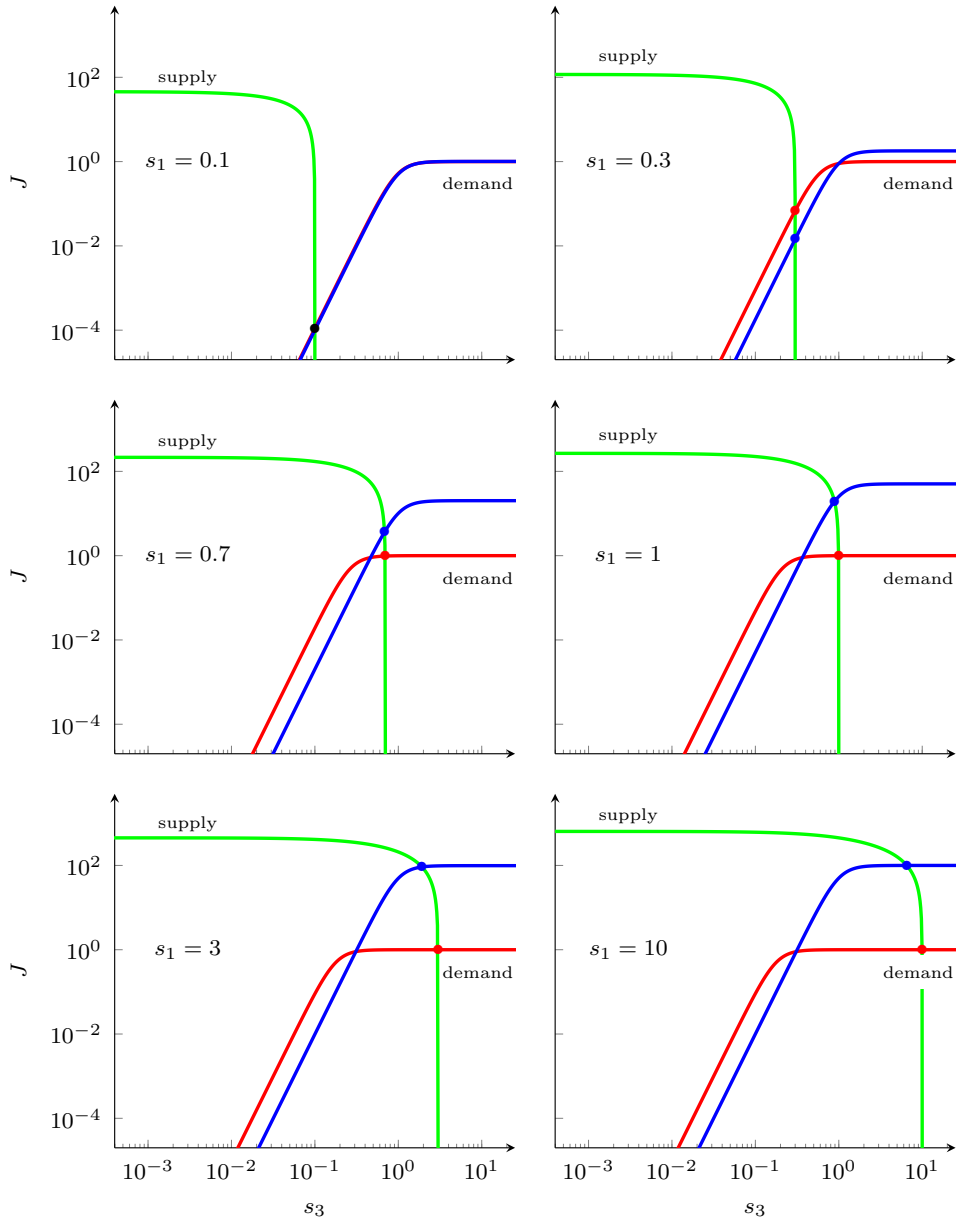

Figure 4.6: Supply and demand rate characteristics with respect to S_3 for the system in Fig. 4.4 at different values of s_1 to compare the effect of K and V-forms of E_4. $K_{4S1} = K_{4S3} = 1$. For K-E_4 $h = 4$, $\alpha = 1000$ and $\gamma = 1$. For V-E_4 $h = 4$, $\alpha = 1$ and $\gamma = 100$.

allosteric effect on v_4 of S_1 which would obtain at constant s_3 and the effect of the thermodynamic increase in s_3 due to the increase in S_1. This means that the s_1-range in which the steady-state J_{234} increases is limited, in this case to s_1-values below about 1 for K-E_4 and below about 3 for V-E_4. In this range $-\varepsilon_{s_3}^{v_{23}} \gg \varepsilon_{s_3}^{v_4}$ and $C_{v_4}^{J_{234}} \to 1$. Above these s_1-values J_{234}-control shifts to the S_3-supply block and feedforward regulation is no longer operative. The difference between the K-E_4 and V-E_4 situations are also clearly visible, in that S_1 not only expands the concentration range where it can activate E_4, but it also increases the limiting rate V_{f4}, thereby increasing the flux-carrying capacity of the S_1-demand block.

Fig. 4.6 provides another perspective on the information in Fig. 4.5. Each graph now combines the supply and demand rate characteristics with respect to S_3 for the K and the V-forms of E_4 at a particular concentration of S_1. At $s_1 = 0.1$ (which corresponds to $s_1/K_{4S1} = 0.1$ since K_{4S1} is by default set to one) there is no difference between the K and V-effects. At higher s_3, within the s_1-range where E_4 is not saturated with S_3, K-E_4 responds to S_3 in a lower s_3-range than V-E_4. This is because the K-effect works both ways: not only does S_1 decrease K_{4S3}, but S_3 also decreases K_{4S1}. This does not happen with a pure V-enzyme where there are no K-effects. What is furthermore clear from the perspective of Fig. 4.6 is the regulatory difference between the K and V-effects: at $s_1 = 0.1$ and $s_1 = 0.3$ both K-E_4 and V-E_4 control J_{234}, but at $s_1 = 0.7$ J_{234}-control has already shifted to the S_3-supply for the system with K-E_4. Only above $s_1 = 3$ does V-E_4 lose control over J_{234}, but by then it has fulfilled its function of increasing J_{234}.

4.2 Graphical analysis of the J_{234}-response to s_1

We now turn to an analysis of the S_1-demand rate characteristics with respect to S_1. Fig. 4.7 shows typical K and V-responses for two values of K_{4S1}. At the point marked (a) the increase in both curves is due to the thermodynamic increase in s_3 linked to the increase in s_1. For $K_{4S1} = 100$ the blue curves describe the situation where S_1 binds so weakly to E_4 that there is no allosteric effect in the s_1-region up to 1; the increase in J_{234} is due solely to

the thermodynamically-linked increase in s_3 with s_1. The allosteric effect is only operational with V-E_4 at the point marked (e) where it increases V_{4f} by a factor of 100. In the situation where S_1 binds strongly to E_4 $K_{4S1} = 0.01$ (the red curves) the allosteric effect increases the J_{234}-response in the region marked (b), either decreasing K_{4S3} of K-E_4 or increasing V_{f4} of V-E_4. In region (c) E_4 is saturated with S_1 so that the increase in J_{234} in region (c) is again due to the thermodynamically-linked increase in s_3 with s_1.

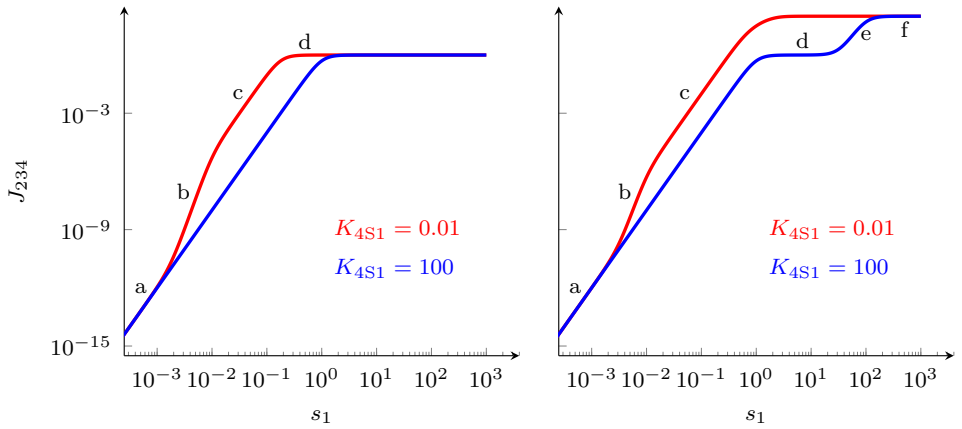

Figure 4.7: Demand rate characteristics with respect to S_1 for the system in Fig. 4.2 with the K-form (left) and the V-form (right) of E_4 at different values of K_{4S1}. The marked regions are discussed in the text. For K-E_4 $h = 4$, $\alpha = 1000$ and $\gamma = 1$. For V-E_4 $h = 4$, $\alpha = 1$ and $\gamma = 100$.

This analysis now makes it much easier to understand Fig. 4.8 in which J_{234}-characteristics with respect to S_1 are plotted for different combinations of K_{4S1} and K_{4S3}. The top two graphs depict the same situation as Fig. 4.7 but at additional intermediate K_{4S1}-values that show how region (b) in Fig. 4.7 shifts to higher s_1 as K_{4S1} increases.

The bottom two graphs in Fig. 4.8 show the converse situation for different values of K_{4S3}. First note the common situation between all four graphs, namely where $K_{4S1} = K_{4S3} = 1$ (the blue curves). For smaller K_{4S3}, S_3 saturates E_4 at lower s_3 so that the response of J_{234} to s_1 is entirely thermodynamically driven (the black and red curves). Weak binding of S_3 ($K_{4S3} > 1$) allows

the allosteric effect to come into play (green and cyan curves); as with the blue curve it is clear in which region there is a steeper allosterically activated response in J_{234} and where the response is thermodynamically driven.

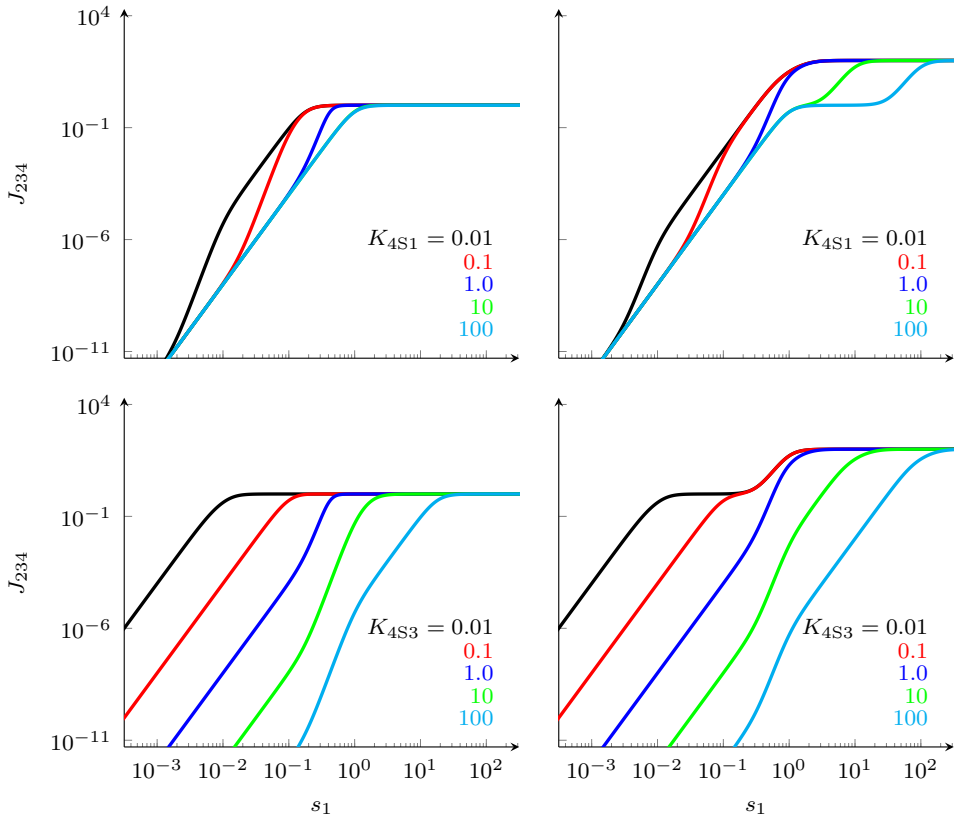

Figure 4.8: Demand rate characteristics with respect to S_1 for the system in Fig. 4.2 with the K-form (left) and the V-form (right) of E_4 at different values of K_{4S3} and K_{4S1}. For K-E_4 $h = 4$, $\alpha = 1000$ and $\gamma = 1$. For V-E_4 $h = 4$, $\alpha = 1$ and $\gamma = 100$.

As Fig. 4.6 provided another perspective on the information in Fig. 4.5, so does Fig. 4.9 on Fig. 4.8. Each graph combines the supply and demand rate characteristics with respect to S_1 for the K and V-forms of E_4 at different values of K_{4S3} and K_{4S1}. Added to these are the (green) curves for an 'unactivated' E_4 that is desensitised to allosteric activation. The graphs in the

left-hand column clearly show how an increase in K_{4S3} allows the K-effect to come into play and how it shifts both the K and the V-curves to lower s_1. The opposite profiles obtain for the different K_{1S4}-values: the K and V allosteric effects only appears at small K_{1S4}-values and the K-effect disappears at high K_{1S4}-values. The other difference is that changes in K_{4S1}-values do not shift the position of the curves relative to each other (they all intersect the J_{234}-axis at the same point).

The broad conclusion from our analysis of feedforward activation is that from a theoretical point of view V-effects are the most effective for ensuring that the allosteric component of feedforward regulation is not affected by the thermodynamic increase in the substrate of the allosteric enzyme, which could saturate the enzyme and thereby abolish K-effects. However, from the review of the literature on allosteric activated enzymes it is clear that both forms occur in practice, and only seldom as the pure V-form or pure K-form. In the next chapter we consider an example of an allosteric enzyme that shows both V and K-effects.

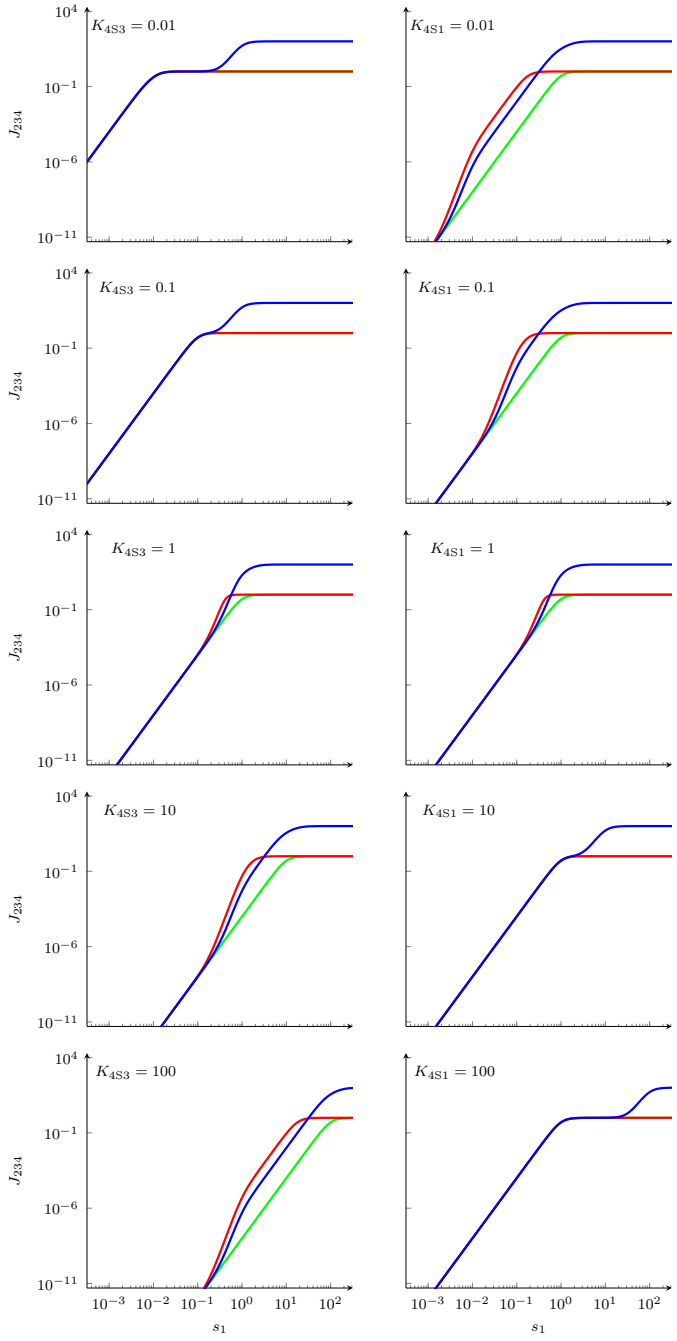

Figure 4.9: Demand rate characteristics with respect to S_1 for the system in Fig. 4.2 to compare the effects of K and V-forms of E_4 at different values of K_{4S3} (left) and K_{4S1} (right). Each graph depicts S_1-demand rate characteristics for a K-activated E_4 ($\alpha = 1000$ and $\gamma = 1$), a V-activated E_4 ($\alpha = 1$ and $\gamma = 100$), and an unactivated E_4 ($\alpha = 1$ and $\gamma = 1$). In all cases $h = 4$.

Chapter 5

Lactate dehydrogenase in *Lactococcus lactis*

Lactococcus lactis (*L. lactis*) is a Gram positive, facultatively anaerobic bacterium with a simple well-characterised metabolism. It lacks a citric acid cycle and the central pathway for glucose utilisation is the Embden-Meyerhof-Parnas (EMP) pathway. High external glucose concentrations result in homolactic fermentation to predominantly lactate via glycolysis, while under glucose-limited conditions the organism switches to mixed-acid (hetero) fermentation. [18]. *L. lactis* is essential in the manufacturing of dairy products and industrial lactic acid production and has recently become the first genetically modified organism to be used alive for the treatment of human disease [4].

Hoefnagel *et al.* [17, 18] constructed a computational model of *L. lactis* glycolysis and the fermentation pathways that branch out from pyruvate. In the metabolic network there is feedforward activation of lactate dehydrogenase by fructose-1,6-bisphosphate and this regulatory loop was incorporated in the model. However, the rate equation for LDH used in this model only incorporated a non-cooperative V-effect of FBP (for which LDH has an absolute requirement), while the kinetic data obtained by Crow and Pritchard [12] clearly showed that the binding of FBP was cooperative, that it had a K-effect on the binding of NADH and pyruvate, and that this K-effect was compet-

itively and cooperatively inhibited by inorganic phosphate. The aim of the investigation described in this chapter was to develop a new rate equation for LDH that incorporated all these additional regulatory features, replace the original LDH rate equation with the new one, and then compare the behaviour of both models to see whether the new features made a significant difference. We also did a number of what-if simulations by removing the different regulatory effects and studying the resulting behaviour of the new model.

Our model, the data and all the rate equations, except the rate equation for LDH, was identical to the model used by Hoefnagel *et al.* [18]. The data for the Hoefnagel-model had been determined by different groups working with different organisms and not always under physiological conditions. All the parameters were based on enzyme kinetics obtained *in vitro*. Where no data were available for *L. lactis* data from another streptococcal species or from other bacteria had been used.

The model consists of 28 reactions with 34 metabolites, and comprises the phosphoenolpyruvate:phosphotransefrase system (PEP:PTS), glycolysis, the pyruvate branches, ATP and NADH utilisation and a reaction for polysaccharide synthesis [18]. Fig. 5.1 is schematic presentation of the model.

The first step is the transport of sugars across the membrane. There are three major sugar uptake systems in bacteria. The phosphoenolpyruvate:phosphotransferase system (PEP:PTS) involves both the transport and phosphorylation of the sugar at the expense of PEP. The PEP:PTS uses a PEP molecule for the transport and concomitant phosphorylation of the imported sugar, and is energetically the most favourable sugar uptake system. The second sugar uptake system is ion-linked and sugar uptake is driven by an ion gradient. The third system involves the transport of sugars by ATPases where ATP hydrolysis is coupled with translocation. *L. lactis* uses the PEP:PTS for the internalisation of different sugars.

Initially all the different sugars are degraded to pyruvate via the EMP-pathway. Pyruvate represents a branch point and has several alternative fates, via either homolactic or mixed-acid fermentation, depending on the environmental and intracellular conditions [6]. ATP is produced by glycolysis

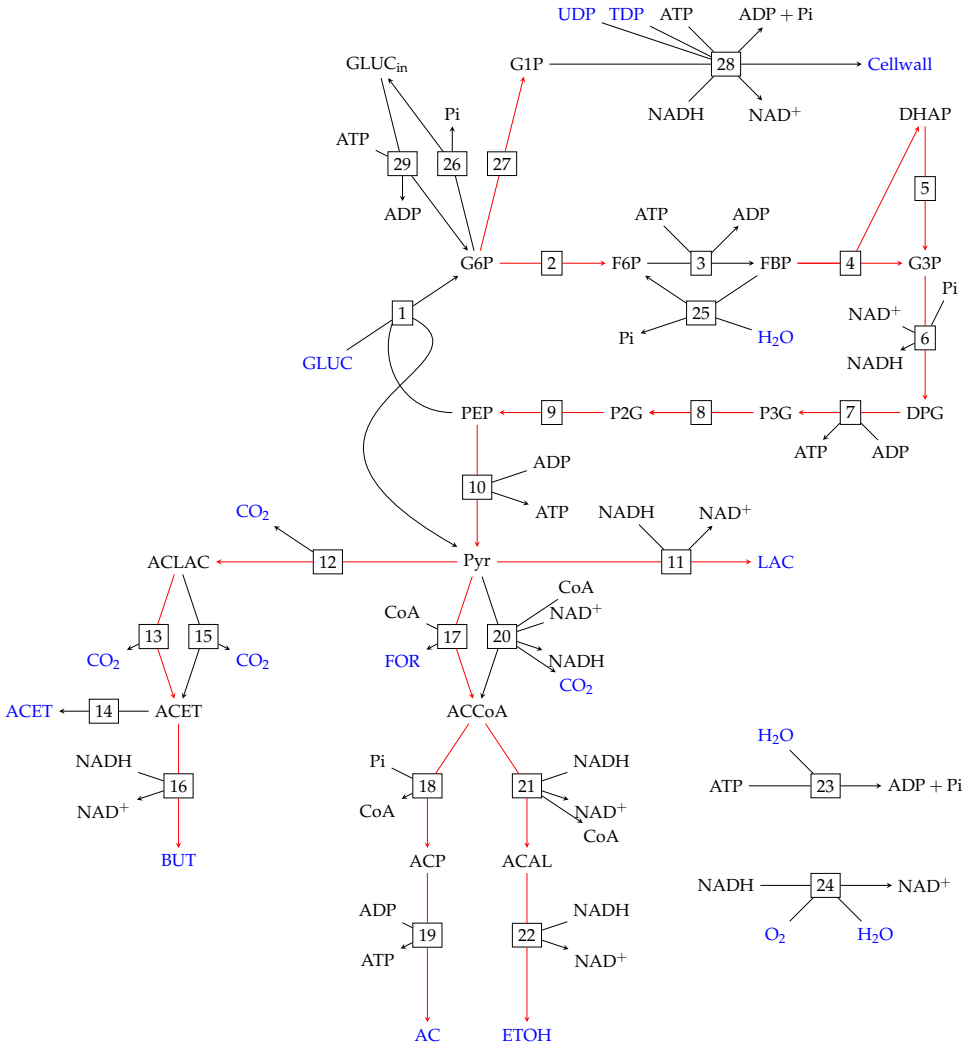

Figure 5.1: Glycolysis and mixed acid fermentation in *Lactococcus lactis*. The red arrows indicate reactions that are modelled with reversible rate equations, while the black arrows indicate irreversible reactions. The metabolites in blue are fixed. Enzyme and metabolite names are listed in Table 5.1.

Table 5.1: Metabolite and enzyme abbreviations and names

AC	acetate	1	PEP:PTS	PEP:phosphotransferase system
ACAL	acetaldehyde	2	PGI	phosphoglucose isomerase
ACCoA	acetyl coenzyme A	3	PFK	phosphofructose kinase
ACET	acetoin	4	ALD	fructose bisphosphate aldolase
ACLAC	α-acetolactate	5	TIP	triosephosphate isomerase
ACP	acetyl phosphate	6	GAPDH	glyceraldehyde-3-phosphate dehydrogenase
ADP	adenosine diphosphate			
ATP	adenosine triphosphate	7	PGK	3-phosphoglycerate kinase
BUT	2,3-butanediol	8	PGM	phosphoglycerate mutase
CO_2	carbon dioxide	9	PPH	enolase
CoA	coenzyme A	10	PK	pyruvate kinase
DHAP	dihydroxy acetonephosphate	11	LDH	lactate dehydrogenase
DPG	1,3-bisphosphoglycerate	12	ALS	α-acetolactate synthase
ETOH	ethanol	13	ALDC	acetolactate decarboxylase
F6P	fructose-6-phosphate	14	ACETEFF	acetoin efflux
FBP	fructose-1,6-bisphosphate	15	NEALC	non-enzymic acetolactate decarboxylase
FOR	formate			
G3P	glyceraldehyde-3-phosphate	16	ACETDH	acetoin dehydrogenase
G6P	glucose-6-phosphate	17	PFL	pyruvate formate-lyase
G1P	glucose-1-phosphate	18	PTA	phosphotransacetylase
GLUC	glucose (extracellular)	19	AK	acetate kinase
$GLUC_{in}$	glucose (intracellular)	20	PDH	pyruvate dehydrogenase
H_2O	water	21	ACALDH	acetaldehyde dehydrogenase
LAC	lactate	22	ADH	alcohol dehydrogenase
NAD	nicotinamide adenine dinucleotide (ox)	23	ATPase	ATPase
NADH	nicotinamide adenine dinucleotide (red)	24	NOX	NADH oxidase
O_2	oxygen	25	FBPase	fructose-1,6-bisphosphatase
Pi	inorganic phosphate	26	G6Pase	glucose-6-phosphatase
P3G	3-phosphoglycerate	27	PGM	phosphoglucomutase
P2G	2-phosphoglycerate	28		Cell wall synthesis
PEP	phosphoenolpyruvate			
PYR	pyruvate			
TDP	thymidine diphosphate			
UDP	uridine diphosphate			

through substrate-level phosphorylation (2 mol of ATP per mol of glucose). A strict balance in the NADH/NAD^+ ratio is maintained; the NAD^+ cofactor reduced during glycolysis is regenerated during pyruvate reduction by LDH.

The first steps in the metabolism of glucose, galactose and lactose all lead to the production of glucose-6-phosphate (G6P), after which the same route through glycolysis follows. G6P is converted to F6P by phosphoglucose isomerase and then to FBP by 6-phosphofructo-1-kinase. FBP is converted to the triose-phosphates dihydroxyacetone phosphate (DHAP) and glyceraldehyde-3-phosphate (GAP) by the enzyme fructose bisphosphate aldolase (ALD). GAP and DHAP can be interconverted by triosephosphate isomerase. 3-Phosphoglycerate (P3G) is formed from GAP by glyceraldehyde-3-phosphate dehydrogenase (GAPDH). P3G is converted to 2-phosphoglycerate (P2G) by phosphoglycerate mutase (PGM). P2G is converted to phosphoenol

pyruvate (PEP) by an enolase and PEP to pyruvate (PYR) by pyruvate kinase (PK). At the level of pyruvate, the metabolic pathway branches [48].

Besides LDH, which converts pyruvate to lactate (LAC), three other enzymes, namely α-acetolactate synthase (ALS), the pyruvate dehydrogenase complex (PDH), and pyruvate formate-lyase (PFL) are able to convert pyruvate under different physiological conditions. ALS is active at high pyruvate concentration and low pH. Conversion of pyruvate through this pathway can produce acetoin (ACET), diacetyl, and 2,3-butanediol (BUT). At low oxygen pyruvate can be converted to diacetyl (an intermediate formed by the non-enzymic decarboxylation of acetolactate—not shown in Fig. 5.1) since the affinity of ALS for pyruvate is very low [26]. PDH is active under aerobic conditions and at low pH, and is inhibited at high NADH concentrations. The end products from this pathway are acetate (AC) and/or ethanol (ETOH) [26]. PFL is active under anaerobic conditions and high pH. The end products are a mixture of formate (FOR), acetate, and/or ethanol [26].

In *L. lactis*, fermentation in resting cells or during rapid growth with high external glucose is predominantly homolactic [18]. Conditions leading to the shift from homolactic fermentation to mixed-acid fermentation include limited glucose availability, growth on maltose, galactose and trehalose, and aerobic conditions [6, 13, 26, 48].

5.1 Constructing the rate equation for nLDH in *L. lactis*

NAD^+-dependent LDH (nLDH) catalyses the conversion of pyruvate and NADH to lactate and NAD^+, and is highly specific for NADH and NAD^+. Crow and Pritchard [12] found that LDH is activated by FBP via a feedforward loop and has an absolute requirement for FBP, while Pi inhibits the binding of FBP to LDH competitively. FBP alters the K_M-values for both pyruvate and NADH as well as the maximum rate V_f. Modifier binding appears to be sigmoidal with a Hill coefficient near 2 (1.7–2.1) for FBP and 2.4 for Pi [12, 14]. Crow and Pritchard [12] concluded from their kinetic study that pyruvate does not affect the K_M for NADH and vice versa.

Previously Hoefnagel *et al.* [17] employed the following reversible random-order bisubstrate-biproduct rate equation in their model:

$$v = \frac{\xi}{1+\xi} V_f \cdot \frac{\sigma_1\sigma_2}{[1+\sigma_1+\pi_1]\,[1+\sigma_2+\pi_2)]} \cdot \left(1 - \frac{\Gamma}{K_{eq}}\right) \tag{5.1}$$

where $\sigma_1 = \frac{[\text{NADH}]}{K_{\text{NADH}}}$, $\sigma_2 = \frac{[\text{PYR}]}{K_{\text{PYR}}}$, $\pi_1 = \frac{[\text{NAD}^+]}{K_{\text{NADH}}}$, $\pi_2 = \frac{[\text{LAC}]}{K_{\text{LAC}}}$, $\Gamma = \frac{[\text{LAC}][\text{NAD}^+]}{[\text{PYR}][\text{NADH}]}$, and $\xi = \frac{[\text{FBP}]}{K_{\text{FBP}}}$.

This equation incorporates an absolute, non-cooperative V-effect of FBP on LDH, but does not account for the cooperative K-effects of FBP and Pi. We were interested whether these additional effects would alter the regulatory behaviour of LDH and we therefore incorporated

- the activation effect of FBP on both the binding of the substrates and products (K-effect) and the limiting rate (V-effect, absolute requirement);
- competitive inhibition of FBP by Pi;
- cooperative binding of FBP and Pi.

The new rate equation for LDH was:

$$v = \frac{\xi^h}{T_1} V_f \cdot \frac{\sigma_1\sigma_2}{\left[\frac{T_1}{T_2} + \sigma_1 + \pi_1\right]\left[\frac{T_1}{T_3} + \sigma_2 + \pi_2\right]} \cdot \left(1 - \frac{\Gamma}{K_{eq}}\right) \tag{5.2}$$

where σ_1, σ_2, π_1, π_2, Γ, and ξ are as above, and

- $T_1 = 1 + \xi^h + \zeta^g$
- $T_2 = 1 + \alpha_1\xi^h + \zeta^g$
- $T_3 = 1 + \alpha_2\xi^h + \zeta^g$
- α_1 and α_2 are the K-effects of FBP on NADH and PYR-binding
- $\zeta = \frac{[\text{Pi}]}{K_{\text{Pi}}}$ (the competitive inhibition of FBP-binding by Pi)
- h, g are the Hill coefficients with respect to FBP and Pi.

Parameter values for modelling with equation 5.2 were either from the original Hoefnagel *et al.* [17] model ($V_f = 3300$U/mg, $K_{eq} = 36000$, $K_{NADH} - 2.4$mM, $K_{LAC} = 100$mM) or from Crow and Pritchard [12] ($K_{FBP} = 0.2$mM, $h = 1.8$). The rest of the parameters (K_{PYR}, K_{Pi}, g, α_1, α_2) had to be calculated from experimental data in [12], as described in the next section.

Determining the parameter values for the LDH rate equation

Experimental data from Crow and Pritchard [12] were employed to determine the parameter values necessary for the construction of the rate equation for LDH. The data in Table 5.2 show the effect of [FBP] on V_f and on the K_M-values of NADH and pyruvate, respectively. These values were used to determine α_1 and α_2.

Table 5.2: Data taken from Table 3 in Crow and Pritchard [12] describing the effect of the activator FBP on the K_M and V_f values for NADH and PYR.

	[PYR] = 10mM		[NADH] = 0.167mM	
FBP (mM)	K_{NADH} (mM)	V_f (U/mg)	K_{PYR} (mM)	V_f (U/mg)
10.0	0.05	2220	ND	ND
1.0	0.07	2020	1.4	1.580
0.5	0.07	1720	1.6	1110
0.1	0.10	347	2.7	215
0.05	0.14	202	4.9	95

To determine K_{NADH} and K_{PYR} in the absence of FBP, as well as α_1 and α_2, which describe the effect of [FBP] on the K_M for NADH and the K_M for PYR respectively, a function was derived by considering, for instance, the term $T_1/T_2 + (\sigma_1 + \pi_1)$ in eqn. 5.2. It can be rewritten as

$$\frac{T_1}{T_2}\left[1 + \frac{T_2}{T_1}\sigma_1 + \frac{T_2}{T_1}\pi_1\right] \tag{5.3}$$

in which

$$\frac{T_2}{T_1}\sigma_1 = \frac{[\text{NADH}]}{\frac{T_1}{T_2}K_{NADH}} \quad \textbf{and} \quad \frac{T_3}{T_1}\pi_1 = \frac{[\text{PYR}]}{\frac{T_1}{T_3}\text{PYR}} \tag{5.4}$$

In the absence of phosphate, i.e., $\zeta = 0$, it follows that:

$$K_{\mathrm{NADH}}(\mathrm{app}) = K_{\mathrm{NADH}} \frac{1 + \left(\dfrac{[\mathrm{FBP}]}{K_{\mathrm{FBP}}}\right)^h}{1 + \alpha_1 \left(\dfrac{[\mathrm{FBP}]}{K_{\mathrm{FBP}}}\right)^h} \tag{5.5}$$

and

$$K_{\mathrm{PYR}}(\mathrm{app}) = K_{\mathrm{PYR}} \frac{1 + \left(\dfrac{[\mathrm{FBP}]}{K_{\mathrm{FBP}}}\right)^h}{1 + \alpha_2 \left(\dfrac{[\mathrm{FBP}]}{K_{\mathrm{FBP}}}\right)^h} \tag{5.6}$$

These functions were fitted to the data in Table 5.2 to provide estimates for α_1, α_2, K_{NADH} and K_{PYR} (see Fig. 5.2).

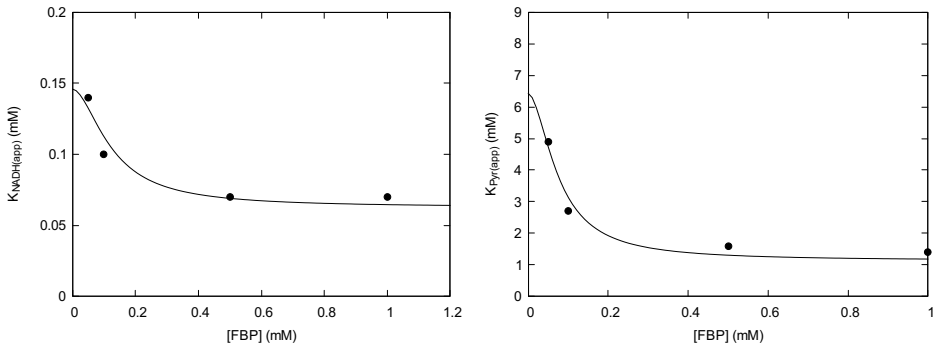

Figure 5.2: Determination of α_1 and K_{NADH} (left-hand) and α_2 and K_{PYR} (right-hand) by fitting eqn. 5.5 and 5.6 to the experimental data in Table 5.2. The parameter values of $K_{\mathrm{FBP}} = 0.2$ mM and $h = 1.8$ were from Table 3 in [12]. Fitting was done with the optimisation function of the plotting program Gnuplot.

Next, K_{Pi} and g had to be determined from Fig. 4 in Crow and Pritchard [12], in which the inhibitory effect of phosphate on FBP activation is plotted. This plot was digitised and the V-effect function, eqn. 5.7 was fitted to the

data to determine values for K_{Pi} and g (see Fig. 5.7).

$$V_{\mathrm{f(app)}} = a \cdot V_{\mathrm{f}} \cdot \frac{\left(\frac{[\mathrm{FBP}]}{K_{\mathrm{FBP}}}\right)^{h}}{1 + \left(\frac{[\mathrm{FBP}]}{K_{\mathrm{FBP}}}\right)^{h} + \left(\frac{[\mathrm{Pi}]}{K_{\mathrm{Pi}}}\right)^{g}} \tag{5.7}$$

where a is a factor used to scale $V_{\mathrm{f(app)}}$ to percentage values.

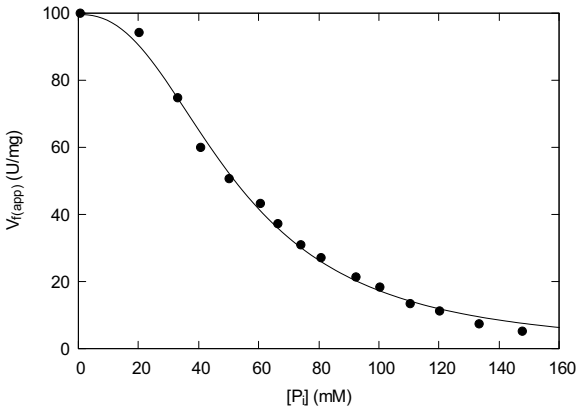

Figure 5.3: Determining values for K_{Pi} and the Hill coefficient, g, to describe competitive inhibition by Pi. The parameter values of $K_{\mathrm{FBP}} = 0.2$ mM and $h = 1.8$ were from Table 3 in [12]. Fitting was done with the optimisation function of the plotting program Gnuplot.

The results of the above fitting procedure are summarised in Table 5.3.

Table 5.3: Parameter values determined from experimental data obtained by Crow and Pritchard [12] for the construction of the LDH-rate equation (K-values in mM).

α_1	K_{NADH}	α_2	K_{PYR}	K_{Pi}	g
2.33	0.15	5.68	6.43	15.3	2.40

5.2 Interlude: An alternative LDH rate equation

Recently Levering *et al.* [31] developed the following rate equation LDH in for *Saccharomyces pyogenes* using convenience kinetics [32, 33]:

$$v = a \cdot V_f \cdot \frac{\sigma_1\sigma_2}{[1+\sigma_1+\sigma_2+\sigma_1\sigma_2+\pi_1+\pi_2+\pi_1\pi_2]} \cdot \left(1 - \frac{\Gamma}{K_{eq}}\right) \tag{5.8}$$

where the activation term

$$a = \left(\frac{\xi}{1+\xi}\right)\left(\frac{\zeta}{1+\zeta}\right)\left(\frac{1}{1+\frac{[NAD^+]}{K_{NAD^+}}}\right) \tag{5.9}$$

This rate equation differs from our eqn. 5.2 in a number of respects: (i) here are no K-effects of FBP, (ii) Pi does not competitively inhibit FBP binding; instead it acts independently and is, as is FBP, an absolute requirement for LDH (in its absence the LDH rate is zero), (iii) neither FBP nor Pi bind co-operatively, (iv) NAD^+ inhibits the enzyme through a non-cooperative V-effect, and (v) the rate equation is based on a rapid-equilibrium random-order mechanism, while ours is based on rapid-equilibrium independent binding of the two substrate/product pairs in which the dead-end complexes pyruvate-NAD^+ and lactate-NADH are also possible besides the productive complexes pyruvate-NADH and lactate-NAD^+.

While interesting, this rate equation is not able to account for the kinetic data of Crow and Pritchard [12] on which our rate equation is based and was therefore not considered any further.

5.3 A comparison of two forms of the Hoefnagel model

Two forms of the model developed by Hoefnagel *et al.* [17, 18]) were compared: the original model (HOEFNAGEL-1) with a model (HOEFNAGEL-2) in which the rate equation for LDH was substituted with eqn. 5.2 with the parameters as listed in the previous sections. Compared to the rate equation in HOEFNAGEL-1, the LDH rate equation in HOEFNAGEL-2 had three

additional features: (i) competitive inhibition of FBP-binding by Pi, (ii) cooperative binding of FBP and Pi, respectively described by h and g, and (iii) the effect of FBP on the binding of NADH and of Pi on the binding of Pyr, respectively described by α_1 and α_2. The PySCeS input file for HOEFNAGEL-1 was obtained from the JWS Online (`http://jjj.biochem.sun.ac.za/`) and only the LDH rate equation and relevant parameters were replaced. The PySCeS input file for HOEFNAGEL-2 is listed in Appendix C.

According to Hoefnagel *et al.* [18], a qualitatively correct model of glucose metabolism by *L. lactis* should describe time-dependent metabolic changes occurring upon glucose depletion (runout) accurately. These changes include a rapid increase in PEP and Pi and a decrease in ATP upon glucose depletion. Also, FBP is relatively slowly depleted. They listed the following features as essential for such a model:

- the activation of PK by FBP and the inhibition by Pi;
- Pi must be modelled as a free metabolite;
- the inhibition of PFK by PEP;
- the inhibition of GAPDH by NADH.

The first two features are important for the rapid increase in PEP and Pi when glucose is depleted. Pi, which is part of a moiety conserved cycle (ATP + G6P + F6P+ 2FBP + G3P + Pi+ P3G + P2G + PEP + DHAP + 2DPG + G1P + ACP = 107.8 mM) is mostly in P2G, P3G, PEP and unbound Pi when glucose is depleted. Two features of the model, the inhibition of PFK by PEP and the inhibition of GAPDH by NADH ensures the gradual decrease in FBP. The inhibition of PFK by PEP ensures the gradual decrease in FBP, G6P and F6P by slowing down the conversion of hexose mono-phosphate to FBP [18].

Upon glucose depletion less Pi is retained in the hexose phosphate pool, resulting in increases in internal Pi and PEP concentration. Since no glucose is available, PEP is not converted to pyruvate via the PEP-PTS and less pyruvate is available as substrate for LDH resulting in rapid accumulation of NADH. GAPDH is severely inhibited by NADH which slows down the conversion of FBP into PEP, explaining the dependence of the rate of glucose

depletion of the hexose phosphate pool (G6P, F6P and FBP) on the rate of NADH oxidation. Under aerobic conditions NADH is oxidized by NADH oxidase, diminishing the inhibition of GAPDH and the model predicts much faster depletion of the hexose phosphate pool than under anoxia [18].

The two models were compared by calculating how their steady-state fluxes and metabolite concentrations changed during a scan of glucose from 0 to 2mM. The scan results for the fluxes are shown in Figs. 5.4 and 5.5 and for the metabolite concentrations in Figs. 5.6 and 5.7. *It should be emphasised that the aim of this comparison was to see whether the more richly regulated LDH in* HOEFNAGEL-2 *made a significant difference to the steady-state profiles and to explain any significant differences as far as possible. We did not aim to analyse and explain the profiles themselves, as this would be a study on its own.*

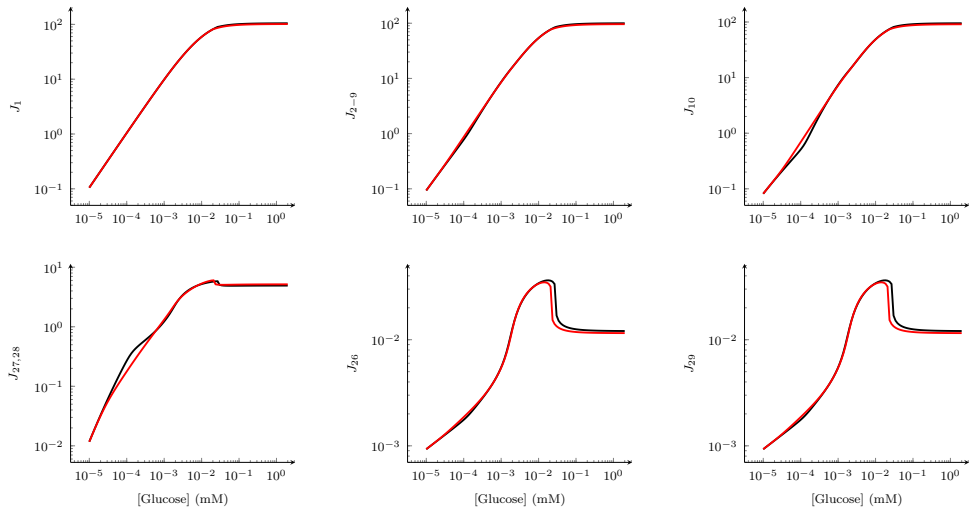

Figure 5.4: A comparison of fluxes in HOEFNAGEL-1 (red) and HOEFNAGEL-2 (black) model in a glucose scan. These fluxes all originate from or end in G6P. Flux unit: J, mmol.(L internal volume)$^{-1}$.min^{-1}.

Above 0.1mM the steady state did not change with a changing glucose concentration. In general, the introduction of the new LDH rate equation had, with one significant exception, very little effect on the steady-state scan profiles of fluxes and concentrations. The changes in the profiles themselves

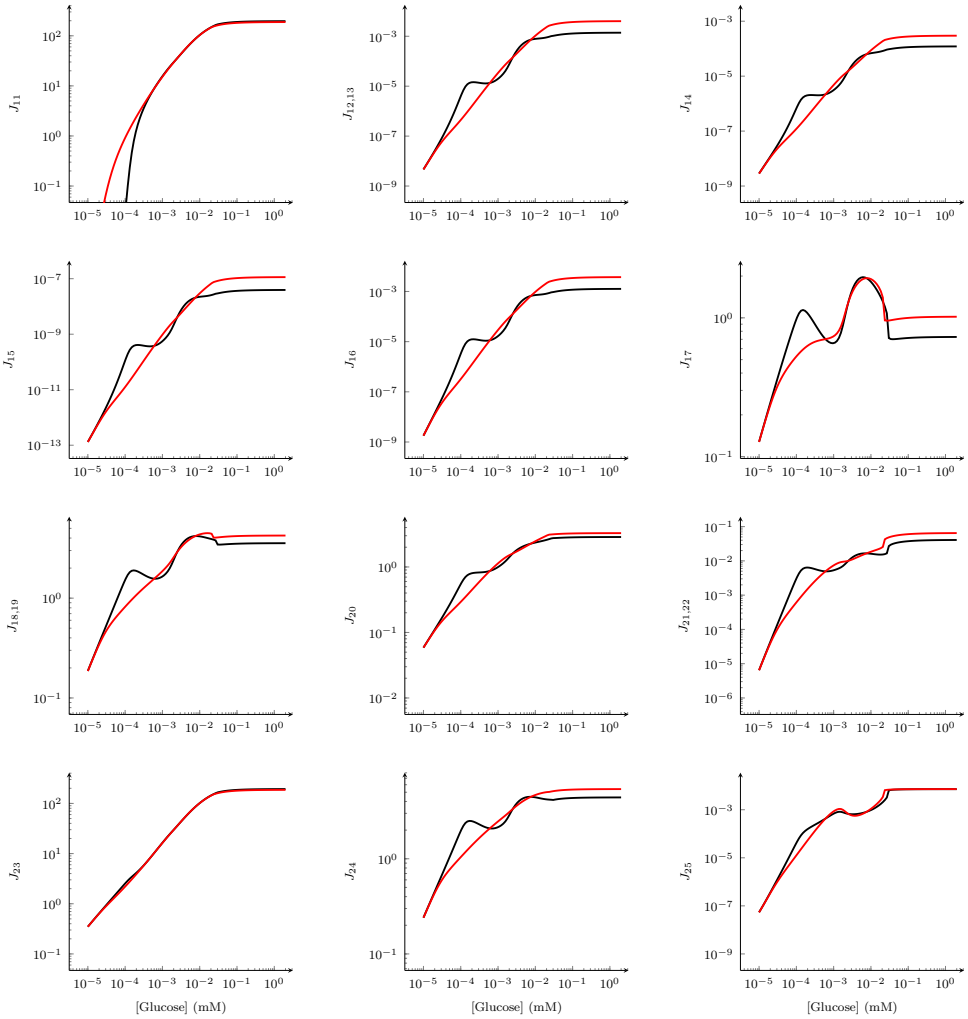

Figure 5.5: A comparison of fluxes in HOEFNAGEL-1 (red) and HOEFNAGEL-2 (black) in a glucose scan. These are fluxes of the fermentation pathways that emanate from Pyr: the LDH branch (J_{11}), the acetoin/butanediol branch (J_{12-16}), and the acetate/ethanol branch (J_{17-22}). Also shown are the ATPase (J_{23}), NADH oxidase (J_{24}), and FBPase (J_{25}) fluxes. Flux unit: J, mmol.(L internal volume)$^{-1}$.min^{-1}.

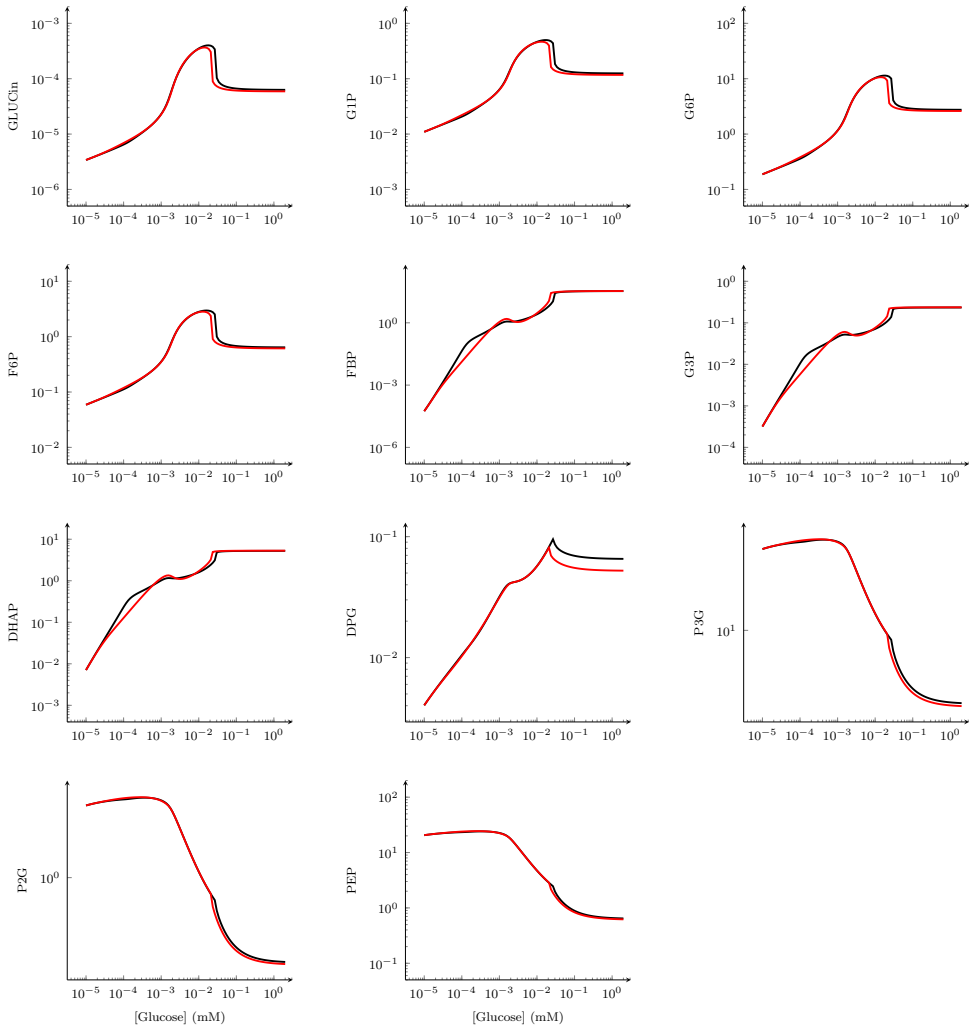

Figure 5.6: A comparison of metabolite concentrations for HOEFNAGEL-1 (red) and HOEFNAGEL-2 (black) in a glucose scan. Y-axis concentration unit: mM.

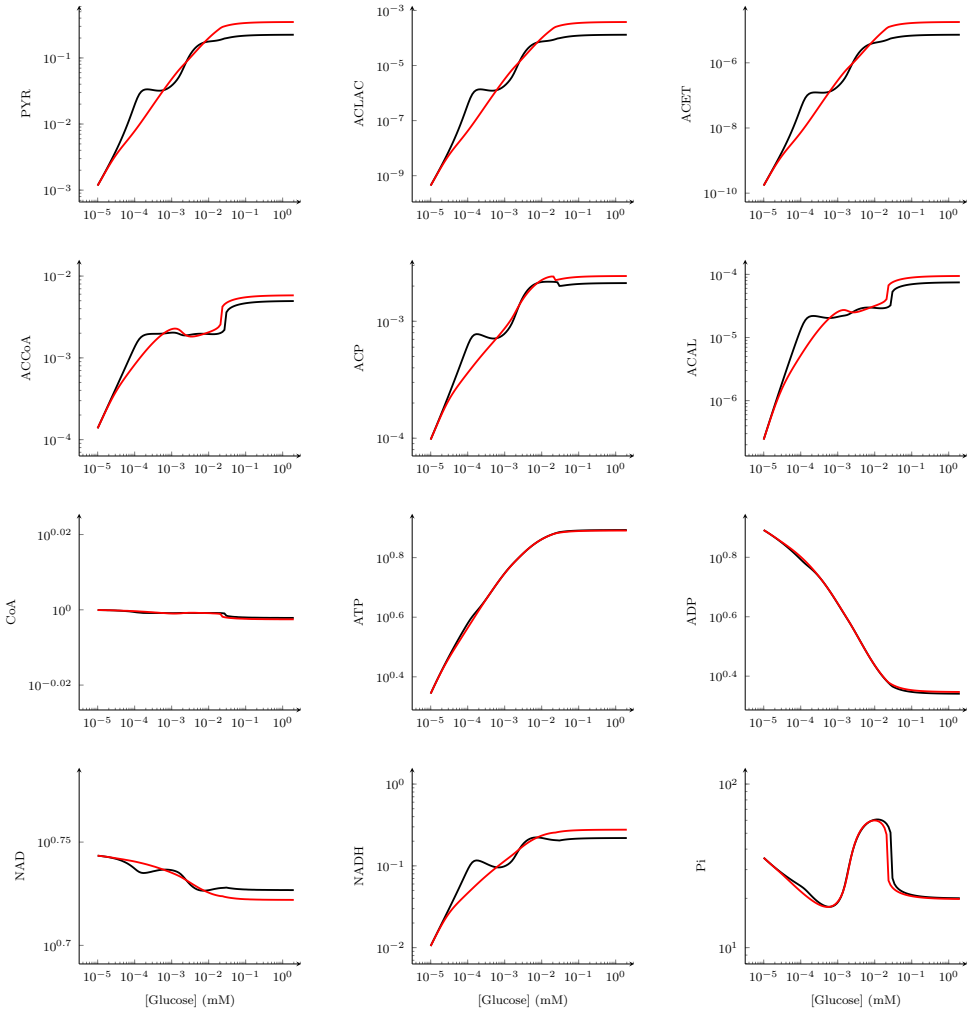

Figure 5.7: A comparison of metabolite concentrations for HOEFNAGEL-1 (red) and HOEFNAGEL-2 (black) in a glucose scan. Y-axis concentration unit: mM.

all occurred at extremely low glucose concentrations (below 50μM) and are probably of physiological significance only in the very last stage of a glucose runout. The fluxes that branch from G6P, including the glycolytic flux to pyruvate J_{2-10}, were slightly increased by the new LDH rate equation (Fig. 5.4), as was the dominating branch flux to lactate, J_{11}) (Fig. 5.5). The steady-state throughout the glucose scan was predominantly homolactic. The relatively minor mixed-acid fermentation fluxes were mainly to acetate and to ethanol, with virtually no flux to acetoin and 2,3-butanediol. However, in all the mixed-acid fermentation branches from pyruvate the new LDH rate equation caused an approximate halving of the fluxes (Fig. 5.5) and, concomitantly, a decrease in the HOEFNAGEL-2 steady-state concentrations of the intermediates in these branches as compared to their HOEFNAGEL-1-values (Fig. 5.7). These decreases in the fermentation fluxes are all related to the decreased concentration of pyruvate, the common substrate for all these branches, and their steady-state profiles in Fig. 5.5 are tightly slaved to that of pyruvate Fig. 5.7).

5.4 Investigating the effect of different forms of the LDH rate equation

Although the results of the comparison of HOEFNAGEL-1 with HOEFNAGEL-2 showed that the new LDH rate eqn. 5.2 certainly changed the steady-state profiles during a glucose scan, it was not clear how the added features contributed to these changes. In order to gain deeper understanding of this question we did a number of what-if experiments that would rarely be possible in practice, and which show the importance of computational modelling as a tool to develop understanding.

A comparison of the V and K-effects on LDH

In this part of the study we compared four forms of LDH in HOEFNAGEL-2:

1. *Our full LDH rate eqn. 5.2.*

2. *An LDH which was completely desensitised to FBP (and, implicitly, to* Pi*).* Although the complete removal of feedforward activation is difficult (but not impossible) to do experimentally, it is possible with modelling to desensitise LDH by removing the V-effect and K-effect terms in the LDH rate equation 5.2 to yield a reversible bi-bi equation that has no absolute requirement for FBP:

$$v = V_f \cdot \frac{\sigma_1\sigma_2}{[1+\sigma_1+\pi_1]\,[1+\sigma_2+\pi_2]} \cdot \left(1 - \frac{\Gamma}{K_{eq}}\right) \tag{5.10}$$

3. *An LDH with only the V-effect of FBP*. The K-effect was removed by setting α_1 and α_2 to one, which sets both T_1/T_2 and T_1/T_3 in eqn. 5.2 to 1. The rate equation differs from the original LDH eqn. 5.1 in that it still contains the competitive inhibition of FBP binding by Pi and cooperativity of FBP and Pi-binding:

$$v = \frac{\xi^h}{1+\xi^h+\zeta^g} V_f \cdot \frac{\sigma_1\sigma_2}{[1+\sigma_1+\pi_1]\,[1+\sigma_2+\pi_2]} \cdot \left(1 - \frac{\Gamma}{K_{eq}}\right) \tag{5.11}$$

4. *An LDH with only the K-effect of FBP*. The V-effect was eliminated by removing the term in eqn. 5.2 that premultiplies V_f:

$$v = V_f \cdot \frac{\sigma_1\sigma_2}{\left[\frac{T_1}{T_2}+\sigma_1+\pi_1\right]\left[\frac{T_1}{T_3}+\sigma_2+\pi_2\right]} \cdot \left(1 - \frac{\Gamma}{K_{eq}}\right) \tag{5.12}$$

The results are presented in Figs. 5.8–5.11. The most general observation is that, where the effects can be clearly distinguished (e.g., Fig. 5.9), the V-effect dominates at glucose concentrations below 10^{-4}mM, and the K-effect dominates at glucose concentrations above 10^{-3}mM, with a contribution from both V and K-effects between 10^{-4} and 10^{-3}mM. What we did find surprising is how little the V-effect on its own contributes to FBP-activation; except for the rather small activation effect below 10^{-4}mM glucose and a barely noticeable activation effect in the region 10^{-3}–10^{-2}mM glucose (e.g., J_{15} in Fig. 5.9) the curve for the V-effect alone (green) coincides with the curve for a completely desensitised LDH (red), i.e., the complete absence of feedforward activation. This implies that the distinct differences between the

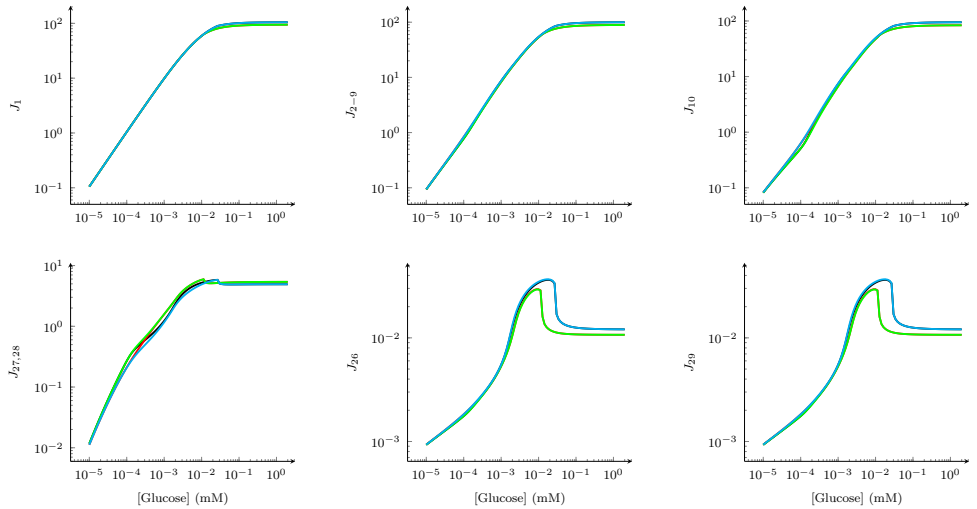

Figure 5.8: The effect of different forms of the LDH rate equation in HOEFNAGEL-2 on the fluxes that originate from or end in G6P. (1) The full rate LDH rate eqn. 5.2 (black), (2) the desensitised LDH (red), (3) an LDH with only the V-effect of FBP (green), and (4) an LDH with only the K-effect of FBP (cyan). In the graphs for J_{26} and J_{20} the cyan and black curves coincide, and the red and green curves coincide. Flux unit: J, mmol.(L internal volume)$^{-1}$.min^{-1}.

.

green/red curves and black/cyan curves are mostly due to the K-effects of FBP. Above 10^{-4}mM glucose the black curves of the full form of the LDH rate equation and the cyan curves of the K-effect LDH form have the same general shape. The 'bumps' on the curves are, however, much more exaggerated on the black curves than on the cyan curves, and this is clearly due to the V-effects that operate in those glucose regions.

It is also clear that the V-effect had no influence on the fluxes J_{26}, J_{29} in Fig. 5.8, and the concentrations of $GLUC_{in}$, G1P, G6P, F6P, DPG, P3G, P2G, and PEP in Fig. 5.10 and CoA, ATP, ADP, and Pi in Fig. 5.11. For these steady-state variables the K-effect (cyan) completely accounts for the scan profiles with the full LDH equation (black).

The only exception to the above general conclusions is the LDH flux itself (J_{11} Fig. 5.9) where the cyan and red curves coincide, and the black and green curves coincide, which means that here the K-effect plays no activatory role,

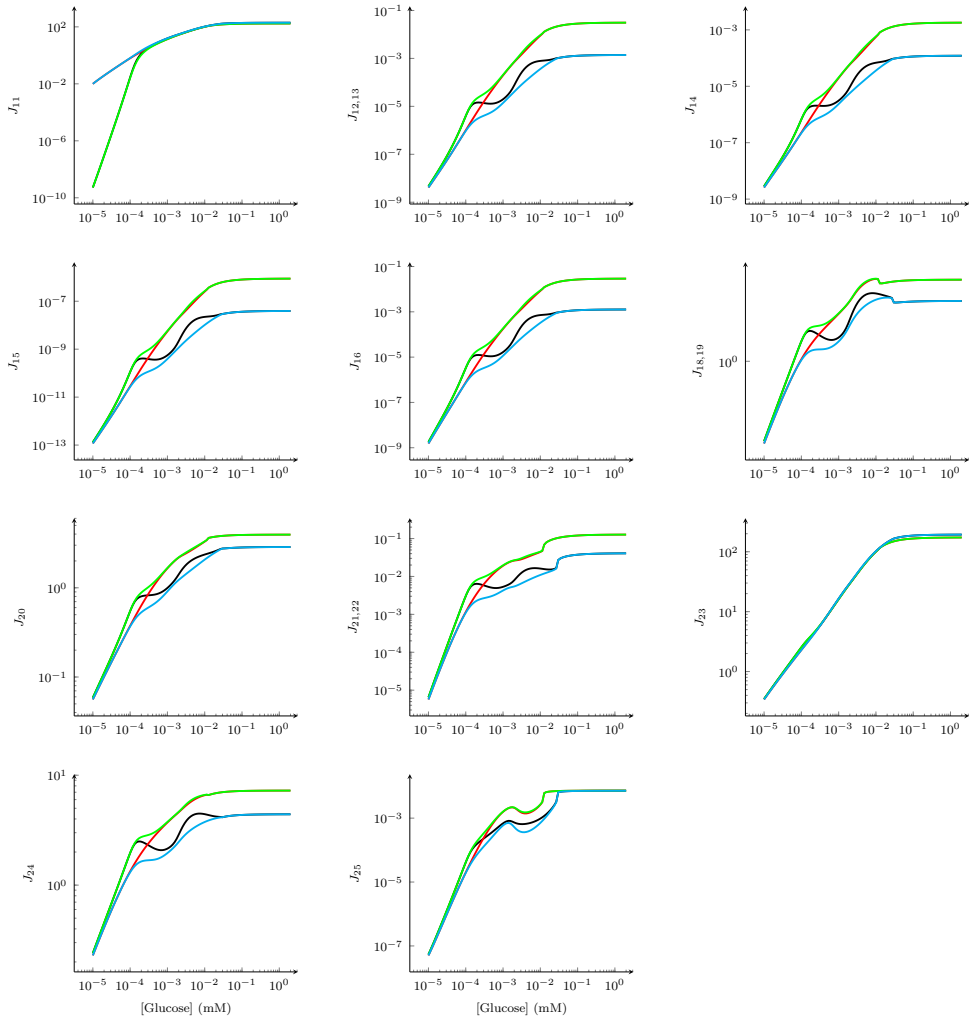

Figure 5.9: The effect of different forms of the LDH rate equation in HOEFNAGEL-2 on the fluxes of the fermentation pathways that emanate from Pyr. (1) The full rate LDH rate eqn. 5.2 (black), (2) the desensitised LDH (red), (3) an LDH with only the V-effect of FBP (green), and (4) an LDH with only the K-effect of FBP (cyan). In the graph for J_{11} the cyan and red curves coincide, and the black and green curves coincide. Flux unit: J, mmol.(L internal volume)$^{-1}$.min^{-1}.

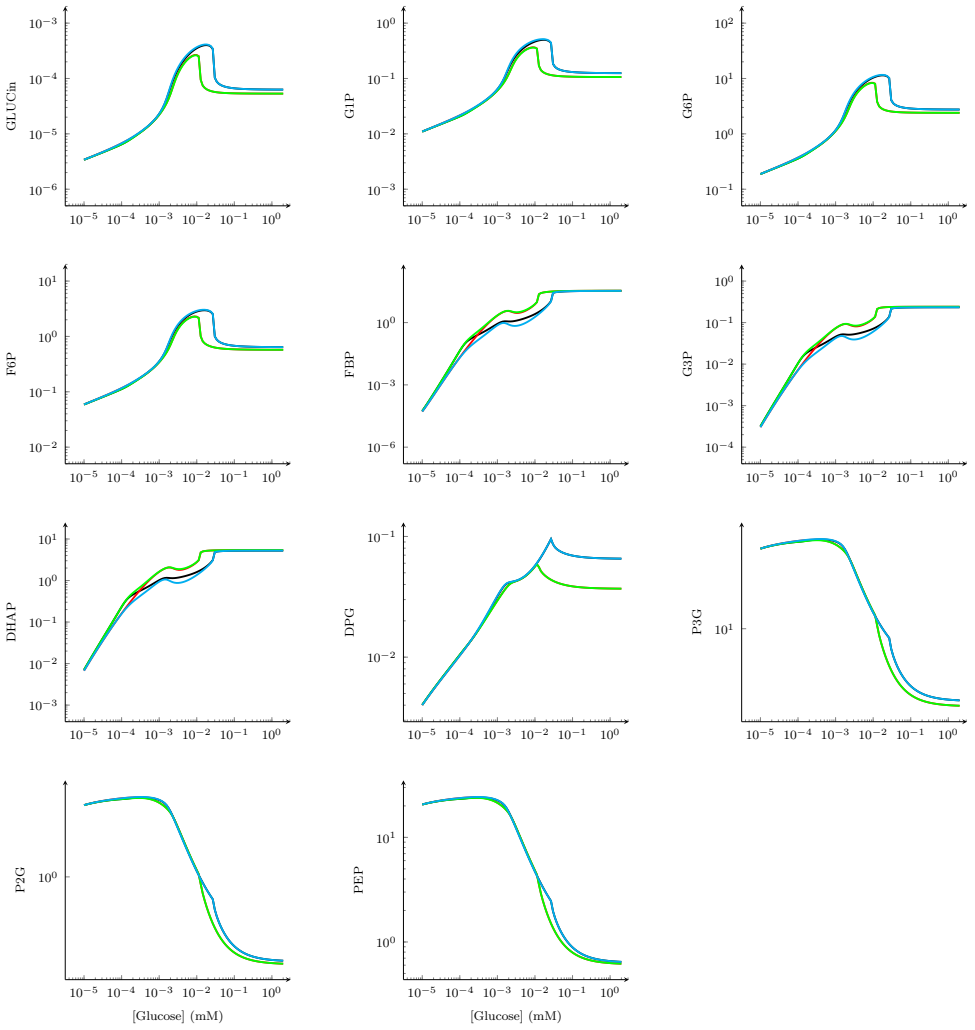

Figure 5.10: The effect of different forms of the LDH rate equation in HOEFNAGEL-2 on the metabolite concentrations. These are all glycolytic intermediates up to PEP. (1) The full rate LDH rate eqn. 5.2 (black), (2) the desensitised LDH (red), (3) an LDH with only the V-effect of FBP (green), and (4) an LDH with only the K-effect of FBP (cyan). Where curves coincide it is cyan/black and red/green. Y-axis concentration unit: mM.

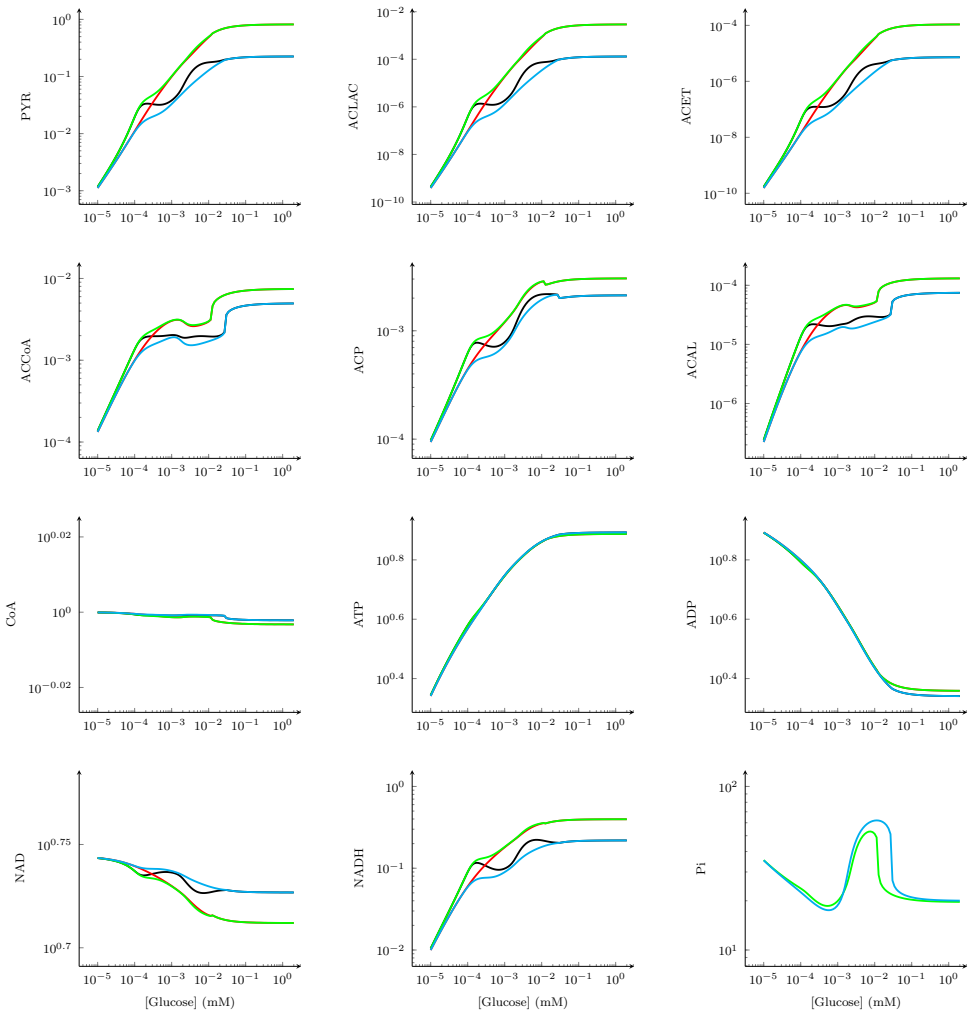

Figure 5.11: The effect of different forms of the LDH rate equation in HOEFNAGEL-2 on the metabolite concentrations. These are the metabolites in the fermentation branches from pyruvate, as well as ATP, ADP, NAD^+, NADH, and Pi. (1) The full rate LDH rate eqn. 5.2 (black), (2) the desensitised LDH (red), (3) an LDH with only the V-effect of FBP (green), and (4) an LDH with only the K-effect of FBP (cyan). Where curves coincide it is cyan/black and red/green. Y-axis concentration unit: mM.

and that the J_{11}-profile is determined completely by the V-effect throughout the full glucose scan range.

The effects of binding cooperativity and Pi-inhibition of FBP-binding

We also determined the effect of removal from the LDH rate equation in HOEFNAGEL-2 of

1. the cooperative binding of FBP and Pi, by setting their respective Hill coefficients h and g in in eqn. 5.2 to one.

2. the competitive inhibition of FBP-binding by Pi, by setting $T_2 = 1 + \alpha_1 \zeta^h$ and $T_3 = 1 + \alpha_2 \zeta^h$ in eqn. 5.2.

The effects of these alterations to the LDH rate eqn. 5.2 are clearly visible only in the fluxes (Fig. 5.12) and some of the metabolite concentrations (Fig. 5.13) of the fermentation pathways that emanate from Pyr, as well as NAD^+ and NADH. The effects on the other fluxes and metabolite concentrations are either much smaller or negligible (not shown).

The effects of cooperative binding of FBP and Pi are quite distinct from the effects of Pi-inhibition of FBP-binding and only visible at low glucose concentrations. The bump in the LDH curve in the glucose concentration region of 10^{-4}–10^{-3}mM is clearly due to the cooperativity of FBP and Pi-binding, while the bump in the 10^{-3}–10^{-2}mM region is due to Pi-inhibition of FBP-binding.

In summary, in HOEFNAGEL-2 the activating V-effect of FBP on LDH operates mostly at very low glucose concentrations, while the K-effect of FBP on LDH operates only at higher glucose concentrations. The K-effect still dominates in the region between exclusively V-effect and exclusively K-effect, and it is only in this region that the cooperative binding of FBP and Pi and the Pi-inhibition of FBP-binding have any visible effect.

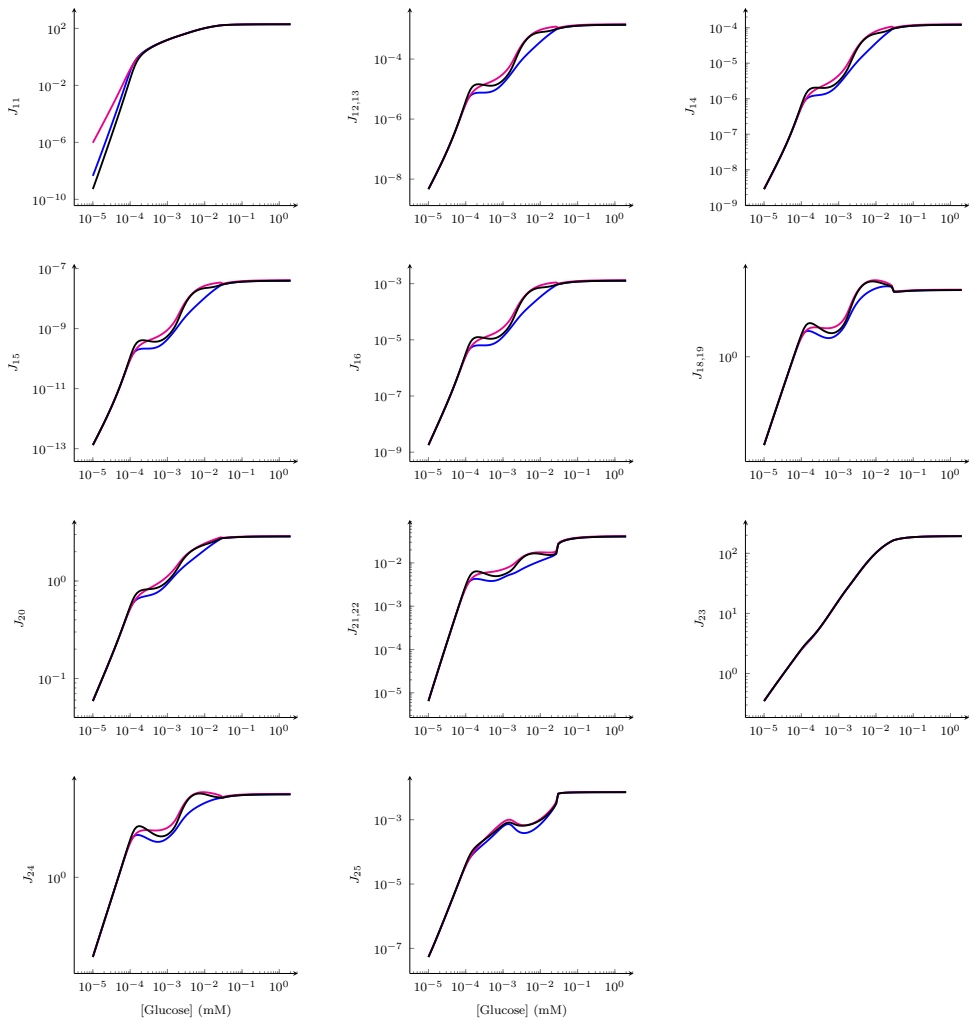

Figure 5.12: The effects of removal of cooperative binding and of Pi-inhibition of FBP-binding in the LDH rate equation in HOEFNAGEL-2 (black) on the fluxes of the fermentation pathways that emanate from Pyr. (1) The cooperativity of FBP and Pi-binding was removed by setting $h = g = 1$ (magenta); (2) the effect of inhibition by Pi was removed by making the enzyme insensitive to Pi (blue). Flux unit: J, mmol.(L internal volume)$^{-1}$.min^{-1}.

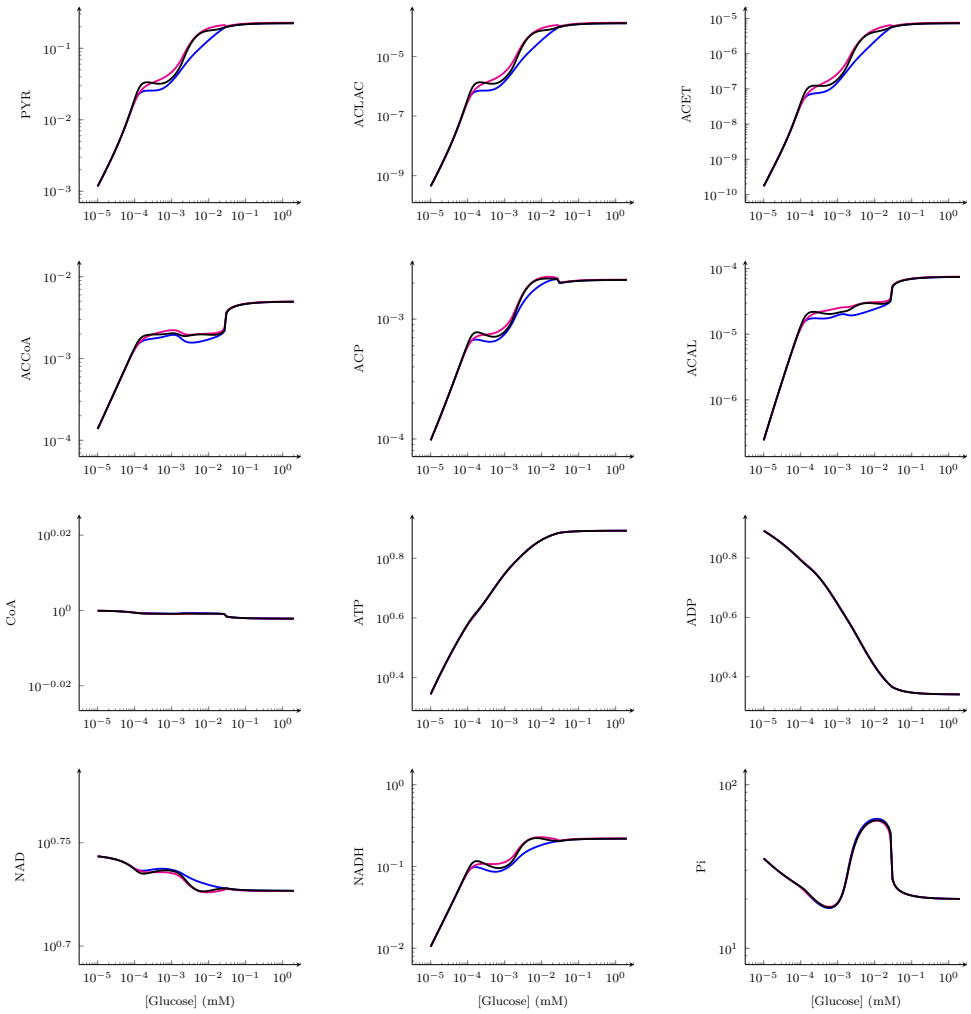

Figure 5.13: The effects of removal of cooperative binding and of Pi-inhibition of FBP-binding in the LDH rate equation in HOEFNAGEL-2 (black) on the metabolite concentrations. These are the metabolites in the fermentation branches from pyruvate, as well as ATP, ADP, NAD^+, NADH, and Pi. (1) The cooperativity of FBP and Pi-binding was removed by setting $h = g = 1$ (magenta); (2) the effect of inhibition by Pi was removed by making the enzyme insensitive to Pi (blue). Y-axis concentration unit: mM.

Chapter 6

Discussion

The study described in this thesis was concerned with the regulatory phenomenon of feedforward activation in metabolism. Feedforward activation was studied by means of metabolic control analysis and supply-demand analysis of a minimal system subject to feedforward activation. An initial control analysis of the full system suggested that saturation of the allosteric enzyme with its substrate would allow it to control the flux through the demand pathway for the allosteric activator. The enzyme kinetics of K-enzymes however showed that under these conditions the allosteric effect is abolished, and other conditions under which the allosteric enzyme controlled its demand flux were searched for using supply-demand analysis, which showed that the allosteric enzyme would have the necessary control of the activator demand flux if the nested supply flux for its substrate was near equilibrium. V-enzymes are not subject to this limitation, and the catalytic allosteric effect operates under conditions of substrate saturation of the allosteric enzyme.

Nevertheless there is still a problem with the nested supply flux of the substrate of the allosteric enzyme needing to be near equilibrium to ensure that the allosteric enzyme controls this flux. In our model we assumed that the equilibrium constant of the E_2-E_3 was one. This ensure that equilibrium concentration of S_3 would the same as s_1. What if this equilibrium constant was very high, as often is the case? This would mean a correspondingly high equilibrium concentration relative to s_1, which could saturate E_3 at very low

s_1 (depending of course the values of K_{4S1} and K_{4E3}). There is one situation that could be exploited to avoid this avoid this problem and that is depicted in Fig. 6.1 in which E_3 is a bisubstrate-biproduct reaction instead of a uni-uni reaction. Such reactions are in fact ubiquitous, whereas uni-uni reactions (which are all isomerisation reactions) are relatively rare. The equilibrium constant for this reaction is:

$$K_{eq3} = \frac{s_3 s_5}{s_2 s_4} \tag{6.1}$$

which can be rearranged to

$$\frac{s_3}{s_2} = K_{eq3}\frac{s_4}{s_5} \tag{6.2}$$

Now assume that E_3 has a high equilibrium constant. It is clear that it is possible to keep the s_3/s_2 ratio low by ensuring an s_4/s_5 ratio that negates the high value of K_{eq3}. For example, to ensure that at equilibrium $s_3/s_2 = 1$ the rate of E_5 must be such that it drives the s_4/s_5 to a value of $1/K_{eq3}$. In such a way metabolic systems could in principle prevent saturation of the allosteric enzyme by its substrate.

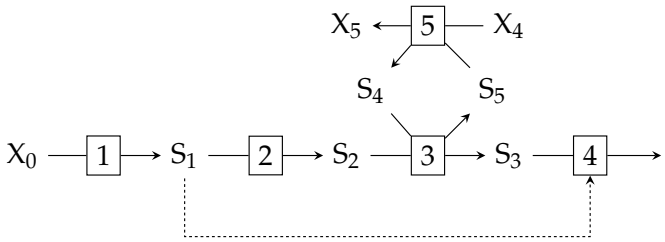

Figure 6.1: The feedforward-regulated pathway in Fig. 4.1 with the E_3-catalysed reaction is altered to a bisubstrate-biproduct reaction, of which the S_4 and S_5 substrate and product pair is reconverted by the E_5-catalysed reaction.

The second part of the study was concerned with a particular allosteric enzyme, lactate dehydrogenase (LDH) in glucose fermentation metabolism in *Lactococcus lactis*, which is activated through feedforward action by fructose-1,6-bisphosphatase (FBP), with the interesting twist that it also has an absolute requirement for FBP. An existing kinetic model of this metabolic pathway contained a rate equation for LDH that only incorporated a non-cooperative V-effect of FBP, but omitted other potentially important effects that have been

described in the literature, such as the competitive inhibition of FBP binding by inorganic phosphate (Pi), cooperative binding of both FBP and Pi, and the alteration of the K_M-values of both the substrates pyruvate and NADH (K-effects). A new rate equation for LDH that incorporated these effects was developed and parameterised with data from the literature. The kinetic model with the original and one with the new rate equation were compared in terms of their steady-state behaviour as the external glucose concentration was increased from 0 to 2mM. The only observable differences occurred at glucose concentrations below 50μM and are probably of physiological significance only in the very last stage of glucose depletion. With our new LDH rate equation there was a decrease in the mixed acid fermentation fluxes as compared to the original model. We were able to relate the observed differences to the different types of allosteric effects through a series of 'what-if' experiments in which we compared the effects of four forms of our rate equation: the full equation, one which was completely desensitised to FBP, one with V-effects only and one with K-effects only. We also studied the effects of binding cooperativity of FBP and Pi-binding, and of Pi-inhibition of FBP-binding. We found that the activating V-effect of FBP on LDH operated mostly at very low glucose concentrations, while the K-effect of FBP onLDH operated only at higher glucose concentrations. The K-effect still dominated in the region between exclusively V-effect and exclusively K-effect, and it is only in this region that the cooperative binding of FBP and Pi and the Pi-inhibition of FBP-binding had any visible effect.

Despite the wealth of metabolic information and available genetic tools, we still do not have a comprehensive understanding of sugar metabolism and regulatory pathways in *L. lactis*. One way that has already contributed to and promises to contribute more to our understanding is through the approach of computational systems biology to the quantitative study of metabolic models. The development of such models depends not only on reliable data of intracellular concentrations of intermediates and metabolic fluxes, but also on accurate and properly parameterised rate equations. Our study of two different rate equations for lactate dehydrogenase in *L. lactis* showed how much understanding can be gained by using a rate equation that ac-

counts for all the known regulatory effects.

Although there is already a great deal of correspondence between models and experimental data of the primary metabolism in *L. lactis*, there are still shortcomings. These include the problems of using too simplistic rate equations, of using possibly inappropriate kinetic data obtained from related organisms, of obtaining kinetic information from databases such as Brenda or Sabio-RK, where assay conditions for each enzyme are often different. Also, differences between results obtained *in vivo* and *in vitro* can cause problems. Important effects are often absent from models either because not enough information is available, or because we do not even know of the existence of the effect. Levering *et al.* [31] reported that incorporation of the effect of extracellular Pi on intracellular phosphorylated glycolytic intermediates is essential to quantitatively fit reported NMR data. Failing to model Pi transport results in much lower [FBP] and intracellular [Pi] levels which affects the regulation of many of the glycolytic processes including PTS, PK and LDH [31]. In both HOEFNAGEL-1 and HOEFNAGEL-2 there is no transport of extracellular phosphate into or out of the cell. Neither model addresses the role of HPr protein in glucose uptake. In *L. lactis* FBP and Pi inhibits the PTS system via a feedback loop. Within the PTS system, the HPr protein has a dual role: when phosphorylated at His-15 phosphate group-transfer leads to uptake and phosphorylation of glucose. When phosphorylated at Ser-46, which is promoted by FBP, HPr acts as a signalling intermediate in glucose repression, thus inhibiting glucose uptake. This feedback loop is considered important during sudden changes in glucose availability affording a degree of robustness.

Despite these shortcomings much has been gained from the modelling studies of glucose metabolism in *L. lactis*. They show that the control of flux resides outside the metabolic pathway. ATP demand controls the flux when working below maximum capacity and when working at maximum capacity glucose transport controls the flux. The glycolytic flux and the fermentation pattern are regulated through the glycolytic allosteric enzymes PFK, LDH and PK. The shift in fermentation products is associated with shifts in the phosphate pools. A rapid increase in PEP and Pi and a decrease in ATP is

observed upon glucose depletion resulting in less Pi in the hexose phosphate pool. The redistribution of the phosphate has important consequences as many enzymes are sensitive to phosphate containing metabolites [39, 47]. PFK is inhibited by PEP, PK is activated by FBP and inhibited by Pi, and LDH is activated by FBP and inhibited by Pi. In the branches the acetate kinase isozymes are inhibited by FBP, G3P and PEP and PFL is inhibited by DHAP and G3P. An important question that remains to be answered is which kinetic parameters are the most important in the distribution of phosphate.

In addition to the distribution of the phosphate pool, oxygen also influences the carbon metabolism of *L. lactis*. Under anaerobic conditions, sugars are converted to lactate or mixed acid products formate, ethanol and acetate. Oxygenation results in an altered redox state and greater NADH oxidase activity and NAD^+ is regenerated through this pathway [43]. Though the factors behind the metabolic switch to mixed acid fermentation remain unclear at least two different allosteric mechanisms, involving the phosphorylated pools (FBP/Pi/ADP/ATP) and the redox balance ($NADH/NAD^+$) are likely to be involved.

Appendix A

The elasticity expressions of $\varepsilon_{s_1}^{v_4}$ for the K and V-forms of E_4

Analytical expressions for $\varepsilon_{s_1}^{v_4}$ of the K and V-forms of E_4 can be obtained by partial differentiation of the logaritmic forms of the rate eqns. 4.9 and 4.9 [25].

K-enzyme

$$\varepsilon_{s_1}^{v_4} = \frac{h(\alpha-1)\left(\frac{s_1}{K_{4S1}}\right)^h}{\left(1+\alpha\left(\frac{s_1}{K_{4S1}}\right)^h\right)\left[\left(\frac{s_3}{K_{4S3}}\right)^h\left(1+\alpha\left(\frac{s_1}{K_{4S1}}\right)^h\right)+1+\left(\frac{s_1}{K_{4S1}}\right)^h\right]} \tag{A.1}$$

The elasticity coefficient $\varepsilon_{s_1}^{v_4}$ depends on the values of h, α, K_{4S1} and K_{4S3}, the latter indicating that the degree of saturation of E_4 by S_3 affects the functioning of the activator. When $\alpha = 1$, $\varepsilon_{s_1}^{v_4} = 0$ and S_1 cannot affect v_4. When $\alpha < 1$ S_1 acts as an activator, and when $\alpha > 1$ as an inhibitor. Fig. A.1 shows how $\varepsilon_{s_1}^{v_4}$ for a K-enzyme varies with s_1 at different combinations of α and s_3/K_{4S3}. The bell-shaped curves tend the maximum of $h = 4$ at high values of α and s_3/K_{4S3} below 0.1. As s_3/K_{4S3} increases above 0.1, $\varepsilon_{s_1}^{v_4}$ decreases and at $s_3/K_{4S3} = 2$ is effectively zero, the phenomenon we previously called the abolishment of activator effect when enzyme becomes saturated with substrate.

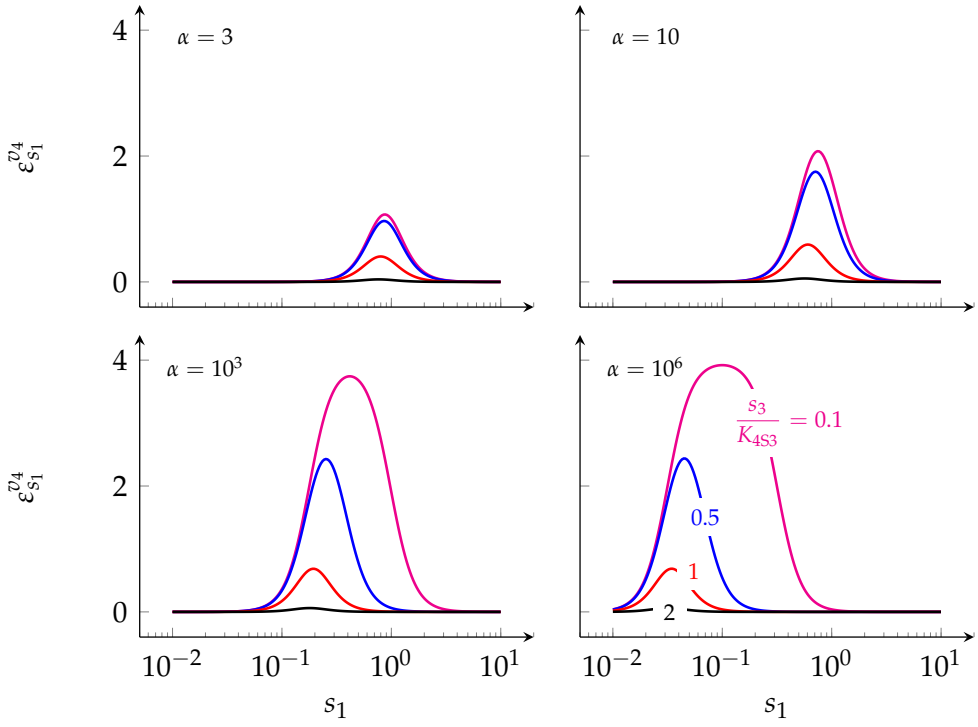

Figure A.1: Variation of $\varepsilon_{s_1}^{v_4}$ of the K-form of E_4 (eqn. A.1) with s_1 at different values of α and s_3/K_{4S3}. Values of s_3/K_{4S3} below 0.1 does not increase the maximum value of $\varepsilon_{s_1}^{v_4}$ any further. In each graph the curve for $s_3/K_{4S3} = 0.1$ represent the maximum $\varepsilon_{s_1}^{v_4}$ that can be reached at the indicated value of α.

V-enzyme

$$\varepsilon_{s_1}^{v_4} = h(\gamma - 1)\frac{\left(\frac{s_1}{K_{4S1}}\right)^h}{\left(1 + \gamma\left(\frac{s_1}{K_{4S1}}\right)^h\right)\left(1 + \left(\frac{s_1}{K_{4S1}}\right)^h\right)} \tag{A.2}$$

The elasticity coefficient $\varepsilon_{s_1}^{v_4}$ depends on the values of h, γ and K_{4S1}. When $\gamma = 1$, $\varepsilon_{s_1}^{v_4} = 0$ and S_1 cannot affect v_4. When $\gamma > 1$ S_1 acts as an activator, and when $\gamma < 1$ as an inhibitor. With increasing γ the maximum value of $\varepsilon_{s_1}^{v_4}$ increases to a limiting value of $h = 4$ and the concentration range in which S_1 activates E_4 expands to lower s_1.

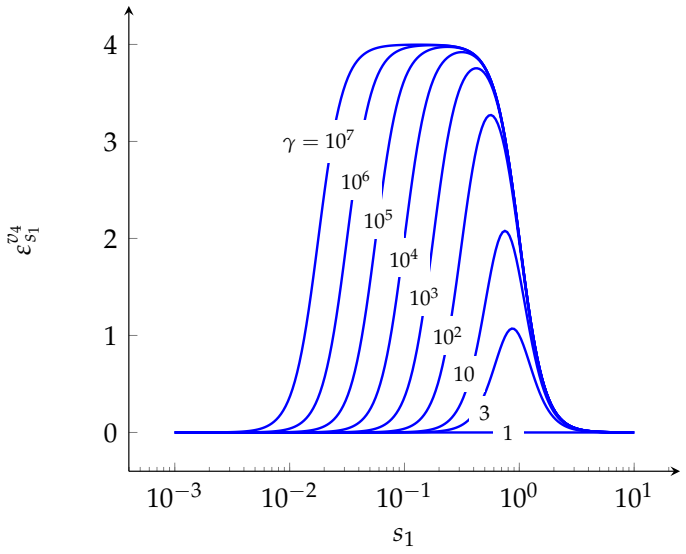

Figure A.2: Variation of $\varepsilon_{s_1}^{v_4}$ of the V-form of E_4 (eqn. A.2) with s_1 at different values of γ.

Appendix B

Pysces input file: FeedForward activation model

```
Modelname: FeedForwardActivation_S1_fixed.psc
Description: Feedforward activation in a 4-step linear metabolic pathway

# X0 <==> S1 <==> S2 <==> S3 <==> X4 with feedforward activation of E4 by S1
#         |____________________|

FIX: X0 S1 X4       # Supply-demand analysis around S1
# FIX: X0 S1 S3 X4  # Supply-demand analysis around S3 at fixed S1

R1: X0 = S1

(Vf1/K1_X0) * (X0 - S1/Keq1)/(1 + X0/K1_X0 + S1/K1_S1)

R2: S1 = S2

(Vf2/K2_S1) * (S1 - S2/Keq2)/(1 + S1/K2_S1 + S2/K2_S2)

R3: S2 = S3

(Vf3/K3_S2) * (S2 - S3/Keq3)/(1 + S2/K3_S2 + S3/K3_S3)

R4: S3 = X4

(Vf4/K4_S3)*(S3 - X4/Keq4)*((S3/K4_S3 + X4/K4_X4)**(h-1))*(1 + g*a*(S1/K4_S1)**h)/
(((S3/K4_S3 + X4/K4_X4)**h)*(1 + a*(S1/K4_S1)**h) + 1 + (S1/K4_S1)**h)

# Fixed metabolites
X0 = 1.0
X4 = 0.0
S1 = 1.0

#Variable metabolites
```

```
S2 = 1.0
S3 = 1.0

#Kinetic parameters
Vf1   = 1.0
Keq1  = 1.0
K1_X0 = 1.0
K1_S1 = 1.0

Vf2   = 1.0
Keq2  = 1.0
K2_S1 = 1.0
K2_S2 = 1.0

Vf3   = 1.0
Keq3  = 1.0
K3_S2 = 1.0
K3_S3 = 1.0

Vf4   = 1.0
Keq4  = 1.0
K4_S3 = 1.0
K4_X4 = 1.0
K4_S1 = 1.0
h     = 1.0
g     = 1.0
a     = 1.0
```

Appendix C

Pysces input file: Hoefnagel2 model

```
Modelname: Hoefnagel_2.psc
Description: A kinetic model of Lactococcus metabolism with a modifed lactate dehydrogenase (v11)
# Original model from:
# Hoefnagel, M. H. N.; van Der Burgt, A.; Martens, D. E.; Hugenholtz, J.; Snoep, J. L.
# Time dependent responses of glycolytic intermediates in a detailed glycolytic model of
# Lactococcus lactis during glucose run-out experiments
# Mol. Biol. Rep., 2002, 29, 157-161
# Pysces file obtained from JWS Online: http://jjj.biochem.sun.ac.za/

FIX: Gluc  Lac  FOR  AC  ETOH  O2  TDP  UDP  Cellwall  ACETOUT  BUT

v1:
{1}Gluc + {1}PEP = {1}G6P + {1}PYR
(Vmax1*(Gluc/km1Gluc)*(PEP/km1PEP))/((1+(Gluc/km1Gluc)+(G6P/km1G6P))*(1+(PEP/km1PEP)+(PYR/km1PYR)))

v2:
{1}G6P = {1}F6P
(Vmax2*(G6P/km2G6P)*(1-(F6P/(G6P*Keq2))))/(1+(G6P/km2G6P)+(F6P/km2F6P))

v3:
{1}F6P + {1}ATP = {1}FBP + {1}ADP
((Vmax3*(1-((PEP**n3PEP/(k3PEP**n3PEP+PEP**n3PEP)))))*(1*(F6P**n3/km3F6P**n3)*(ATP/km3ATP)))/
((1+((F6P**n3)/(km3F6P**n3))+(FBP/km3FBP))*(1+(ATP/km3ATP)+(ADP/km3ADP)))

v4:
{1}FBP = {1}G3P + {1}DHAP
Vmax4* FBP/K4FBP*(1-((G3P*DHAP)/(FBP*Keq4)))/
(1+(FBP/K4FBP)+(DHAP/K4DHAP)+(G3P/K4G3P)+((FBP*G3P)/( K4FBP*Ki4G3P))+((DHAP*G3P)/( K4DHAP* K4G3P)))

v5:
{1}DHAP = {1}G3P
(Vmax5*(DHAP/km5DHAP)*(1-(G3P/(DHAP*Keq5))))/(1+(DHAP/km5DHAP)+(G3P/km5G3P))
```

```
v6:
{1}G3P + {1}NAD + {1}P = {1}DPG + {1}NADH
(Vmax6*(1-((DPG*NADH)/(G3P*NAD*P*Keq6)))*(G3P/km6G3P)*(NAD/km6NAD)*(P/km6P))/
((1+(G3P/km6G3P)+(DPG/km6DPG))*(1+(P/km6P))*(1+(NAD/km6NAD)+(NADH/km6NADH)))

v7:
{1}DPG + {1}ADP = {1}P3G + {1}ATP
(Vmax7*(DPG/km7DPG)*(ADP/km7ADP)*(1-((P3G*ATP)/(DPG*ADP*Keq7))))/
((1+(DPG/km7DPG)+(P3G/km7P3G))*(1+(ADP/km7ADP)+(ATP/km7ATP)))

v8:
{1}P3G = {1}P2G
(Vmax8*(P3G/km8P3G)*(1-(P2G/(P3G*Keq8))))/(1+(P3G/km8P3G)+(P2G/km8P2G))

v9:
{1}P2G = {1}PEP
(Vmax9*(P2G/km9P2G)*(1-(PEP/(P2G*Keq9))))/(1+(P2G/km9P2G)+(PEP/km9PEP))

v10:
{1}PEP + {1}ADP = {1}PYR + {1}ATP
(Vmax10*((PEP/km10PEP)**n10)*(ADP/km10ADP)*(1-((PYR*ATP)/(PEP*ADP*Keq10))))/
(((1+(PEP/km10PEP)**n10)+(PYR/km10PYR))*(1+(ADP/km10ADP)+(ATP/km10ATP)))*
(1/(1+P**3/(Ki10*(1+(FBP/K10FBP)+(G6P/K10G6P))**3)))

v11:
{1}PYR + {1}NADH = {1}Lac + {1}NAD

((FBP/km11FBP)**n11_FBP/T1)*(Vmax11/(km11PYR*km11NADH))*(PYR*NADH - Lac*NAD/Keq11) /
((T1/T2 + (NADH/km11NADH + NAD/km11NAD))*(T1/T3 +(PYR/km11PYR + Lac/km11Lac)))

!F self.T1 = 1+(self.FBP/self.km11FBP)**self.n11_FBP+(self.P/self.k11P)**self.n11_P
!F self.T2 = 1+self.alfa_NADH*(self.FBP/self.km11FBP)**self.n11_FBP+(self.P/self.k11P)**self.n11_P
!F self.T3 = 1+self.alfa_PYR*(self.FBP/self.km11FBP)**self.n11_FBP +(self.P/self.k11P)**self.n11_P

# Original LDH rate equation from Hoefnagel et al. (2002)
#  (FBP/(FBP+km11FBP))*(Vmax11*(PYR/km11PYR)*(NADH/km11NADH)*(1-((Lac*NAD)/(PYR*NADH*Keq11))))/
#  ((1+(PYR/km11PYR)+(Lac/km11Lac))*(1+(NADH/km11NADH)+(NAD/km11NAD)))

# K-LDH (no V-effect) Exp. 4l in Lactis_experiments_log_scan.py
#  (Vmax11/(km11PYR*km11NADH))*(PYR*NADH - Lac*NAD/Keq11) /
#  (T1/T2 + (NADH/km11NADH + NAD/km11NAD))*(T1/T3 +(PYR/km11PYR + Lac/km11Lac)))

# No activation by FBP; no inhibition by Pi (reversible bi-bi Hill equation)
#  (Vmax11/(km11PYR*km11NADH))*(PYR*NADH - Lac*NAD/Keq11) /
#  ((1 + (NADH/km11NADH + NAD/km11NAD))*(1 +(PYR/km11PYR + Lac/km11Lac)))
```

```
v12:
{2}PYR = {1}ACLAC
Vmax12*(PYR/K12PYR)*(1-(ACLAC/(PYR*Keq12)))*(((PYR/K12PYR)+(ACLAC/K12ACLAC))**(h12-1))/
(1+(((PYR/K12PYR)+(ACLAC/K12ACLAC))**h12))

v13:
{1}ACLAC = {1}ACET
Vmax13*ACLAC/Km13ACLAC*(1-ACET/(ACLAC*Keq13))*(ACLAC/Km13ACLAC + ACET/Km13ACET)**(h13-1)/
(1+(ACLAC/Km13ACLAC + ACET/Km13ACET)**h13)

v14:
{1}ACET = {1}ACETOUT
Vmax14*(ACET/Km14ACET)/(1+ACET/Km14ACET)

v15:
{1}ACLAC = {1}ACET
Vmax15*ACLAC

v16:
{1}ACET + {1}NADH = {1}BUT + {1}NAD
(Vmax16*(ACET/km16ACET)*(NADH/km16NADH)*(1-((BUT*NAD)/(ACET*NADH*Keq16))))/
((1+(ACET/km16ACET)+(BUT/km16BUT))*(1+(NADH/km16NADH)+(NAD/km16NAD)))

v17:
{1}PYR + {1}COA = {1}FOR + {1}ACCOA
(Vmax17*(PYR/km17PYR)*(COA/km17COA)*(1-((FOR*ACCOA)/(PYR*COA*Keq17))))/
((1+((G3P+DHAP)/ki17))*(1+(PYR/km17PYR)+(FOR/km17FOR))*(1+(COA/km17COA)+(ACCOA/km17ACCOA)))

v18:
{1}ACCOA + {1}P = {1}ACP + {1}COA
(Vmax18*(ACCOA/km18ACCOA)*(P/km18P)*(1-((ACP*COA)/(ACCOA*P*Keq18))))/
((1+(ACCOA/km18ACCOA)+(ACP/km18ACP))*(1+(P/km18P)+(COA/km18COA)))

v19:
{1}ACP + {1}ADP = {1}AC + {1}ATP
(Vmax19*(ACP/km19ACP)*(ADP/km19ADP)*(1-((AC*ATP)/(ACP*ADP*Keq19))))/
((1+(ACP/km19ACP)+(AC/km19AC))*(1+(ADP/km19ADP)+(ATP/km19ATP)))

v20:
{1}PYR + {1}NAD + {1}COA = {1}NADH + {1}ACCOA
(Vmax20*(PYR/k20PYR)*(NAD/k20NAD)*(COA/k20COA)/
((1+(PYR/k20PYR))*(1+(NAD/k20NAD)+(NADH/k20NADH))*(1+(COA/k20COA)+(ACCOA/k20ACCOA))))*
(1/(1+(Ki20*(NADH/NAD))))

v21:
{1}NADH + {1}ACCOA = {1}NAD + {1}COA + {1}ACAL
(Vmax21*(NADH*ACCOA)/(K21NADH*K21ACCOA)-(Vmax21*NAD*COA*ACAL)/
```

```
(K21NADH*K21ACCOA*KEQ21))/((1+NADH/K21NADH+NAD/K21NAD)*(1+ACCOA/K21ACCOA+COA/K21COA)
*(1+ACAL/K21ACAL))

v22:
{1}ACAL + {1}NADH = {1}ETOH + {1}NAD
(Vmax22*(ACAL/km22ACAL)*(NADH/km22NADH)*(1-((ETOH*NAD)/
(ACAL*NADH*Keq22))))/((1+(ACAL/km22ACAL)+(ETOH/km22ETOH))*(1+(NADH/km22NADH)+(NAD/km22NAD)))

v23:
{1}ATP = {1}ADP + {1}P
Vmax23*((ATP/ADP)**N23)/((K23ATP**N23+((ATP/ADP)**N23)))

v24:
{1}NADH + {1}O2 = {1}NAD
(Vmax24*NADH/KM24OXNADH*O2/KM24OXO)/((1+NADH/KM24OXNADH+NAD/KM24OXNAD)*(1+O2/KM24OXO))

v25:
{1}FBP = {1}F6P + {1}P
(Vmax25*(FBP/km25FBP))/(1+(FBP/km25FBP)+(F6P/km25F6P))

v26:
{1}G6P = {1}Glucin + {1}P
Vmax26*(G6P/K26G6P)/(1 + G6P/K26G6P)

v27:
{1}G6P = {1}G1P
(Vmax27*(G6P/km27G6P)*(1-(G1P/(G6P*Keq27))))/(1+(G6P/km27G6P)+(G1P/km27G1P))

v28:
{5}G1P + {5}ATP + {2}NADH + {3}UDP + {2}TDP = {5}ADP + {10}P + {2}NAD + {1}Cellwall
(Vmax28*(G1P/k28g1p)*(ATP/k28atp) *(NADH/k28nadh))/
((1+( G1P/k28g1p)+(P/k28p))*(1+(ATP/k28atp)+(ADP/k28ADP))*
(1+(NADH/k28nadh)+(NAD/k28nad)))

v29:
{1}Glucin + {1}ATP = {1}G6P + {1}ADP
(Vmax29*(Glucin/km29Glucin)*(ATP/km29ATP))/
((1+(Glucin/km29Glucin)+(G6P/km29G6P))*(1+(ATP/km29ATP)+(ADP/km29ADP)))

#InitVar
PEP       = 0.05
G6P       = 3.0
F6P       = 0.7
ATP       = 5.0
FBP       = 30.0
ADP       = 5.0
G3P       = 1.0
```

```
DHAP     = 11.0
NAD      = 5.2
DPG      = 0.1
NADH     = 0.35
P3G      = 20.0
P2G      = 1.8
PYR      = 0.3
COA      = 0.89
ACCOA    = 0.11
P        = 5.0
ACP      = 0.03145
ACAL     = 0.11
G1P      = 0.02
Glucin   = 0.00001
ACLAC    = 0.01
ACET     = 0.1

#initext
Gluc = 2.0
Lac = 0.1
FOR = 0.02
AC = 0.02
ETOH = 0.0
O2 = 0.1
TDP = 0.1
UDP = 0.1
Cellwall = 0.00001
ACETOUT = 0.1
BUT = 0.0


#initpar
Vmax1 =  160.0
km1Gluc =  0.015
km1PEP =  0.3
km1G6P =  500.0
km1PYR =  2.0
Vmax2 =  1280.0
km2G6P =  1.5
Keq2 =  0.314
km2F6P =  0.2
Vmax3 =  227.0
n3PEP =  1.0
k3PEP =  2.0
n3 =  2.9
km3F6P =  0.25
km3ATP =  0.18
```

```
km3FBP =  5.8
km3ADP =  0.3
Vmax4 =  1100.0
K4FBP =  0.17
Keq4 =  0.056
K4DHAP =  0.13
K4G3P =  0.03
Ki4G3P =  0.23
Vmax5 =  17500.0
km5DHAP =  2.8
Keq5 =  0.045
km5G3P =  0.3
Vmax6 =  4984.0
Keq6 =  0.0007
km6G3P = 0.25
km6NAD = 0.2
km6P =  2.35
km6DPG =  0.05
km6NADH =  0.067
Vmax7 =  920.0
km7DPG =  0.003
km7ADP =  0.2
Keq7 =  3200.0
km7P3G =  0.53
km7ATP =  0.3
Vmax8 =  1340.0
km8P3G =  1.2
Keq8 =  0.1
km8P2G =  0.1
Vmax9 =  1600.0
km9P2G =  0.04
Keq9 =  4.6
km9PEP =  0.5
Vmax10 =  2030.0
km10PEP =  0.17
n10 =  1.4
km10ADP =  1.0
Keq10 =  6500.0
km10PYR =  21.0
km10ATP =  10.0
Ki10 =  0.77
K10FBP =  9.1
K10G6P =  0.48
Vmax11 =  3300.0
# Nuwe waarde vir LDH (reaksie 11)
km11FBP   = 0.2
km11PYR   = 6.429
```

```
km11NADH  = 0.146
k11P      = 15.32
n11_FBP   = 1.8
n11_P     = 2.4
alfa_PYR  = 5.678
alfa_NADH = 2.329
Keq11 =  360000.0
km11Lac =  100.0
km11NAD =  2.40
#gecopy uit hoefnagel
#Vmax11 =  3300.0
#k11FBP =  0.003
#km11PYR =  1.5
#km11NADH =  0.2
#Keq11 =  360000.0
#km11Lac =  100.0
#km11NAD =  2.40
Vmax12 =  600.0
K12PYR =  50.0
Keq12 =  900000.0
K12ACLAC =  100.0
h12 =  2.4
Vmax13 =  106.0
Keq13 =  900000.0
Km13ACLAC =  10.0
Km13ACET =  100.0
h13 =  1.0
Vmax14 =  83.3
Km14ACET =  5.0
Vmax15 =  0.0003
Vmax16 =  43.3
km16ACET =  0.06
km16NADH =  0.02
Keq16 =  1400.0
km16BUT =  2.6
km16NAD =  0.16
Vmax17 =  114.0
km17PYR =  1.0
km17COA =  0.007
Keq17 =  650.0
ki17 =  0.2
km17FOR =  24.0
km17ACCOA =  0.05
Vmax18 =  720.0
km18ACCOA =  0.06
km18P =  5.0
Keq18 =  0.0281
```

```
km18ACP =  0.48
km18COA =  0.1
Vmax19 =  500.0
km19ACP =  0.16
km19ADP =  0.5
Keq19 =  174.22
km19AC =  7.0
km19ATP =  7.0
Vmax20 =  60.0
k20PYR =  1.0
k20NAD =  0.4
k20COA =  0.014
k20NADH =  0.1
k20ACCOA =  0.008
Ki20 =  49.36
Vmax21 =  100.0
K21NADH =  0.025
K21ACCOA =  0.007
KEQ21 =  1.0
K21NAD =  0.08
K21COA =  0.008
K21ACAL = 10.0
Vmax22 =  270.0
km22ACAL =  0.03
km22NADH =  0.05
Keq22 =  12355.0
km22ETOH =  1.0
km22NAD =  0.08
Vmax23 =  1000.0
N23 =  2.58
K23ATP =  6.196
Vmax24 =  30.0
KM24OXNADH =  0.041
KM24OXO =  0.01
KM24OXNAD =  0.2
Vmax25 =  0.01
km25FBP =  10.0
km25F6P =  2.0
Vmax26 =  0.1
K26G6P =  20.0
Vmax27 =  35.0
km27G6P =  0.05
Keq27 =  0.0585
km27G1P =  0.004
Vmax28 =  10.0
k28g1p =  0.05
k28atp =  7.0
```

```
k28nadh =  0.02
k28p =  30.0
k28ADP =  1.0
k28nad =  1.0
Vmax29 =  60.0
km29Glucin =  0.2
km29ATP =  0.05
km29G6P =  5.0
km29ADP =  5.0

# Disequilibrium ratios for reversible reactions

!F self.dr2 = (self.F6P/self.G6P)/self.Keq2
!F self.dr4 = (self.G3P*self.DHAP/self.FBP)/self.Keq4
!F self.dr5 = (self.G3P/self.DHAP)/self.Keq5
!F self.dr6 = ((self.DPG*self.NADH)/(self.G3P*self.NAD*self.P))/self.Keq6
!F self.dr7 = (self.P3G*self.ATP)/(self.DPG*self.ADP)/self.Keq7
!F self.dr8 = (self.P2G/self.P3G)/self.Keq8
!F self.dr9 = (self.PEP/self.P2G)/self.Keq9
!F self.dr10 = (self.PYR*self.ATP)/(self.PEP*self.ADP)/self.Keq10
!F self.dr11 = (self.Lac*self.NAD)/(self.PYR*self.NADH)/self.Keq11
!F self.dr12 = (self.ACLAC/self.PYR**2)/self.Keq12
!F self.dr13 = (self.ACET/self.ACLAC)/self.Keq13
!F self.dr16 = (self.BUT*self.NAD)/(self.ACET*self.NADH)/self.Keq16
!F self.dr17 = (self.FOR*self.ACCOA)/(self.PYR*self.COA)/self.Keq17
!F self.dr18 = (self.ACP*self.COA)/(self.ACCOA*self.P)/self.Keq18
!F self.dr19 = (self.AC*self.ATP)/(self.ACP*self.ADP)/self.Keq19
!F self.dr21 = (self.NAD*self.COA*self.ACAL)/(self.NADH*self.ACCOA)/self.KEQ21
!F self.dr22 = (self.ETOH*self.NAD)/(self.ACAL*self.NADH)/self.Keq22
!F self.dr27 = (self.G1P/self.G6P)/self.Keq27
```

Bibliography

[1] Amir, J. and Preiss, J. [1982] "Kinetic characterization of spinach leaf sucrose-phosphate synthase." *Plant Physiol.* **69**, 1027–30.

[2] Assa, P., Ozkan, M. and Ozcengiz, G. [2005] "Thermostability and regulation of *Clostridium thermocellum* L-lactate dehydrogenase expressed in *Escherichia coli*" *Annals Micriobiol.* **55**, 193–197.

[3] Bond, C. J., Jurica, M. S., Mesecar, A. and Stoddard, B. L. [2000] "Determinants of allosteric activation of yeast pyruvate kinase and identification of novel effectors using computational screening" *Biochemistry (Mosc.)* **39**, 15333–15343.

[4] Braat, H., Rottiers, P., Hommes, D., Huyghebaert, N., Remaut, E., Remon, J., van Deventer, S., Neirynck, S., Peppelenbosch, M. and Steidler, L. [2006] "A phase I trial with transgenic bacteria expressing interleukin-10 in Crohn's disease" *Clin. Gastroenterol. Hepatol.* **4**, 754–759.

[5] Brown, A. T. and Wittenberger, C. L. [1972] "Fructose-1, 6-diphosphate-dependent lactate dehydrogenase from a cariogenic streptococcus: Purification and regulatory properties" *J. Bacteriol.* **110 (2)**, 604–615.

[6] Cao, R., Zeidan, A., Radström, P. and van Niel, E. W. J. [2010] "Inhibition kinetics of catabolic dehydrogenases by elevated moieties of atp and adp–implication for a new regulation mechanism in *Lactococcus lactis*" *FEBS J.* **277**, 1843–1852.

[7] Chen, W.-J., Huang, D.-J., Liu, P.-H., Wang, H.-J., Su, J.-C. and Lee, P.-D. [2001] "Purification and characterization of sucrose phosphate synthase from sweet potato tuberous roots" *Bot. Bull. Acad. Sin.* **42**, 123–129.

[8] Christensen, C. D., Hofmeyr, J.-H. S. and Rohwer, J. M. [2015] "Tracing regulatory routes in metabolism using generalised supply-demand analysis." *BMC Syst. Biol.* **9**, 89.

[9] Clarke, A. R., Atkinson, T. and Holbrook, J. J. [1989] "From analysis to synthesis: new ligand binding sites on the lactate dehydrogenase framework. part 2" *Trends Biochem. Sci.* **14**, 145–148.

[10] Collins, L. and Thomas, T. D. [1974] "Pyruvate kinase of *Streptococcus lactis*" *J. Bacteriol.* **120**, 52–58.

[11] Cornish-Bowden, A. [2002] *Fundamentals of Enzyme Kinetics* Portland Press.

[12] Crow, V. L. and Pritchard, G. G. [1977] "Fructose 1,6-diphosphate-activated L-lactate dehydrogenase from *Streptococcus lactis*: Kinetic properties and factors affecting activation" *J. Bacteriol.* **131**, 82–91.

[13] Garrigues, C., Loubiere, P., Lindley, N. D. and Cocaign-Bousquet, M. [1997] "Control of the shift from homolactic acid to mixed-acid fermentation in *Lactococcus lactis*: predominant role of the NADH/NAD^+ ratio." *J. Bacteriol.* **179**, 5282–7.

[14] Garvie, E. I. [1980] "Bacterial lactate dehydrogenases" *Microbiol. Rev.* **44**, 106–139.

[15] Hardman, M. J., Crow, V. L., Cruickshank, D. S. and Pritchard, G. G. [1985] "Kinetics of activation of L-lactate dehydrogenase from *Streptococcus lactis* by fructose 1,6-biphosphate" *Eur. J. Biochem.* **146**, 179–183.

[16] Heinrich, R. and Rapoport, T. A. [1974] "A linear steady-state treatment of enzymatic chains. general properties, control and effector strength." *Eur. J. Biochem.* **15**, 89–95.

[17] Hoefnagel, M. H. N., Starrenburg, M. J. C., Martens, D. E., Hugenholtz, J., Kleerebezem, M., Van Swam, I. I., Bongers, R., Westerhoff, H. V. and Snoep, J. L. [2002] "Metabolic engineering of lactic acid bacteria, the combined approach: kinetic modelling, metabolic control and experimental analysis." *Microbiology* **148**, 1003–13.

[18] Hoefnagel, M. H. N., van der Burgt, A., Martens, D. E., Hugenholtz, J. and Snoep, J. L. [2002] "Time dependent responses of glycolytic intermediates in a detailed glycolytic model of *Lactococcus lactis* during glucose run-out experiment" *Mol. Biol. Rep.* **29**, 157–161.

[19] Hofmeyr, J. H. [1995] "Metabolic regulation: a control analytic perspective." *J. Bioenerg. Biomembr.* **27**, 479–90.

[20] Hofmeyr, J.-H. and Cornish-Bowden, A. [1997] "The reversible Hill equation: how to incorporate cooperative enzyme into metabolic models" *CABIOS* **13**, 377–385.

[21] Hofmeyr, J.-H. S. [1989] "Control-pattern analysis of metabolic pathways" *Eur. J. Biochem.* **186**, 343–354.

[22] Hofmeyr, J.-H. S. and Cornish-Bowden, A. [1991] "Quantative assessment of regulation in metabolic systems" *Eur. J. Biochem.* **200**, 223–236.

[23] Hofmeyr, J.-H. S. and Cornish-Bowden, A. [2000] "Regulating the cellular economy of supply and demand" *FEBS Lett.* **476**, 47–51.

[24] Hofmeyr, J.-H. S. and Rohwer, J. M. [2011] "Supply-demand analysis: A framework for exploring the regulatory design of metabolism" *Methods Enzymol.* **500**, 533–554.

[25] Hofmeyr, J.-H. S., Rohwer, J. M. and Snoep, J. L. [2006] "Conditions for effective allosteric feedforward and feedback in metabolic pathways" *IEE Proc.-Syst. Biol.* **153**, 327–331.

[26] Hols, P., Ramos, A., Hugenholtz, J., Delcour, J., de Vos, W. M., Santos, H. and Kleerebezem, M. [1999] "Acetate utilization in *Lactococcus lactis*

deficient in lactate dehydrogenase: a rescue pathway for maintaining redox balance." *J. Bacteriol.* **181**, 5521–5526.

[27] Huber, S. C. and Huber, J. L. [1992] "Role of sucrose-phosphate synthase in sucrose metabolism in leaves" *Plant Physiol.* **99**, 1275–1278.

[28] Jonas, H. A., Anders, R. F. and Jago, G. R. [1972] "Factors affecting the activity of the lactate dehydrogenase of *Streptococcus cremoris*" *J. Bacteriol.* **111**, 397–403.

[29] Jurica, M. S., Mesecar, A., Heath, P. J., Shi, W., Nowak, T. and Stoddard, B. L. [1998] "The allosteric regulation of pyruvate kinase by fructose-1,6-bisphosphate" *Structure* **6**, 195–210.

[30] Kacser, H. and Burns, J. A. [1973] "The control of flux" *Symp. Soc. Exp. Biol.* **27**, 65—104.

[31] Levering, J., Mark W. J. M. Musters, M. W. J. M., Martijn Bekker, M., Bellomo, D., Fiedler, T., de Vos, W. M., Hugenholtz, J., Kreikemeyer, J. B., Kummer, U. and Teusink, B. [2012] "Role of phosphate in the central metabolism of two lactic acid bacteria – a comparative systems biology approach" *FEBS J.* **279**, 1274–1290.

[32] Liebermeister, W. and Klipp, E. [2006] "Bringing metabolic networks to life: convenience rate law and thermodynamic constraints" *Theor. Biol. Med. Model.* **3**, 1–4.

[33] Liebermeister, W. and Klipp, E. [2006] "Bringing metabolic networks to life: integration of kinetic, metabolic, and proteomic data" *Theor. Biol. Med. Model.* **3**, 42.

[34] Loewe, A., Einig, W. and Hampp, R. [1996] "Coarse and fine control and annual changes of sucrose-phosphate synthase in norway spruce needles." *Plant Physiol.* **112**, 641–649.

[35] Melchiorsen, C. R., Jensen, N. B., Christensen, B., Vaever Jokumsen, K. and Villadsen, J. [2001] "Dynamics of pyruvate metabolism in *Lactococcus lactis*" *Biotechnol. Bioeng.* **74**, 271–9.

[36] Michaelis, L. and Menten, M. M. L. [2013] "The kinetics of invertin action: Translated by T.R.C. Boyde" *FEBS Lett.* **587**, 2712–2720.

[37] Monod, J., Wyman, J. and Changeux, J.-P. [1965] "On the nature of allosteric transitions: a plausible model" *J. Mol. Biol.* **12**, 88–118.

[38] Moreno-Sanchez, R., Saavedra, E., Rodrıguez-Enrıquez, S. and Olın-Sandoval, V. [2008] "Metabolic control analysis: a tool for designing strategies to manipulate metabolic pathways" *J. Biomed. Biotechnol.* **2008**, 1–30.

[39] Moreno-Sánchez, R., Saavedra, E., Rodríguez-Enríquez, S. and Olín-Sandoval, V. [2008] "Metabolic control analysis: a tool for designing strategies to manipulate metabolic pathways" *J. Biomed. Biotechnol.* **2008**, 597913.

[40] Munday, M. R. [2002] "Regulation of mammalian acetyl-CoA carboxylase" *Biochem. Soc. Trans.* **30**, 1059–1064.

[41] Munoz, E. and Ponce, E. [2003] "Pyruvate kinase : current status of regulatory and functional properties" *Comparative* **135**, 197–218.

[42] Neuhaus, H. E., Quick, W. P., Siegl, G. and Stitt, M. [1990] "Control of photosynthate partitioning in spinach leaves" *Planta* **181**, 583–592.

[43] Neves, A. R., Pool, W. a., Kok, J., Kuipers, O. P. and Santos, H. [2005] "Overview on sugar metabolism and its control in *Lactococcus lactis* — the input from in vivo NMR" *FEMS Microbiol. Rev.* **29**, 531–54.

[44] Olivier, B. G., Rohwer, J. M. and Hofmeyr, J.-H. S. [2005] "Modeling cellular systems with PySCeS" *Bioinformatics* **21**, 560–561.

[45] Olivier, B. G. and Snoep, J. L. [2004] "Web-based kinetic modelling using JWS Online" *Bioinformatics* **20**, 2143–2144.

[46] Palm, D. C., Rohwer, J. M. and Hofmeyr, J.-H. S. [2013] "Regulation of glycogen synthase from mammalian skeletal muscle – a unifying view of allosteric and covalent regulation" *FEBS J.* **280**, 2–27.

[47] Papagianni, M., Avramidis, N. and Filiousis, G. [2007] "Glycolysis and the regulation of glucose transport in *Lactococcus lactis* spp. *lactis* in batch and fed-batch culture" *Microb. Cell Fact.* **6:16**.

[48] Pool, W. A. [2008] *Engineering of sugar metabolism in* Lactococcus lactis Ph.D. thesis Rijksuniversiteit Groningen.

[49] Popova, S. V. and Sel'kov, E. E. [1975] "Generalization of the model by Monod, Wyman and Changeux for the case of a reversible monosubstrate reactions S $<=$ (R, T) $=>$ P" *FEBS Lett.* **53**, 269–273.

[50] Popova, S. V. and Sel'kov, E. E. [1976] "Generalization of the Monod-Wyman-Changeux model to the case of a multisubstrate reaction" *Mol. Biol. (Moskva)* **10**, 1116–1126.

[51] Popova, S. V. and Sel'kov, E. E. [1978] "Description of the kinetics of two-substrate reactions of the type $s_1 + s_2 \rightleftharpoons s_3 + s_4$ by a generalised Monod, Wyman, and Changeux model" *Mol. Biol. (Moskva)* **13**, 129–139.

[52] Popova, S. V. and Sel'kov, E. E. [1978] "Reversible regulatory enzymatic reactions. A theoretical analysis" *Mol. Biol. (Moskva)* **12**, 1139–1151.

[53] Reimholtz, R., GeigenbStitt, P. and Stitt, M. [1994] "Sucrose-phosphate synthase is regulated via metabolites and protein phosphorylation in potato tubers, in a manner analogous to the enzyme in leaves" *Planta* **192**, 480–488.

[54] Rohwer, J. M., Hanekom, A. J. and Hofmeyr, J.-H. S. [2007] "A universal rate equation for systems biology" in *Proceedings of 2nd International ESCEC Symposium on Experimental Standard Conditions on Enzyme Characterizations, March 19th – 23rd, 2006, Ruedesheim/Rhein, Germany* (Kettner, C. and Hicks, M. G., eds.) pp. 175–188 Beilstein Institute, Frankfurt.

[55] Rohwer, J. M. and Hofmeyr, J.-H. S. [2008] "Identifying and characterising regulatory metabolites with generalised supply-demand analysis." *J. Theor. Biol.* **252**, 546–54.

[56] Savijoki, K. and Palva, a. [1997] "Molecular genetic characterization of the L-lactate dehydrogenase gene (LdhL) of *Lactobacillus helveticus* and biochemical characterization of the enzyme." *Appl. Environ. Microbiol.* **63**, 2850–6.

[57] Stoll, V. S., Kimber, M. S. and Pai, E. F. [1996] "Insights into substrate binding by D-2-ketoacid dehydrogenases from the structure of *Lactobacillus pentosus* D-lactate dehydrogenase" *Structure* **4**, 437–447.

[58] Teusink, B., Bachmann, H. and Molenaar, D. [2011] "Systems biology of lactic acid bacteria: a critical review" *Microb. Cell Fact.* **10 Suppl 1**, S11.

[59] Thampy, K. G. and Wakil, J. [1985] "Activation of acetyl-CoA carboxylase. purification and properties of a Mn^{2+}-dependent phosphatase" *J. Biol. Chem.* **260(10)**, 6318–6323.

[60] Thomas, T. D. [1976] "Regulation of lactose fermentation in group n *Streptococci*" *Appl. Environ. Microbiol.* **32**, 474–478.

[61] Tong, L. [2005] "Acetyl-coenzyme A carboxylase: crucial metabolic enzyme and attractive target for drug discovery" *Cell Mol Life Sci.* **62 (16)**, 1784–803.

[62] Turunen, M., Parkkinen, E., Londesborough, J. and Korhola, M. [1987] "Distinct forms of lactate dehydrogenase purified from ethanol- and lactate-producing cells of *Clostridum thermohydrosulfuricum*" *J. Gen. Microbiol.* **133**, 2865–2873.

[63] Valentini, G., Chiarelli, L., Fortin, R., Speranza, M. L., Galizzi, A. and Mattevi, A. [2000] "The allosteric regulation of pyruvate kinase: A site-directed mutagenesis study" *J. Biol. Chem.* **275**, 18145–18152.

[64] Veith, N., Feldman-Salit, A., Cojocaru, V., Henrich, S., Kummer, R. and Wade, C. [2013] "Organism-adapted specificity of the allosteric regulation of pyruvate kinase in lactic acid bacteria" *PLoS Comput. Biol.* **9**, 1–15.

[65] Westermark, P. O., Hellgren-Kotaleski, J. and Lansner, A. [2004] "Derivation of a reversible hill equation with modifiers affecting catalytic properties" *WSEAS Trans. Biol. Med.* **1**, 91–98.

[66] Wittenberger, C. L. and Angelo, N. [1970] "Purification and properties of a fructose-1,6-diphosphate-activated lactate dehydrogenase from *Streptococcus faecalis*" *J. Bacteriol.* **101**, 717–724.